This is to certify that the
dissertation entitled

UNDERSTANDING LIPID BLAYER DYNAMICS USING
FLUORESCENCE SPECTROSCOPY

presented by

MONIQUE MARIE LAPINSKI

has been accepted towards fulfillment
of the requirements for the

Ph.D. degree in Chemistry

Major Professor's Signature

7/30/07

Date

MSU is an affirmative-action, equal-opportunity employer

UNDERSTANDING LIPID BILAYER DYNAMICS USING FLUORESCENCE SPECTROSCOPY

By

Monique Marie Lapinski

A DISSERTATION

Submitted to
Michigan State University
in partial fulfillment of the requirements
for the degree of

DOCTOR OF PHILOSOPHY

Department of Chemistry

2007

ABSTRACT

UNDERSTANDING LIPID BILAYER DYNAMICS USING FLUORESCENCE SPECTROSCOPY

By

Monique Marie Lapinski

Lipid vesicles are important because of their use as models for biological membranes. We were particularly interested in using the rotational and translational dynamics of chromophores sequestered within the bilayers comprising vesicles so that we may understand more about the factors that govern interactions between bilayer constituents. We find that two common methods for vesicle preparation yield the same rotational and translational diffusion dynamics for chromophores imbedded in them indicating that the molecular scale organization of bilayers is determined by interactions between bilayer constituents, which themselves do not depend on the manner in which the bilayer is formed. We report that small concentrations of certain bilayer species can have substantial effects on the overall properties of the bilayer systems. In particular, it is possible to have interactions between chromophores which perturb the system in such a way that the bilayer itself is not being interrogated properly. This finding emphasizes the necessity in using small concentrations of fluorescent probes when performing bilayer studies. We were successful in using the reorientation dynamics of a nonpolar chromophore to determine the phase transition temperature of a lipid comprising the bilayers in vesicles. We found that the introduction of an unsaturated lipid into the same system, in small concentrations, caused a substantial and measureable change in the phase transition temperature of the system owing to the order was disrupted in the

system. We studied the effects that the radius of curvature of vesicles has on the measured phase transition temperature of lipids in the bilayers and found that we could detect the phase change in vesicles up to 800 nm in diameter. At sizes larger than this, the data suggested that the chromophore changes location in the bilayer with the decrease in the radius of curvature, underscoring the effect that the size of the vesicle has in mediating the dynamics of bilayer constituents.

To Dr. Robert Stach,
the professor that inspired me to pursue chemistry in college

ACKNOWLEDGEMENTS

There are several people that I need to thank that have helped me along the way during my graduate career at Michigan State University. First and foremost, I must thank my parents, who instilled in me, from a very young age, the importance and value of education. My father once told me that "education is the one thing, that once acquired, can never be taken away." Now, as my formal education is drawing to a close, I realize how true that statement is, and also how truly blessed I am to have parents that value education so dearly.

My husband, Steve, has been just as encouraging and equally supportive of each of my endeavors. It must be a true challenge to be married to a scientist, especially when the day's experiments prove to not go as planned. The patience that he has shown for me through the years is definitely a blessing, and I am lucky to have someone in my life that is so devoted to me and my love for chemistry.

Dr. Robert Stach, my undergraduate mentor and advisor, is the person responsible for developing my real love for biochemistry. His enthusiasm for teaching and his encouragement of learning during my undergraduate education challenged me in every way possible. It was at his insistence that I became an undergraduate chemistry tutor and developed my own passion for teaching. And now, I will continue to follow in his footsteps.

Dr. Gary Blanchard, my graduate advisor, provided guidance and support from the first day that I joined his research group. His willingness to help and his overall

dedication to research made him an excellent advisor. Over the years, with true patience, he never once doubted my abilities. He continued to challenge me on all levels and has now provided me with the tools that I need to be successful.

Finally, I must thank my committee members, Dr. David Weliky, Dr. Greg Swain and Dr. Gavin Reid for serving on my committee. In addition, I must also thank Dr. Robert Ofoli and his research group in the Chemical Engineering and Material Science department on campus, as they were instrumental in conducting the experiments using supported lipid bilayers in Chapter 3.

TABLE OF CONTENTS

LIST OF TABLES

LIST OF FIGURES

LIST OF ABBREVIATIONS

TCSPC ..... Time correlated single photon counting

CFD ..... Constant fraction discriminator

TAC ..... Time to amplitude converter

MCP ..... Microchannel plate

PMT ..... Photomultiplier tube

MCA ..... Multichannel analyzer

TEM .....Transmission electron microscopy

DLS ..... Dynamic light scattering

FRAPP ..... Fluorescence recovery after pattern photobleaching

sBLM ..... Supported bilayer membrane

SUV ..... Small unilamellar vesicle

DOPC 1,2-dioleoyl-*sn*-glycero-3-phosphocholine

NBD-PC ..... 1-oleoyl-2-[12-[(7-nitro-2-1,3-benzoxadiaz l-4-yl)amino]dodecanoyl]-*sn*-glycero-3-phosphocholine

HEPES .....N-2-Hydroxyethylpiperazine-N'-2-ethanesulfonic acid

NBD 7-nitrobenz-2-oxa-1,3-diazol-4-yl

SPM ..... Sphingomyelin

DMPC 1,2-dimyristoyl-*sn*-phosphatidylcholine

NBD-cholesterol ..... 25-(N-(7-nitrobenz-2-oxa-1,3-diazol-4-yl-methyl)amino)-27-norcholesterol

Rhodamine-PE ..... 1,2-Dimyristoyl-*sn*-Glycero-3-Phosphoethanolamine-N- (Lissamine Rhodamine B Sulfonyl Ammonium salt)

DMPE 1,2-Dimyristoyl-*sn*-Glycero-3-Phosphoethanolamine

NMR ..... Nuclear magnetic resonance

Tris® ..... Tris hydroxymethylaminoethane

14:1 PC 1,2-dimyristoleoyl-*sn*-glycero-3-phosphocholine

HEPES® ..... N-2-Hydroxyethylpiperazine-N'-2-ethanesulfonic acid

Chapter 1

INTRODUCTION

Lipids and lipid bilayers have recently attracted a great deal of attention from researchers because of their use in a variety of scientific, medical and pharmacological applications. The lipid bilayers that are used are often in the form of liposomes; small, spherical structures that can form when a lipid comes into contact with an aqueous phase. The driving force for this self assembly process is the tendency of the hydrophobic portion of the lipid molecule to minimize its contact with water. Therefore, the hydrophilic polar heads of the lipid molecule will face the aqueous surroundings and the hydrophobic tail portions of the lipid will constitute the interior of the bilayers. If this structure closes on itself, a lipid vesicle (liposome) is formed. The utility of this vesicular structure lies in the ability to trap various constituents within the small confines of the bilayer. In doing so, researchers are able to further study the physical and molecular factors that affect lipids and lipid bilayers.

The first researchers to study lipids found in cell membranes were Evert Gorter and his assistant, F. Grendel. In their classic experiment with red blood cells,[1] the researchers were able to demonstrate that lipid molecules could from a double layer, as well as a monolayer. In addition, by using a modified device similar to a Langmuir trough, they were able to show that the surface area of the lipids extracted from the red blood cells was approximately twice the area of the cells themselves. Gorter and Grendel repeated their initial studies with red blood cells using erythrocytes from several animals

and humans and concluded that "[red blood cells] are covered by a layer of fatty substances that is two molecules thick[1]."

Later, researchers discovered that the work of Gorter and Grendel was limited by the measurement techniques available at the time. They had not extracted the lipids from the red blood cells quantitatively, and had also underestimated the surface area of the erythrocytes. These two errors essentially cancelled and their conclusions were basically correct.[2] This finding ultimately led to the idea that cell membranes may, in fact, consist of lipid bilayers.

In 1957, J.D. Robertson proposed one version of the membrane model, which was based primarily on electron microscopy studies that he had conducted.[3] Under the high magnification of the transmission electron microscope (TEM), membranes displayed a characteristic outer shaded region that was darker in color than the inner shaded region. Robertson proposed that the outer layers were protein layers and the inner region was the lipid bilayer. However, Robertson's description was not entirely correct.

Once a more detailed understanding of proteins and their interactions with membranes was developed, the current model for the cell membrane was proposed. This model, known as the fluid mosaic model, was proposed by Singer and Nicolson in 1972,[4] and continues as the membrane model in use today. The fluid mosaic model includes the basic lipid structure first proposed by Gorter and Grendel, but also describes globular proteins (both integral and peripheral) that are able to reside within the lipid bilayer, rather than just on the membrane surface, as Robertson had once proposed.

Using modern molecular dynamics methods and a host of spectroscopic techniques, much work is in progress to understand more about membranes and lipid bilayers. It is known that the lipid bilayer that forms cell membranes is a two-dimensional liquid,[5] but the organization of this liquid continues to be an ongoing study among researchers. There have been repeated attempts to introduce lateral heterogeneities and lipid microdomains into systems to order to provide further insight into the structures and dynamics of the lipids that govern membrane bilayers and the ordering of these systems.[6-8] Because a large fraction of all biological membranes are believed to exist in a fluid state under physiological conditions, it is of particular importance to establish the factors and mechanisms that govern the ordering of lipid bilayers.[9]

A drastic change in the order of a bilayer system occurs at the so-called main phase transition temperature (T_m). At this temperature, the hydrocarbon tails undergo a change from being predominantly *trans* in configuration to a structure that is dominated by a significant number of *trans-gauche* conformers.[10] There are several factors that can affect phase changes in a lipid system. These factors include, but are not limited to pressure, temperature, the amount of hydration and the basic structural properties of the lipid(s), including the length of the hydrocarbon chain and the composition of the headgroup. We were interested in studying various regions of lipid bilayers to understand more about the factors that affect the ordering and measured transition temperatures of various systems.

For most of our studies, we prepared lipid vesicles using the extrusion method,[11-16] where a lipid solution is forced via syringe through polycarbonate membranes with defined pore sizes. The advantage in using the extrusion method for vesicle preparation is that we are able to control the sizes of the vesicles and can be assured the samples are unilamellar in structure. With the lipid vesicles, we then chose to explore some factors that would affect the phase transition temperature including the radius of curvature of the vesicles and the addition of an unsaturated lipid into the systems.

For these studies, we employed Time Correlated Single Photon Counting (TCSPC) as a means of determining the time-domain fluorescent properties of chromophores either embedded within or tethered to the lipid bilayers. In doing so, we were able to gain insight into the lipid bilayer environment in which the fluorescent probe was residing, including the polarity and viscosity of the surrounding area. In addition, we were able to use the data that we obtained from TCSPC to evaluate the effects that the addition of an unsaturated lipid and a fluorescent probe has on the measured transition temperature of the system. We were also able to determine the effects that the size of the size of the liposome has on the transition temperature.

For the time-resolved fluorescence spectroscopy measurements that we include in this dissertation, the light source was a continuous wave (CW) mode-locked Nd:YAG laser (Coherent Antares 76-s) that produced 100 ps pulses at a 76 MHz repetition rate. A cavity-dumped dye laser (Coherent 702-2) was operated with either Stilbene 420 dye (Exciton) and excited by the third harmonic of the source laser, or was operated with Pyromethene 567 dye (Exciton) that was excited by the second harmonic of the source

laser. Sample fluorescence was detected using a microchannel plate – photomultiplier tube (MCP-PMT, Hamamatsu R3809U), and the electronics used to temporally resolve the fluorescence transients were a constant fraction discriminator (CFD, Tennelec 454) and a time-to-amplitude converter/biased amplifier (TAC, Tennelec 864), (Figure 1.1). The fluorescence lifetime data were collected at 54.7° with respect to the vertical excitation polarization, while the reorientation data were collected at polarizations parallel (0°) and perpendicular (90°) to the vertically-polarized incident light.

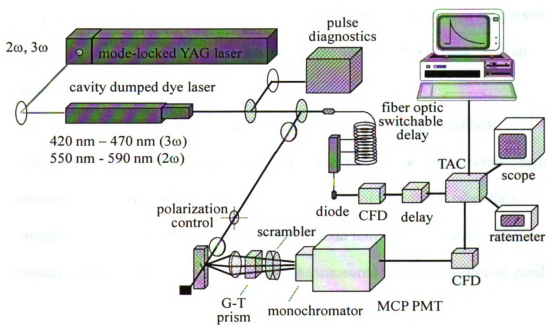

Figure 1.1. Schematic of the Time Correlated Single Photon Counting (TCSPC) system.

One of the parameters that we can determine using a chosen chromophore and the lipid bilayer structures is the fluorescence lifetime of the probe. The fluorescence lifetime can be described as the average amount of time that the chromophore molecule remains in the excited state before the emission of a photon takes place. The data contained in the fluorescence lifetime measurements therefore provide valuable insight into the environment in which the chromophore resides. When the exponential lifetime decay is analyzed, the resulting number of fluorescence lifetimes corresponds to the number of different environments that the chromophore senses. A single exponential lifetime decay indicates that the chromophore is sensing a single environment, and the lifetime value (measured in picoseconds) can, for certain chromophores, provide a gauge for the polarity of that environment. Multiple exponential lifetime decays are possible, especially for tethered chromophores that exhibit the ability to "loop back" into an environment with differing polarity.[17-20]

Another parameter that we can measure using TCSPC is the rotational reorientation time(s) of the chromophore. The reorientation time, usually measured in nanoseconds or picoseconds, is described as the amount of time that it takes for a chromophore to reorient itself to a random distribution following excitation. The reorientation time is derived by incorporating the measured intensities collected parallel ($I_{\parallel}(t)$) and perpendicular ($I_{\perp}(t)$) to the polarized incident light to form the induced anisotropy function shown in Eqn. 1.1.

$$R(t) = \frac{I_{\parallel}(t) - I_{\perp}(t)}{I_{\parallel}(t) + 2I_{\perp}(t)} \qquad (1.1)$$

The generated exponential decay curve is then fitted to determine the reorientation time(s) of the chromophore. The number of exponential decays contained in R(t) is determined by the effective rotor shape of the probe, and in principle, can contain up to five exponential decays. However, it is often difficult to resolve more than two of these decays simply based on symmetry conditions and the limitations in the signal-to-noise of the measurements.

The recovered reorientation time(s) can be used in the modified Debye-Stokes-Einstein Equation[21-23] shown in Eqn. 1.2, to determine the viscosity of the environment in which the chromophore resides.

$$\tau_{OR} = \frac{\eta V f}{k_B T S} \qquad (1.2)$$

In this equation, η represents the viscosity, V is the hydrodynamic volume of the chromophore, k_B is the Boltzmann constant and T is the temperature. The terms, f and S, are added to this equation to account for deviations from ideal behavior. The frictional coefficient, f, is equal to unity in the "stick" limit, which applies to very strong solute-solvent interactions. For weaker interactions, the "slip limit" is applied.[23,24] The shape factor term, S, is derived from Perrin's equations[21] and added to the Debye-Stokes-Einstein equation to account for deviations of the chromophores from perfectly spherical shapes. This term can vary from close to zero to 1, where unity represents a spherical reorienting chromophore.

The utility of these studies resides in the fact that we were able to use several chromophores with varying structural properties to probe different areas of the lipid vesicles. In Chapter 2, we used a chromophore tethered to a lipid, 1-oleoyl-2-[12-[(7-

nitro-2-1,3-benzoxadiazol-4-yl)amino]dodecanoyl]-*sn*-glycero-3-phosphocholine (18:1-12:0 NBD-PC), to determine whether two widely used methods of lipid vesicle preparation yield the same results, both in the rotational and translational dynamics of the chromophore. In Chapter 3, two tethered chromophores that are localized in different regions of the vesicles, NBD-cholesterol and Rhodamine-PE, to determine how compositional changes in one region give rise to structural changes in other bilayer regions. Chapter 4 addresses the use of a tethered polar chromophore, Rhodamine-PE, and the effects that the concentration of this probe has on the recorded rotational dynamics of the chromophore in the polar region of the lipid bilayer systems. In Chapter 5, a nonpolar chromophore, perylene, is used in varying lipid systems to determine whether the measured reorientation time of perylene can be used as a suitable means for detecting the phase transition temperature of lipid bilayer systems. Also, in this chapter, the effect that an unsaturated lipid has on the transition temperature of the system is evaluated. Chapter 6 uses the same probe and lipid system as the one tested in Chapter 3, but the diameter of the vesicles is varied from 100 nm to 5 μm to determine how the radius of curvature affects the measured transition temperature of the systems. Chapter 7 contains some final conclusions and possible representative future studies.

Literature Cited

(1) Gorter, E.; Grendel, F. *Journal of Experimental Medicine* **1925**, *41*, 439.

(2) Sadava, D. E. *Cell Biology: Organelle Structure and Function*; Jones and Bartlett: Boston, 1993.

(3) Robertson, J. D. *J Biophys Biochem Cytol FIELD Full Journal Title:The Journal of biophysical and biochemical cytology* **1957**, *3*, 1043.

(4) Singer, S. J.; Nicolson, G. L. *Science FIELD Full Journal Title:Science (New York, N.Y.)* **1972**, *175*, 720.

(5) Simons, K.; Vaz, W. L. C. *Annual Review of Biophysics and Biomolecular Structure* **2004**, *33*, 269.

(6) Glaser, M. *Current Opinion in Structural Biology* **1993**, *3*, 475.

(7) Jain, M. K.; White, H. B., III. *Advances in Lipid Research* **1977**, *15*, 1.

(8) Vaz, W. L.; Almeida, F. F. *Current Opinion in Structural Biology* **1993**, *3*, 482.

(9) Metso, A. J.; Jutila, A.; Mattila, J.-P.; Holopainen, J. M.; Kinnunen, P. K. J. *Journal of Physical Chemistry B* **2003**, *107*, 1251.

(10) Pabst, G.; Amenitsch, H.; Kharakoz, D. P.; Laggner, P.; Rappolt, M. *Physical Review E: Statistical, Nonlinear, and Soft Matter Physics* **2004**, *70*, 021908/1.

(11) Driessen, A. J.; van den Hooven, H. W.; Kuiper, W.; van de Kamp, M.; Sahl, H. G.; Konings, R. N.; Konings, W. N. *Biochemistry* **1995**, *34*, 1606.

(12) Hunter, D. G.; Frisken, B. J. *Biophysical Journal* **1998**, *74*, 2996.

(13) MacDonald, R. C.; MacDonald, R. I.; Menco, B. P.; Takeshita, K.; Subbarao, N. K.; Hu, L. R. *Biochimica et Biophysica Acta* **1991**, *1061*, 297.

(14) Mayer, L. D.; Hope, M. J.; Cullis, P. R. *Biochimica et Biophysica Acta* **1986**, *858*, 161.

(15) Subbarao, N. K.; MacDonald, R. I.; Takeshita, K.; MacDonald, R. C. *Biochimica et Biophysica Acta* **1991**, *1063*, 147.

(16) Unger, E. C.; MacDougall, P.; Cullis, P.; Tilcock, C. *Magnetic Resonance Imaging* **1989**, *7*, 417.

(17) Chattopadhyay, A.; London, E. *Biochimica et Biophysica Acta, Biomembranes* **1988**, *938*, 24.

(18) Fery-Forgues, S.; Fayet, J.-P.; Lopez, A. *Journal of Photochemistry and Photobiology, A: Chemistry* **1993**, *70*, 229.

(19) Feng, Z. V.; Spurlin, T. A.; Gewirth, A. A. *Biophysical Journal* **2005**, *88*, 2154.

(20) Mazeres, S.; Schram, V.; Tocanne, J.-F.; Lopez, A. *Biophysical Journal* **1996**, *71*, 327.

(21) Perrin, F. *Journal de Physique et le Radium* **1936**, *7*, 1.

(22) Debye, P. Polar Molecules. In *Chemical Catalog Co.* New York, 1929.

(23) Zwanzig, R.; Harrison, A. K. *Journal of Chemical Physics* **1985**, *83*, 5861.

(24) Youngren, G. K.; Acrivos, A. *Journal of Chemical Physics* **1975**, *63*, 3846.

Chapter 2

A COMPARISON OF LIPOSOMES FORMED BY SONICATION AND EXTRUSION: ROTATIONAL AND TRANSLATIONAL DIFFUSION OF AN IMBEDDED CHROMOPHORE

Introduction

Lipid bilayers are fundamental structures for all cellular systems, and a great deal of research effort has been expended on understanding how to create and interrogate native and model bilayer structures. Phospholipids are known to form liposome structures in an aqueous environment, and these structures can be created by any of a number of methods.[1-4] The resulting, nominally spherical structure is comprised of a phospholipid bilayer surrounding an aqueous core, with the size of the vesicle ranging from tens of nm to μm, depending on the manner in which the liposomes are formed. Two common protocols used in the preparation of liposomes are extrusion[5-10] and bath sonication,[11] with each method yielding liposome structures with different average sizes and size distributions.

Extrusion is currently one of the most common methods for controlling vesicle size and for producing unilamellar liposomes.[5-10] With this method, a lipid suspension is forced through a polycarbonate membrane with a well defined pore size to produce vesicles with a characteristic diameter near the pore size of the membrane used in its preparation. This technique avoids problems associated with the removal of organic solvents or detergents from the final preparations used in other protocols, and the technique can be applied to a wide variety of lipid species and mixtures.[12] Perhaps of

most significance is that the resulting vesicle average size and size distribution are reproducible from batch-to-batch due to the physical processing method.

Sonication is also used widely for the preparation of liposomes. With this method, lipid suspensions are mixed using acoustic energy from either a bath or a probe tip sonicator. The induced pressure breaks up the larger, multilamellar vesicles present in the sample and forms smaller vesicles that may be either unilamellar or multilamellar in composition.[11] The time over which lipid solutions are sonicated affects the size of the vesicles, with the smallest radius for phospholipid vesicles being in the range of 10.25 ± 0.55 nm, independent of the phospholipid hydrocarbon chain length.[13] The primary advantage of sonication over extrusion is that sonication is less time-consuming. However, the resulting mean liposome batch-to-batch diameter and size distribution are not as reproducible as those made by extrusion.

The goal of this study was to evaluate the behavior of small unilamellar vesicles (SUVs) prepared by bath sonication and by extrusion, to determine if the method of preparation has any influence on selected bilayer properties. This is an important issue because it bears on whether or not experimental data acquired for bilayer lipid membranes formed by these two different methodologies can be compared directly. We are interested in the mean diameter and size distribution of liposomes formed by the two techniques, and examine this issue using dynamic light scattering (DLS) and transmission electron microscopy (TEM). We are also interested in the molecular scale and mesoscopic properties of the lipid bilayers formed by the two methods. We address this issue through the measurement of the rotational motion of the chromophore incorporated

in the liposomes using time correlated single photon counting (TCSPC), and its translational diffusion in planar supported bilayer lipid membranes (sBLMs) using fluorescence recovery after pattern photobleaching (FRAPP). We find that, while the physical morphology (mean diameter and size distribution) of the liposomes formed by the two methods is outwardly different, the molecular scale diffusional behavior of species within the bilayers is essentially the same. The addition of cholesterol to the liposomes alters the observed dynamics of the tethered chromophore, with similar dynamical results for liposomes formed using both methods.

Experimental

Vesicle preparation by extrusion. Phospholipids 1,2-dioleoyl-*sn*-glycero-3-phospho-choline (DOPC), 1-oleoyl-2-[12-[(7-nitro-2-1,3-benzoxadiazol-4-yl)amino]dodecanoyl]-*sn*-glycero-3-phosphocholine (18:1-12:0 NBD-PC) and cholesterol were purchased from Avanti Polar Lipids Inc. (Alabaster, AL) and used as received. For each sample, 1 mM lipid solutions containing DOPC/NBD-PC (98:2 mol/mol) or DOPC/cholesterol/NBD-PC (68:30:2 mol/mol) were prepared. The chloroform solvent was evaporated from the lipid mixtures and the dry film was hydrated using HEPES® buffer (Sigma-Aldrich, St. Louis, MO) containing NaCl (Fisher Scientific, Fair Lawn, NJ). The goal was to obtain a final lipid concentration of 1 mg/mL. The buffer (10 mM HEPES®, 150 mM NaCl, pH 7.4) was prepared using purified water from a Milli-Q Plus water purification system (Millipore, Bedford, MA). The mixtures were processed five times through a freeze-thaw-vortex cycle to ensure complete mixing of the sample constituents. Each cycle consisted of immersion in liquid nitrogen for five minutes, followed by immersion in a 60°C water bath for five minutes, then vortexing the thawed sample for ca. two minutes. After the freeze-thaw-vortex cycling, the solutions were extruded through two 400 nm pore diameter polycarbonate membrane filters using a mini-extruder (Avanti Polar Lipids Inc., Alabaster AL). The pre-extruded vesicle suspension was then extruded eleven times through two polycarbonate membranes (Avanti Polar Lipids Inc., Alabaster, AL) with a nominal pore diameter of 100 nm. All extrusions were performed at room temperature.

Vesicle preparation by sonication. Lipid mixtures with the same compositions as those used for the extrusion experiments were used to form liposomes by sonication. The chloroform-solvated lipid mixtures were dried under nitrogen and placed under vacuum at -45°C for 3 hours. The dried lipid mixtures were then hydrated in buffer (10 mM HEPES®, 150 mM NaCl, pH 7.4), and sonicated for 20 minutes using a bath ultrasonic cleaner (Branson 1510, Branson Ultrasonic Corporation, Danbury, CT). Fresh liposome solutions were prepared prior to the beginning of each experiment.

Transmission Electron Microscopy (TEM) Imaging. A 10 μL aliquot of each sample was fixed on a Formvar® nickel-coated grid using a solution containing 2% uranyl acetate stain in water. Images were acquired using a transmission electron microscope (TEM, JEOL 100CX) operated at an accelerating voltage of 100 kV.

Dynamic Light Scattering (DLS). DLS was performed with a Protein Solutions DynaPro-MS/X system (Wyatt Technology Corporation, Santa Barbara, CA) on DOPC/NBD-PC liposome solutions, with and without cholesterol, to determine mean vesicle sizes and size distributions. Liposome solutions were diluted by a factor of ten with buffer and placed in a polyethylene cuvette for measurement.

Steady state spectroscopy. Steady state excitation and emission spectra (Figure 2.1) were acquired for vesicle samples for the purpose of characterizing the NBD chromophore band positions. We used an emission spectrometer (Spex Fluorolog 3, Edison, NJ) for all measurements, set to a spectral bandpass of 3 nm for both excitation and emission monochromators.

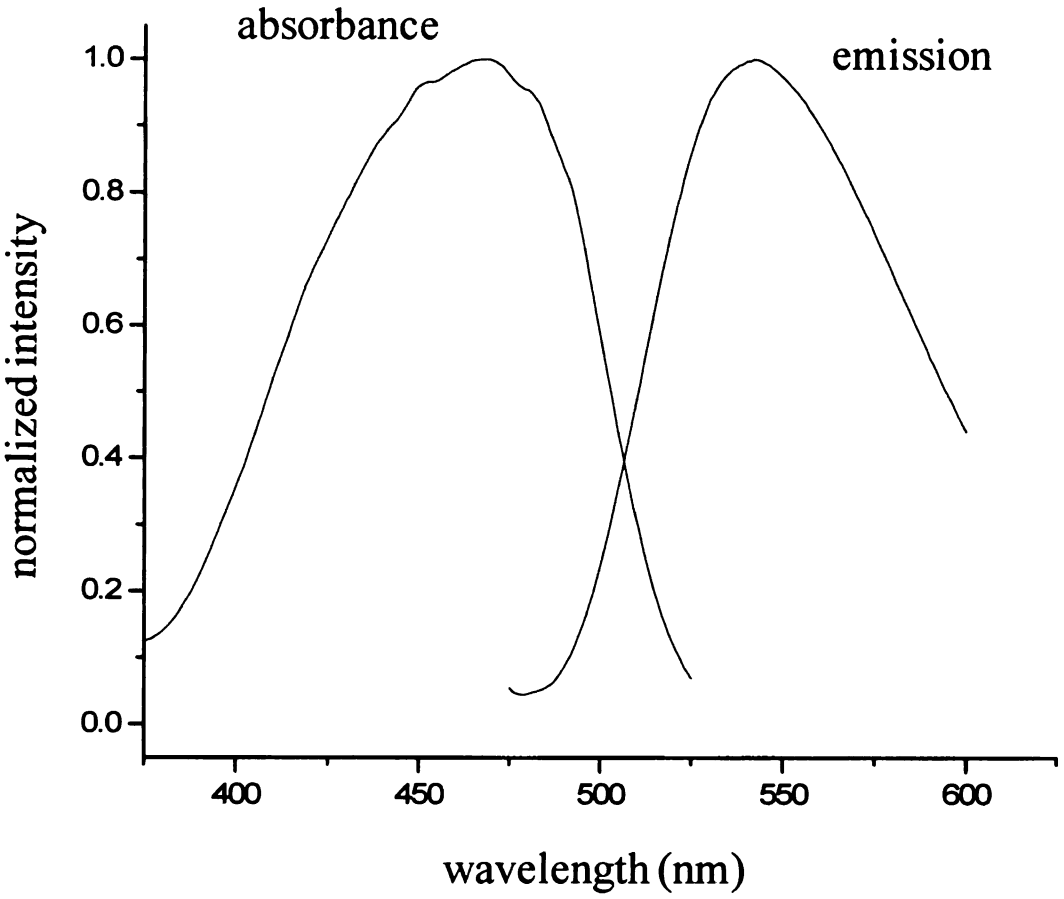

Figure 2.1. Solution phase absorption and emission spectra of NBD-PC and DOPC vesicles. Spectra have been normalized for clarity of presentation.

Time-resolved fluorescence measurements. Time-domain polarized fluorescence intensity decays were acquired using a time-correlated single-photon counting (TCSPC) system. This system has been described in detail elsewhere,[14,15] and we present only a brief recap of the essential features here. The light source is a CW mode-locked Nd:YAG laser (Coherent Antares 76-s) that produces 100 ps 1064 nm pulses at 76 MHz repetition rate. The third harmonic of the Nd:YAG laser output is used to excite a cavity-dumped dye laser (Coherent 702-2) operated with Stilbene 420 dye (Exciton) at 460 nm. The average output power of this laser is approximately 25 mW, with 5 ps pulses at a 4 MHz repetition rate. The sample fluorescence emission is measured with a microchannel plate photomultiplier tube (MCP-PMT, Hamamatsu R3809U-51). The electronics used to temporally resolve the fluorescence transients included a constant fraction discriminator (CFD, Tennelec 454) and a time-to-amplitude converter/biased amplifier (TAC, Tennelec 864). The collection wavelength (545 nm, 10 nm detection bandwidth) and polarization were computer controlled using LabVIEW® 7.1 code. The fluorescence lifetime data were collected at 54.7° with respect to the vertical excitation polarization, while the reorientation data were collected at polarizations parallel (0°) and perpendicular (90°) to the vertically-polarized incident light.

Fluorescence Recovery After Pattern Photobleaching (FRAPP). FRAPP was used to measure lateral diffusion coefficients of fluorescently-tagged lipids in supported bilayer lipid membranes (sBLMs) on fused silica microscope slides. The experimental setup consists of a double syringe pump system (Harvard Apparatus, Model 551382) used to simultaneously infuse and withdraw solutions from a custom made 1 mL flow

cell, an inverted microscope (Zeiss Axiovert 135M, Carl Zeiss, Thornwood, NY) with a 32X objective lens (Carl Zeiss, Thornwood, NY), an argon ion laser (95 Lexel Laser, Fremont, CA), a side-on photomultiplier tube (Hamamatsu R4632, Bridgewater, NJ), a photon counter (SR400 Stanford Research Systems, Sunnyvale, CA), and a fast preamplifier (SR445 Stanford Research Systems, Sunnyvale, CA). The 488 nm laser line was directed through a 5X beam expander (Edmund Optics, Inc., Barrington, NJ), a system of optical flats[16] used to toggle between a low intensity (20μW) monitoring beam for continuous fluorescence detection and a high intensity (500mW) beam for photobleaching of fluorophores. A Ronchi ruling (50 lines per inch, Edmund Optics, Inc., Barrington, NJ) was placed in the back image plane of the microscope to create a fringe pattern on the silica slide. The beam was then directed through a filter cube (Ex: 450-490/DM: 510/ Em: 515-565*)*. An aperture placed in the image plane in front of the PMT was used to restrict the observation area. Thus, the illuminated area was approximately 200 μm, while the observed area was 75 μm. This was done to prevent unbleached fluorophores from outside of the patterned area from reaching the observation zone during fluorescence recovery measurements. Stripe periodicity in the sample plane was 25 μm.

Deposition of Supported Lipid Bilayers (sBLMs). Fused silica microscope slides (75x25x1 mm) were purchased from Technical Glass Products, Inc. (Paineville, OH). The substrates were cleaned by bath sonication (Branson 1510, Branson Ultrasonic Corporation, Danbury, CT) in detergent solution for 20 minutes, rinsed with DI water, baked at 160°C for 4 hours and plasma treated (Harrick Plasma, Ithaca, NY) with oxygen

under vacuum (200 mTorr) for 10 minutes immediately before bilayer deposition. Supported bilayer lipid membranes (sBLMs) were deposited by vesicle fusion in a custom made flow cell. The flow cell was initially washed with buffer, followed by one hour incubation with liposome solution and a final buffer wash to remove any unadsorbed liposomes. All experiments were performed at room temperature.

Results and Discussion

The purpose of this work was to compare two methods of liposome preparation, extrusion and bath sonication, to determine if the method of preparation affects the physical and dynamical properties of the resulting liposomes. DOPC was chosen as the primary lipid in our studies because of its low transition temperature (-20°C),[17] ensuring that the resulting lipid bilayers are fluid at room temperature. The specific choice of chromophore (NBD-PC, 18:1 – 12:0) was made to ensure structural similarity to the phospholipid to which it is tethered (DOPC, 18:1). In addition, there is a significant body of knowledge extant on the properties of this chromophore,[18-20] making it an attractive choice for probing our structures.

We were primarily concerned with three issues in this work: the physical attributes (mean diameter and size distribution) of liposomes formed by the two methods, the molecular scale environment of the lipids comprising the liposomes, and the fluidity of bilayer structures resulting from the two liposome-forming methods. We are also concerned with how incorporating cholesterol in the liposome affects each of these issues. We expected that there would be a marked change in the organization of the liposomes and bilayer lipid membranes on a molecular scale with the addition of this component. We consider each of these issues individually.

Liposome mean diameter and size distribution. We used TEM and DLS to evaluate the mean diameter and size distribution of liposomes formed by extrusion and sonication. TEM images (Figures 2.2a and 2.2b) indicated liposomes formed by the two

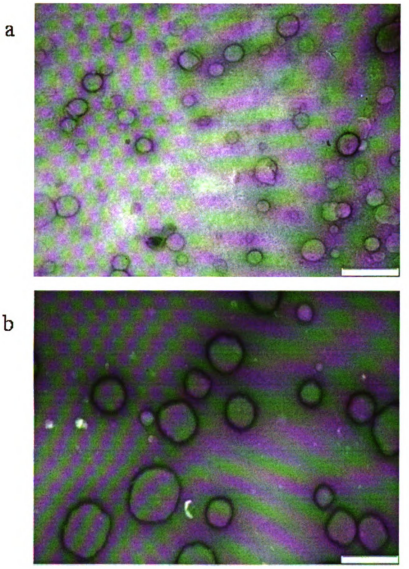

Figure 2.2. TEM images of vesicles produced by extrusion and sonication. (a) Extruded vesicles without cholesterol. (b) Sonicated vesicles without cholesterol. The scale bar is 500 nm in both images.

methods are both unilamellar in structure. However, while these images are useful in comparing relative sizes of liposomes, they provide little utility in evaluating absolute sizes because the liposomes may be distorted by the vacuum and the high energy electron beam used in imaging could, in principle, damage liposome structures. Such distortions may appear in the form of non-spherical structures (Figures 2.2a and 2.2b). An additional issue is that, while appealing from a visual perspective, TEM data do not lend themselves readily to the evaluation of the size distribution of the liposomes. To address these issues, we also characterized our liposomes by dynamic light scattering (DLS), a technique that measures the diameter of particles suspended in solution. Because DLS collects scattering information on an ensemble of particles, it is a relatively simple matter to obtain information on the particle size distribution.[21-24]

The mean diameters of vesicles formed by extrusion were 112 ± 6 nm with cholesterol and 112 ± 6 nm without cholesterol (Table 2.1). Thus cholesterol has no apparent influence on the sizes of liposomes formed by extrusion. This is not surprising since we expected that the extruded vesicles would be close to 100 nm in diameter with or without cholesterol, based on the sizes of pores in the polycarbonate membranes used to prepare them.[5-10] On the other hand, the results for liposomes formed by sonication gave values of 28 ± 2 nm without cholesterol and 64 ± 3 nm with cholesterol, showing significant cholesterol influence on size. While the ultimate sizes of sonicated vesicles were smaller than those from extrusion, this can controlled by the sonication time.[11] We also note that liposomes formed by sonication had a bimodal size distribution with or without cholesterol, and liposomes formed by extrusion also had a bimodal size

Table 2.1. Dynamic Light Scattering (DLS) results for the extruded and sonicated liposomes. Uncertainties in the data are estimated to be ± 5% of the average values.

	Average diameters of extruded liposomes (nm)	Average diameters of sonicated liposomes (nm)
DOPC / NBD-PC	112 ± 6	28 ± 2 and 196 ± 10
DOPC / cholesterol / NBD-PC	112 ± 6 and 600 ± 30	64 ± 3 and 259 ± 13

distribution if they contained cholesterol (Table 2.1). It is not clear if there is a compositional difference between vesicles in the two distribution zones, an issue that is currently under investigation. The physical size and distribution information is not necessarily correlated with the molecular scale properties of the bilayer structures.

Molecular-scale motion in the bilayers. To gain information on the molecular scale dynamical properties of the liposomes, we have measured the fluorescence lifetime and induced orientational anisotropy of the tethered NBD chromophores contained within the bilayer structures. The data provided by lifetime and anisotropy measurements are different but complementary. For all of the liposome systems examined here (sonicated and extruded, with and without cholesterol), we observed a fluorescence population decay that can be fitted with a two-component exponential model. For a chromophore such as NBD, the observation of multiple lifetime components is indicative of the existence of at least two environments that do not exchange population on the timescale of the excited state relaxation. This behavior has been reported for NBD tethered to phospholipids in a variety of environments,[25-30] and we interpret it in the following context. The fluorescence lifetime of NBD is sensitive to the polarity of its immediate environment, where the shorter lifetime corresponds to the NBD chromophore existing in a more polar environment.[31] For NBD chromophores tethered to the acyl chain of a phospholipid, it has been established that the chromophore can "loop back" to position itself in close proximity to the polar headgroup region of the bilayer in which it resides.[18-20,32] The longer lifetime component in this model corresponds to the NBD chromophore residing closer to the nonpolar region of the lipid bilayer. The fact that we observe two

lifetime values that differ by more than 4500 ps while the proposed environments for NBD are only separated by a few Ångströms is consistent with the chromophore existing in a dielectric gradient that changes substantially over the length scale of the chromophore itself.[33,34] Thus, our lifetime results are consistent with previous reports and this information, combined with the recovery of a single anisotropy decay time constant for each system (*vide infra*) points to the chromophore residing in a range of locations, all in close spatial proximity to the bilayer polar head groups.

For the anisotropy decay measurements reported here, the chemical information contained in these experiments is in the form of the decay functionality of R(t), (Eq. 2.1).

$$R(t) = \frac{I_{\parallel}(t) - I_{\perp}(t)}{I_{\parallel}(t) + 2I_{\perp}(t)} \tag{2.1}$$

where $I_{\parallel}(t)$ and $I_{\perp}(t)$, are the emission intensities polarized parallel and perpendicular to the vertically polarized incident excitation pulse, respectively. In our experiments, the NBD chromophore was tethered to a membrane bilayer constituent, and the anisotropy decay for this system was treated in the context of the hindered rotor model.[35-38] The tethered NBD chromophore does not have the structural freedom to orientationally re-randomize fully within its environment following excitation, which gives rise to an infinite time anisotropy, $R(\infty)$. For such systems, the function R(t) exhibits is governed by Eq. 2.2,

$$R(t) = R(\infty) + (R(0) - R(\infty))\exp(-t/\tau_{HR}) \tag{2.2}$$

where $R(\infty)$ is the infinite time anisotropy and R(0) is the zero time anisotropy. The value of R(0) is determined by the angle between the excited and emitting transition

dipole moments of the chromophore and R(∞) serves as a gauge for the orientational confinement that the chromophore experiences. The term τ_{HR} is related to the orientational relaxation of the chromophore within its confining volume, and is approximated by Eq. 2.3,[38,39]

$$\tau_{HR} = \frac{7\theta_0^2}{24 D_w} \tag{2.3}$$

where θ_0 is the semi-angle of the confining cone. The semi-angle of the confining conic volume of the chromophore is related to the zero- and infinite-time anisotropies by Eq. 2.4,[39]

$$\left[\frac{R(\infty)}{R(0)}\right]^{1/2} = 0.5\left(\cos\theta_0\left(1+\cos\theta_0\right)\right) \tag{2.4}$$

where the values of R(∞) and R(0) are determined from the experimental data. We have determined the values for θ_0 for the extruded and sonicated vesicles, both with and without cholesterol (Tables 2.2 and 2.3). For each of the systems tested, the cone angles are the same within experimental uncertainty, regardless of the method of vesicle preparation. We note that, for the systems containing cholesterol, the recovered cone angles are measurably smaller (ca. 60° vs. ca. 40°) for both the extruded and sonicated liposomes in comparison to the systems containing only the phospholipid and the chromophore. This finding is consistent with literature reports indicating that the addition of cholesterol to a bilayer serves to make the bilayer less fluid.[40-44] Our data point to not only a slightly longer reorientation time for the cholesterol-containing system, but also a more restricted volume (θ_0). From these data we find $D_w \sim 100$ MHz

Table 2.2. Results from Time Correlated Single Photon Counting (TCSPC) studies using extruded and sonicated liposomes with DOPC and NBD-PC.

	DOPC / NBD-PC				
	τ_1 (ps)	τ_2 (ps)	τ_{HR} (ps)	θ_0(°)	D_w (MHz)
Extruded	1547 ± 143	6014 ± 57	3025 ± 215	62 ± 5	113 ± 27
Sonicated	1931 ± 261	6098 ± 73	2944 ± 94	57 ± 5	98 ± 21

Table 2.3. Results from Time Correlated Single Photon Counting (TCSPC) studies using extruded and sonicated liposomes with DOPC, cholesterol and NBD-PC.

	DOPC / cholesterol / NBD-PC				
	τ_1 (ps)	τ_2 (ps)	τ_{HR} (ps)	θ_0(°)	D_w (MHz)
Extruded	1671 ± 92	6041 ± 81	3591 ± 277	42 ± 3	44 ± 10
Sonicated	2299 ± 182	5909 ± 104	3002 ± 220	37 ± 2	41 ± 8

for the phospholipid bilayer with no cholesterol, and $D_w \sim 45$ MHz with the addition of cholesterol. It is interesting to note that there is an apparent difference in the reorientation times for the cholesterol-containing liposomes. This difference in time constant, while suggestive of a different environment formed by the two methods, cannot be taken simply at face value. The observed time constant is related to both the confining cone angle and to the "wobbling" diffusion coefficient, D_w. The cone angles recovered for these two liposomes are the same to within experimental uncertainty, and when the fundamental quantity D_w is extracted from the θ_0 and τ_{HR} data, we find that there is no statistically discernible difference for the liposomes formed by extrusion vs. those by sonication.

It is important to emphasize that, in all of the anisotropy data we do not find any measurable difference between the molecular environments of the liposomes formed by extrusion and sonication. While there is a slight difference in the fast component of the NBD fluorescence lifetime for sonicated vs. extruded liposomes containing cholesterol, this finding is not reflected in the anisotropy decay dynamics, which are arguably a more sensitive probe of the local environment of the chromophore. With this information, we turn next to the translational diffusion behavior of the tethered chromophore in planar lipid bilayers formed from each type of liposome.

Translational diffusion in the bilayers. Measurement of translational diffusion in a sBLM provides information on the mobile fraction and diffusion coefficient of lipids within the membrane. It is not possible to directly quantitate the translational motion of

chromophores while embedded in liposomes. Therefore, to measure the translational diffusion of chromophores, it is common to reconstitute the liposome in the form of sBLMs on a planar substrate such as fused silica. The transformation of liposomes to planar bilayer lipid membranes is accomplished by a series of steps that include vesicle adsorption, vesicle surface and vesicle-vesicle interactions and vesicle fusion.[45-47] Once the bilayer is formed on a planar substrate, fluorescence recovery after pattern photobleaching (FRAPP) measurements can be used to characterize the translational motion of the chromophores. In such measurements, a selected region of the planar bilayer is exposed to intense electromagnetic radiation, causing photodegradation of chromophores in the illuminated region. Following photobleaching, the recovery of fluorescence intensity in the bleached region occurs at a rate determined by the translational diffusion coefficient of the chromophore.

In our FRAPP protocol, a Ronchi ruling placed in the rear image plane of the microscope projects a pattern of alternating dark and bright fringes on the sample plane. The recovery of fluorescence emission intensity in the sample following photobleaching provides information about the diffusion of the fluorescent probe.[48] Figure 2.3 shows a fluorescence recovery curve obtained for a supported lipid bilayer of DOPC containing NBD-PC as a fluorescent probe. The equation describing pattern photobleaching recovery in this system is[49]

$$f(t) = f(0) + \frac{m}{2}\left[1 - f(0)\right]\left[1 - \left(\frac{8}{\pi^2}\right)\left\{\exp\left(-\frac{4\pi^2 Dt}{a^2}\right) + \frac{1}{9}\exp\left(-\frac{36\pi^2 Dt}{a^2}\right)\right\}\right] \qquad (2.5)$$

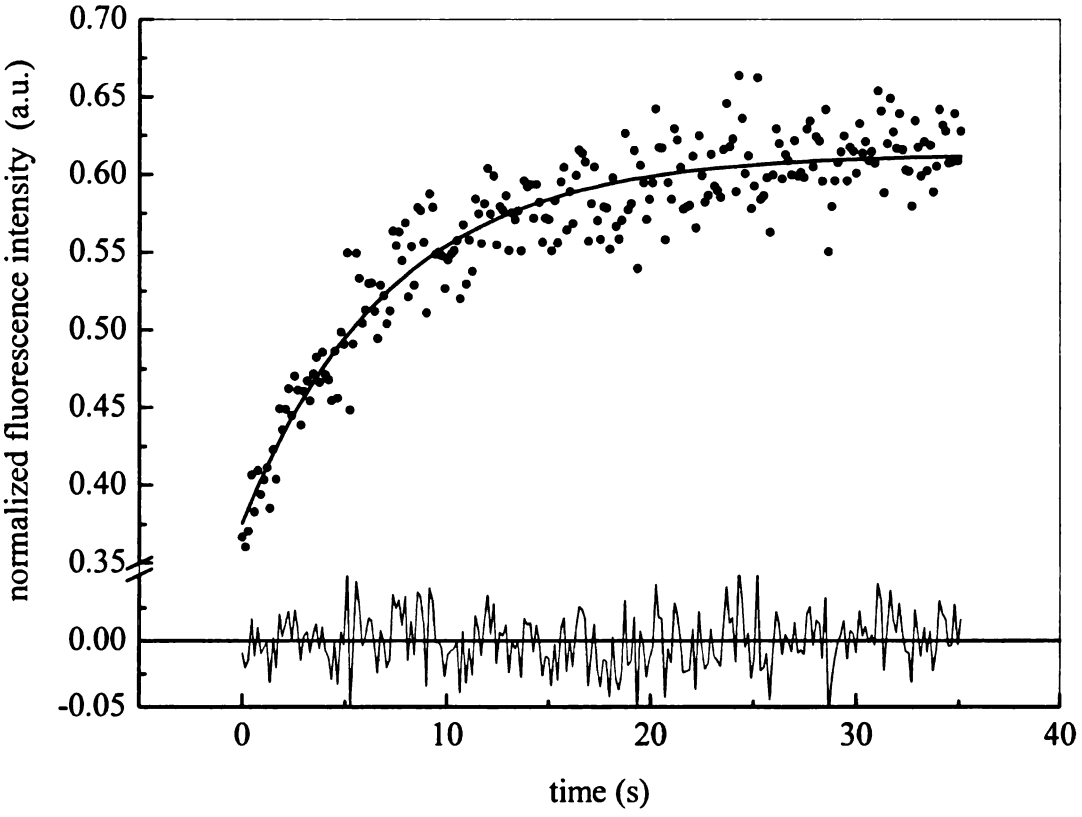

Figure 2.3. Representative plot of a FRAPP recovery curve for a DOPC/NBD-PC supported bilayer membrane.

where $f(t)$ is the post-bleach fluorescence ($t>0$) normalized with respect to the constant pre-bleach fluorescence ($t<0$), with $t=0$ being the time of the bleach pulse, D is the average diffusion coefficient of the fluorophores, and m is the mobile fraction. The parameter a is the stripe periodicity of the Ronchi ruling in the sample plane, 25 μm in our experiments. Equation 2.5 was fitted to the FRAPP data for each of the systems, and the average best-fit values of D and m were obtained (Tables 2.4 and 2.5). The physical significance of these quantities is that D is the translational diffusion coefficient, a direct measure of molecular mobility on mesoscopic length scales, and m is the mobile fraction of the chromophore. These data provide two important pieces of information (Tables 2.4 and 2.5). The first is that, for a given liposome composition, the fitted values of D and m are the same for liposomes made by extrusion and sonication. Thus, differences in size between liposomes prepared by extrusion and sonication do not seem to affect the fluidity of the resulting bilayer membranes. This corroborates evidence from a quartz crystal microbalance (QCM) study showing that liposomes ranging in size from 25 nm to 200 nm can form viable bilayer lipid membranes.[50] The second important finding is that, as expected, the presence of cholesterol in the bilayer serves to make the chromophore less mobile (i.e. less fluid). This result is fully consistent with the anisotropy decay data presented above, as well as previous findings that the addition of cholesterol to a phospholipid bilayer decreases the translational diffusion of the lipid.[51]

Table 2.4. Results from Fluorescence Recovery After Pattern Photobleaching (FRAPP) using supported bilayer membranes from extruded and sonicated vesicles. The samples contained DOPC and NBD-PC.

	Diffusion coefficient (10^{-8} cm^2 s^{-1})	Mobile fraction of NBD-PC (%)
Extruded	2.24 ± 0.25	78 ± 18
Sonicated	2.02 ± 0.15	81 ± 11

Table 2.5. Results from Fluorescence Recovery After Pattern Photobleaching (FRAPP) using supported bilayer membranes from extruded and sonicated vesicles. The samples contained DOPC, cholesterol and NBD-PC.

	Diffusion coefficient (10^{-8} cm^2 s^{-1})	Mobile fraction of NBD-PC (%)
Extruded	1.65 ± 0.22	73 ± 10
Sonicated	1.72 ± 0.04	69 ± 6

Conclusions

The goal of this study was to compare the properties of liposomes prepared by sonication to those prepared by extrusion on several length scales. Our findings demonstrate that, while the physical appearance, mean diameter and size distributions of the liposomes do indeed depend on the manner by which they are prepared, the molecular and nanoscale organization of the bilayers, as sensed through the dynamics of a tethered chromophore, does not depend on the manner of liposome formation. Liposomes formed by the two schemes were characterized in solution and in planar supported lipid membranes formed via liposome fusion on a fused silica substrate. The effect of cholesterol on the properties of the liposomes and supported lipid bilayers was also evaluated. Our data clearly show that whether the liposomes are formed by sonication or extrusion does not affect the molecular scale organization of these systems. Rather, the molecular scale organization of the bilayers is determined by interactions between the constituent species, which themselves do not depend on the manner in which the bilayer is formed. This finding indicates that, all other factors being equal, data on bilayer systems formed by sonication can in fact be compared directly to data on bilayer systems formed by extrusion.

Literature Cited

(1) Manconi, M.; Isola, R.; Falchi, A. M.; Sinico, C.; Fadda, A. M. *Colloids and Surfaces, B: Biointerfaces* **2007**, *57*, 143.

(2) Wang, S.; Huang, J.; Song, Q.; Fu, H. *Journal of Colloid and Interface Science* **2007**, *311*, 296.

(3) Kim, S. H.; Haimovich-Caspi, L.; Omer, L.; Talmon, Y.; Franses, E. I. *Journal of Colloid and Interface Science* **2007**, *311*, 217.

(4) Chen, K.; Luo, W.; Rahman, Z. U.; Guo, Y.; Schulte, A. *Journal of Dispersion Science and Technology* **2007**, *28*, 471.

(5) Driessen, A. J.; van den Hooven, H. W.; Kuiper, W.; van de Kamp, M.; Sahl, H. G.; Konings, R. N.; Konings, W. N. *Biochemistry* **1995**, *34*, 1606.

(6) Hunter, D. G.; Frisken, B. J. *Biophysical Journal* **1998**, *74*, 2996.

(7) MacDonald, R. C.; MacDonald, R. I.; Menco, B. P.; Takeshita, K.; Subbarao, N. K.; Hu, L. R. *Biochimica et Biophysica Acta* **1991**, *1061*, 297.

(8) Mayer, L. D.; Hope, M. J.; Cullis, P. R. *Biochimica et Biophysica Acta* **1986**, *858*, 161.

(9) Subbarao, N. K.; MacDonald, R. I.; Takeshita, K.; MacDonald, R. C. *Biochimica et Biophysica Acta* **1991**, *1063*, 147.

(10) Unger, E. C.; MacDougall, P.; Cullis, P.; Tilcock, C. *Magnetic Resonance Imaging* **1989**, *7*, 417.

(11) Maulucci, G.; De Spirito, M.; Arcovito, G.; Boffi, F.; Castellano, A. C.; Briganti, G. *Biophysical Journal* **2005**, *88*, 3545.

(12) Feitosa, E.; Barreleiro, P. C. A.; Olofsson, G. *Chemistry and Physics of Lipids* **2000**, *105*, 201.

(13) Cornell, B. A.; Fletcher, G. C.; Middlehurst, J.; Separovic, F. *Biochimica et Biophysica Acta, Biomembranes* **1982**, *690*, 15.

(14) DelaCruz, J. L.; Blanchard, G. J. *Journal of Physical Chemistry B* **2003**, *107*, 7102.

(15) DeWitt, L.; Blanchard, G. J.; LeGoff, E.; Benz, M. E.; Liao, J. H.; Kanatzidis, M. G. *Journal of the American Chemical Society* **1993**, *115*, 12158.

(16) Gajraj, A.; Ofoli, R. Y. *Langmuir* **2000**, *16*, 4279.

(17) Schroeder, R.; London, E.; Brown, D. *Proceedings of the National Academy of Sciences of the United States of America* **1994**, *91*, 12130.

(18) Chattopadhyay, A.; London, E. *Biochimica et Biophysica Acta: Biomembranes* **1988**, *938*, 24.

(19) Fery-Forgues, S.; Fayet, J.-P.; Lopez, A. *Journal of Photochemistry and Photobiology A: Chemistry* **1993**, *70*, 229.

(20) Mazeres, S.; Schram, V.; Tocane, J.-F.; Lopez, A. *Biophysical Journal* **1996**, *91*, 327.

(21) Berne, B. J.; Pecora, R. *Dynamic Light Scattering - with Application to Chemistry, Biology and Physics*; Wiley: New York, 1976.

(22) Aragon, S. R.; Pecora, R. *Journal of Chemical Physics* **1976**, *64*, 2395.

(23) Hallett, F. R.; Craig, T.; Marsh, J.; Nickel, B. *Canadian Journal of Spectroscopy* **1989**, *34*, 63.

(24) Hupfeld, S.; Holsaeter, A. M.; Skar, M.; Frantzen, C. B.; Brandl, M. *Journal of Nanoscience and Nanotechnology* **2006**, *6*, 3025.

(25) Chattopadhyay, A.; London, E. *Biochimica et Biophysica Acta, Biomembranes* **1988**, *938*, 24.

(26) Chattopadhyay, A.; London, E. *Biochemistry* **1987**, *26*, 29.

(27) Huster, D.; Mueller, P.; Arnold, K.; Herrmann, A. *European Biophysics Journal* **2003**, *32*, 47.

(28) Huster, D.; Muller, P.; Arnold, K.; Herrmann, A. *Biophysical Journal* **2001**, *80*, 822.

(29) Mukherjee, S.; Raghuraman, H.; Dasgupta, S.; Chattopadhyay, A. *Chemistry and Physics of Lipids* **2004**, *127*, 91.

(30) Raghuraman, H.; Shrivastava, S.; Chattopadhyay, A. *Biochimica et Biophysica Acta, Biomembranes* **2007**, *1768*, 1258.

(31) Greenough, K. P.; Blanchard, G. J. *Journal of Physical Chemistry A* **2007**, *111*, 558.

(32) Feng, Z. V.; Spurlin, T. A.; Gewirth, A. A. *Biophysical Journal* **2005**, *88*, 2154.

(33) Kreiter, M.; Prummer, M.; Hecht, B.; Wild, U. P. *Journal of Chemical Physics* **2002**, *117*, 9430.

(34) Drexhage, K. H. *Proc. Int. Conf. Lumin.* **1970**, 693.

(35) Karpovich, D. S.; Blanchard, G. J. *Langmuir* **1996**, *12*, 5522.

(36) Kinosita, K., Jr.; Ikegami, A.; Kawato, S. *Biophysical Journal* **1982**, *37*, 461.

(37) Kinosita, K., Jr.; Kawato, S.; Ikegami, A. *Biophysical Journal* **1977**, *20*, 289.

(38) Szabo, A. *Journal of Chemical Physics* **1984**, *81*, 150.

(39) Lipari, G.; Szabo, A. *Biophysical Journal* **1980**, *30*, 489.

(40) Filippov, A.; Oradd, G.; Lindblom, G. *Biophysical Journal* **2003**, *84*, 3079.

(41) Kahya, N.; Schwille, P. *Journal of Fluorescence* **2006**, *16*, 671.

(42) Liu, J.; Yang, L. *Bioorganic & Medicinal Chemistry* **2006**, *14*, 2225.

(43) Nishimura, S. Y.; Vrljic, M.; Klein, L. O.; McConnell, H. M.; Moerner, W. E. *Biophysical Journal* **2006**, *90*, 927.

(44) Cullis, P. R. *FEBS Letters* **1976**, *70*, 223.

(45) Zhdanov, V. P.; Kasemo, B. *Langmuir* **2001**, *17*, 3518.

(46) Seifert, U.; Lipowsky, R. *Physical Review A: Atomic, Molecular, and Optical Physics* **1990**, *42*, 4768.

(47) Nollert, P.; Kiefer, H.; Jaehnig, F. *Biophysical Journal* **1995**, *69*, 1447.

(48) Smith, B. A.; McConnell, H. M. *Proceedings of the National Academy of Sciences of the United States of America* **1978**, *75*, 2759.

(49) Starr, T. E.; Thompson, N. L. *Biophysical Chemistry* **2002**, *97*, 29.

(50) Reimhult, E.; Hook, F.; Kasemo, B. *Journal of Chemical Physics* **2002**, *117*, 7401.

(51) Oradd, G.; Lindblom, G.; Westerman, P. W. *Biophysical Journal* **2002**, *83*, 2702.

Chapter 3

UNDERSTANDING INTERMOLECULAR INTERACTIONS IN UNILAMELLAR VESICLES COMPRISED OF MULTIPLE CONSTITUENTS

Introduction

Lipid bilayer structures play a critical role, either directly or indirectly, in essentially all cellular processes. A central issue in understanding the function of lipid bilayers is the structural relationship between different, phase-segregated regions of these complex structures. Plasma membranes are thought to contain one hundred or more different constituents, and at this point in time, understanding structure and dynamics in such a complex system is not a tractable problem. A substantial body of work has been performed on comparatively simple three-component model bilayer structures. Model bilayers containing a phospholipid, a sphingolipid and cholesterol have been shown to demonstrate phase segregation,[2-7] depending on the amount of each constituent, and this property has caused some to speculate on the relationship of such heterogeneous model systems to "lipid raft" structures[8-15] that are thought to exist in plasma membranes. In this work, we report on our initial efforts to understand how perturbations to one phase of these bilayer structures influence the organization and dynamics of other phases that coexist in the same system. Our data on the fluorescence lifetime, rotational motion and excitation transport behavior of chromophores tethered to specific bilayer constituents, point to the presence of structural perturbations in one region having an easily measurable effect on the other region(s). Our data on NBD-cholesterol also shed some

light on the orientation of this molecule within the bilayer structure, an issue that is unresolved at the present time despite significant, ongoing attention in the literature.[14,16-18]

For any chemical system, it is the interactions between molecules that determine both the microscopic and bulk properties. Lipid bilayers are interesting because they are both fluid and heterogeneous, and understanding the intermolecular interactions that are responsible for the existence of such structures remains to be achieved. For three-component systems containing phospholipids, sphingolipids and cholesterol, it is thought by some that the sphingolipids associate most closely with cholesterol owing to the ability of this family of lipids to form hydrogen bonds with the cholesterol hydroxyl functionality.[5] It is also important to consider the acyl chains of the phospholipids and sphingolipids because, depending on the extent of chain saturation, this region of the bilayer can exhibit significant organization, which can be perturbed by the introduction of unsaturations.[19] Indeed, it is the lipid acyl chain length and degree of unsaturation that is thought to determine the melting point of the resulting bilayer structure. Lipid headgroup structure can also influence lipid packing. Phosphatidylethanolamines, for example, have much higher phase transition temperatures and do not exhibit the same steric hindrance that the corresponding length phosphatidylcholines do, because of the small headgroup size and hydrogen-bonding capability of the former. The structural complexity of even relatively simple bilayer model systems requires that experiments be planned carefully if they are to distinguish between the different intermolecular interactions that collectively produce the mesoscopic behavior seen experimentally.

One of the first issues to be considered in the examination of a heterogeneous system is the extent to which the organization of one phase or region influences that of other phases in the overall system. To address this issue we use structurally well characterized chromophores that are covalently bound to bilayer constituents. This strategy is the same as that we have employed for "lock and key" interrogation of crystallization processes,[20] and is well established as a means of providing chromophore localization. We have studied the fluorescence lifetime, fluorescence anisotropy decay dynamics and excitation transport behavior of these localized chromophores to understand local organization and longer range order within lipid bilayer structures. We have incorporated selected chromophores into the bilayer regions of a series of unilamellar vesicles of varying composition. Phase separation in multi-component bilayer systems has been noted in a variety of bilayer structural motifs, including unilamellar vesicles with diameters comparable to those we use in this work.[11]

A key issue that we address in this work is in determining how to probe for the presence of such phase segregation in structures that are ca. 100 nm in diameter. Our fluorescence lifetime and anisotropy data indicate that the role of sphingomyelin (SPM) in mediating bilayer organization is not as significant as expected, and that the existence of chromophores in these bilayers can influence the dynamical properties of the bilayers themselves. While essentially any bilayer constituent can cause structural perturbations, the identity and location of the perturbing constituent play important roles in determining the consequences of the perturbation. Specifically, there is a clear correlation between the behavior of the chromophores imbedded in the cholesterol phase and the amount of

fluorophore-tagged lipid present in the phospholipid phase. Our data reveal interactions between tagged lipids in the phospholipid phase and provide insight into the structural details of the cholesterol phase.

Experimental

Vesicle Preparation. Powdered cholesterol, the phospholipid 1,2-dimyristoyl-*sn*-phosphatidylcholine (DMPC) and egg sphingomyelin (SPM) were purchased from Avanti Polar Lipids Inc. (Alabaster, AL) and used as received. The chromophores 25-(N-(7-nitrobenz-2-oxa-1,3-diazol-4-yl-methyl)amino)-27-norcholesterol (NBD-cholesterol) and 1,2-Dimyristoyl-*sn*-Glycero-3-Phosphoethanolamine-N-(Lissamine Rhodamine B Sulfonyl Ammonium salt), (Rhodamine-PE) were purchased from Avanti Polar Lipids Inc., and used as received. For each sample, the lipids, cholesterol, and optical probes were mixed in selected ratios and the chloroform solvent was evaporated. The samples all contained a total concentration of 33 mol% cholesterol (the sum of 32.5 mol% powdered cholesterol and 0.5 mol% NBD-cholesterol). Several different concentrations of SPM (0, 11, 22 and 33 mol%) were used, and for all of the resulting systems, the dynamical behavior of the NBD chromophore remained the same to within the experimental uncertainty for a given concentration of Rhodamine-PE. The rhodamine-PE concentration was varied between 0 and 1.0 mol%, and NBD cholesterol dynamics were found to depend sensitively on Rhodamine-PE concentration. The balance of the vesicle composition was comprised of the C_{14} phospholipid, DMPC. An appropriate volume of Tris® buffer (Sigma-Aldrich, Milwaukee, WI) was added to each mixture so that the final concentration of lipid in the mixture was 1 mg/mL. The buffer (10 mM, pH 7.8) was prepared using purified water from a Milli-Q Plus water purification system (Millipore, Bedford, MA). The mixtures were processed five times through a freeze-thaw-vortex cycle to ensure thorough mixing of the constituents. Each cycle involves

freezing the solution by immersion in liquid nitrogen for five minutes, followed by thawing via immersion in 60°C water (five minutes), and concluding with vortexing (2 minutes). After the freeze-thaw-vortex processing, the solutions were extruded once through two polycarbonate membrane filters with 400 nm diameter pores using a mini-extruder (Avanti Polar Lipids Inc.). The resulting extruded vesicle suspension was then extruded eleven times through two polycarbonate membranes (Avanti Polar Lipids Inc.) with a nominal pore diameter of 100 nm. The resulting solution contained vesicles with a size distribution centered around 100 nm as estimated from TEM data (Figure 3.1).[21-26]

Steady state spectroscopy. Absorption spectra were obtained using a Cary 300 UV-visible spectrophotometer. Quartz cuvettes with a 1 cm pathlength were used for all measurements. Background samples without the fluorophore were used for baseline correction because of scattering from the vesicle-containing solutions. NBD exhibits steady state absorption and emission features that depend sensitively on the chromophore local environment. The 480 nm band position we observe experimentally is fully consistent with the chromophore residing in a relatively nonpolar environment.[27]

Steady state fluorescence measurements were performed using a SPEX Fluorolog-3 spectrophotometer using 1 cm pathlength quartz cuvettes. Excitation and emission slits with a nominal bandpass of 3 nm were used for all experiments. For recording excitation spectra, the emission wavelength was kept fixed at 535 nm and experiments were performed at 298 K. Background intensities of samples in which NBD-cholesterol was not added were subtracted from each sample spectrum to cancel out any scattering contributions.

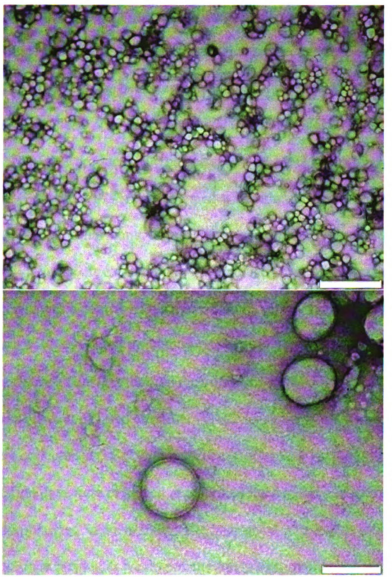

Figure 3.1. Transmission electron microscopy (TEM) image of a unilamellar vesicle. Top pane: Wide area view of aggregated vesicles. Scale bar = 1 μm. Bottom pane: Images of individual vesicles under higher magnification conditions. Scale bar = 200 nm.

Time-resolved fluorescence measurements. Time-domain fluorescence intensity decays were measured at a sample temperature of 27°C (above the melting transition temperature of DMPC, 24°C) using a time-correlated single-photon counting (TCSPC) system. This system has been described in detail elsewhere,[28,29] and we briefly recap its salient features here. The light source is a CW mode-locked Nd:YAG laser (Coherent Antares 76-s) that produces 100 ps pulses at a 76 MHz repetition rate. A cavity-dumped dye laser (Coherent 702-2) was operated with either Stilbene 420 dye (Exciton) and excited by the third harmonic of the source laser, or was operated with Pyromethene 567 dye (Exciton) and was excited by the second harmonic of the source laser. Sample fluorescence was detected with a microchannel plate – photomultiplier tube (MCP-PMT, Hamamatsu R3809U) and the electronics used to temporally resolve the fluorescence transients were a constant fraction discriminator (CFD, Tennelec 454) and a time-to-amplitude converter/biased amplifier (TAC, Tennelec 864). The fluorescence lifetime data were collected at 54.7° with respect to the vertical excitation polarization, while the reorientation data were collected at polarizations parallel and perpendicular to the vertically-polarized incident light. The instrument response function for this system is typically 35 ps fwhm and we do not attempt to deconvolute the response function from the recorded fluorescence transients.

Results and Discussion

The primary purpose of this work is to examine the dynamics of chromophores imbedded in specific bilayer regions and the interactions between different, spectrally overlapped chromophores where each is sequestered in a different bilayer phase. We are interested in establishing ways to probe local organization in structures on the order of 100 nm in diameter, with the goal being to elucidate structural heterogeneity on length scales that are well beneath the far field optical diffraction limit. We have used NBD-tagged cholesterol and a rhodamine-tagged C_{14} phospholipid (Figure 3.2), and find that the transient response of these chromophores individually, as well as the excitation transport dynamics between them, provides insight into the extent of organization within different regions of the bilayer structure. We have also examined the effect of sphingomyelin[8,10,12,13,30] in the bilayers on the dynamics of these chromophores, and find that the chromophore behavior is essentially sphingomyelin-independent.

The first chromophore we have used is 7-nitrobenz-2-oxa-1,3-diazol-4-yl (NBD). NBD is very weakly fluorescent in water, but in a hydrophobic medium such as a lipid bilayer, this chromophore exhibits a high fluorescence quantum yield;[31] the fluorescence lifetime of the NBD group is sensitive to the polarity of its environment.[32,33] In this work, we have used the NBD chromophore bound covalently to the aliphatic terminus of cholesterol, NBD-cholesterol (Figure 3.2). This probe has been used in a variety of bilayer studies, and there is an ongoing discussion in the literature regarding the orientation of this molecule in cholesterol-rich regions of the bilayers studied. Some reports indicate that the NBD chromophore is located closest to the polar phospholipid

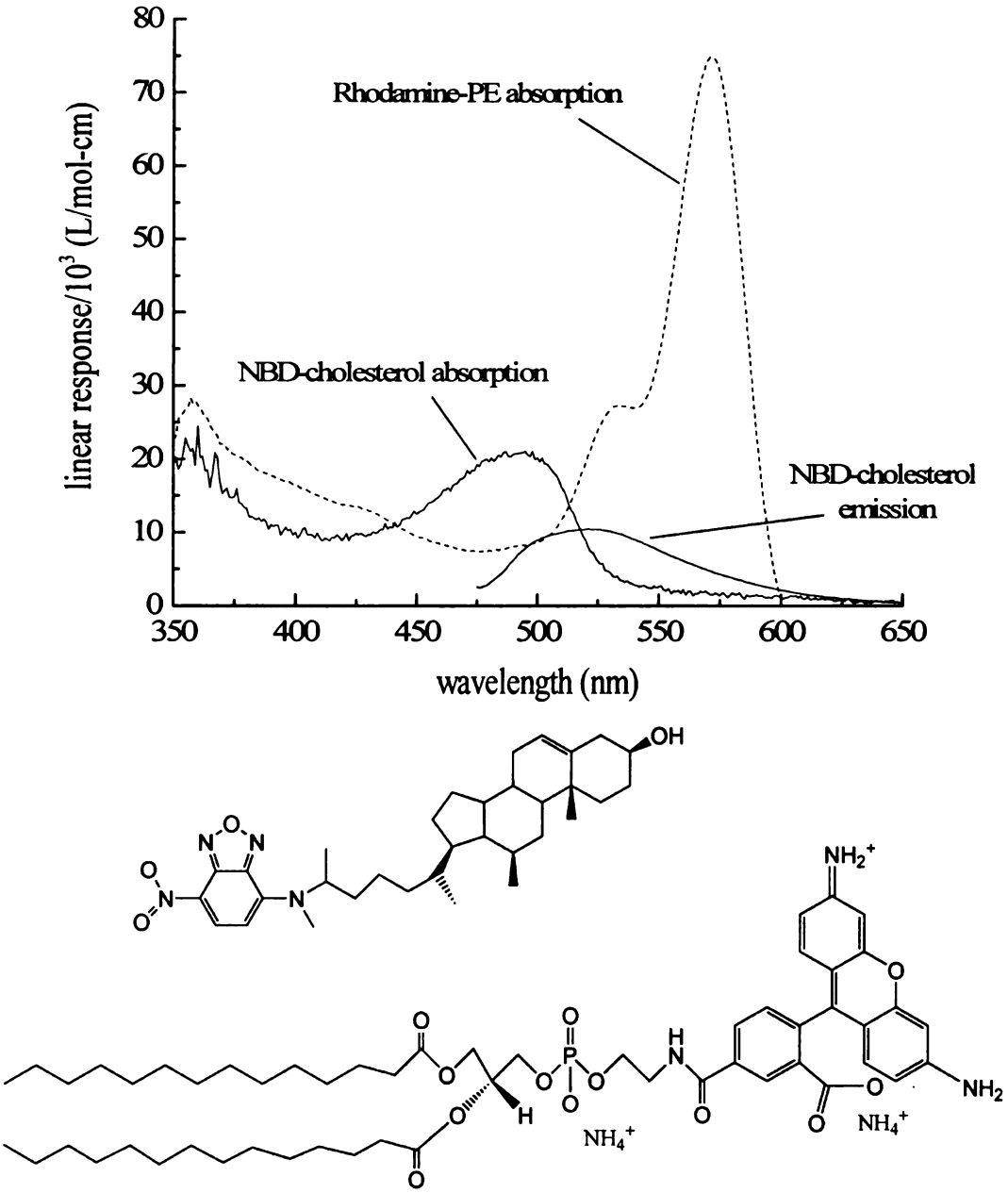

Figure 3.2. Top: Absorption and emission spectra of NBD-cholesterol, and the absorption spectrum of Rhodamine-PE, Tris® buffer. The spectra have been corrected for the extinction coefficients of the two compounds, and the fluorescence quantum yield of NBD-cholesterol is assumed to be 0.5 for the sake of presentation. Bottom: Structures of NBD-cholesterol and Rhodamine-PE.

head group region, with the cholesterol moiety oriented in opposition to that of native cholesterol.[14,17] There are also reports that indicate NBD is oriented in some systems such that the cholesterol moiety lies in correspondence with the other, non-substituted cholesterol molecules, positioning the chromophore within the nonpolar interior region of the bilayer.[16,18]

Our experimental data shed some light on this issue. Based on the fluorescence lifetime data ($\tau_{fl} \sim 2.8$ ns) and the functional form of the motional relaxation data (*vide infra*), we believe that the NBD-labeled cholesterol molecule is oriented such that the NBD moiety is sequestered within the nonpolar region of the membrane.[5] Specifically, our NBD-cholesterol fluorescence lifetimes in the absence of Rhodamine-PE are ca. 2.8 ns, and the anisotropy decay times are ca. 1.3 ns. In aqueous environments, NBD has a fluorescence lifetime that is typically hundreds of ps at most, and the reorientation times for this chromophore in an aqueous environment are on the order of 100 ps. Our lifetime data thus indicate a nonpolar environment and the reorientation data reveal a viscosity of ca. 10 – 15 cP, consistent with the interior of a bilayer membrane.[19,34] This orientation is consistent with the cholesterol –OH functionality being in contact with the polar solvent medium, where it is capable of participating in hydrogen bonding with phospholipids and sphingolipids.

In contrast to the NBD-cholesterol chromophore, there is less uncertainty with respect to the location of the rhodamine chromophore bound to DMPE because it is attached to the polar head group of the phospholipid (Figure 3.2). We thus expect it to

interact most strongly with the aqueous solvent in the immediate proximity of the bilayer head groups.

For fluorescence lifetime measurements of complex organic chromophores, there is not a single clear theoretical framework within which to interpret the data.[35-39] The fluorescence lifetime of NBD is sensitive to the polarity of its immediate environment, but there is little other than an empirical correlation to apply to the interpretation of such data. For systems where only one of the chromophores is present, we recover a single exponential fluorescence intensity decay, indicative of a single environment for each chromophore (Figure 3.3). For systems where both chromophores are present, we recover multiple exponential decay components under certain circumstances, and we understand this behavior in the context of Förster energy transfer between chromophores. The lifetime and reorientation behavior of NBD-cholesterol depend very sensitively on the amount of Rhodamine-PE present. The first issue to consider is excitation transport between the chromophores, as expected from their spectral overlap (Figure 3.2). We show in Figure 3.4 the fluorescence lifetime(s) and their fractional contributions as a function of Rhodamine-PE concentration in the bilayers. We understand these data as follows. Based on a significant body of data that exhibit phospholipid-cholesterol phase separation, we believe that our vesicles exhibit a non-homogeneous distribution of cholesterol within the bilayer.[2-7] It is known that even for small amounts of cholesterol and NBD-cholesterol in unilamellar vesicles that phase separation and organization occurs,[31] and our experimental results (*vide infra*) are fully consistent with that structural motif. While it would be ideal to have a direct measure of the morphology of our

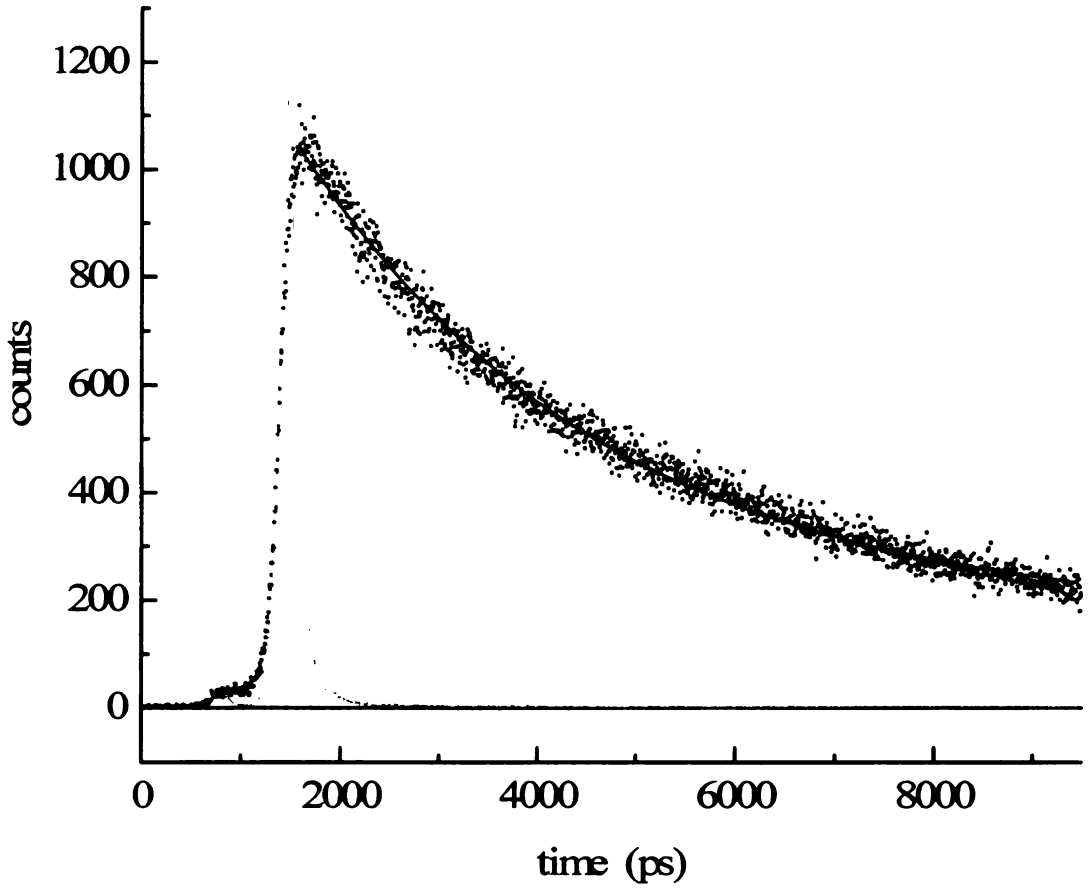

Figure 3.3. Fluorescence lifetime decay of NBD-cholesterol in a unilamellar vesicle containing 33 mol% cholesterol, 11 mol% sphingomyelin and 56 mol% DMPC. The recovered time constant of this decay is 3150 ± 30 ps.

vesicles, providing information such as the domain size of the phase separated regions, we do not have the capability of producing such data. Owing to the small size of the vesicles, far field optical microscopic techniques cannot provide adequate resolution. The creation of larger vesicles or the deposition of these bilayers onto a planar substrate may yield some information, but translational diffusion within such structures could serve to cloud the correspondence across bilayer structural formats. A significant goal of this work is to explore the utility of spectroscopic probes in providing structural information on vesicle structures of such small dimensions.

With the *ansatz* that NBD-cholesterol is located in the cholesterol-rich regions of the bilayers, and the Rhodamine-PE is located in the phospholipid regions, for low Rhodamine-PE concentrations there is only one NBD-cholesterol lifetime, which decreases with increasing Rhodamine-PE concentration. At 0.25 mol% Rhodamine-PE, we observe a change in decay functionality from one to two exponential components. We can interpret these data either in terms of induced structural heterogeneity in the system where the NBD chromophore finds itself distributed between two non-exchanging environments, or in terms of excitation transport. Because of the modest amounts of Rhodamine-PE used and the fact that the rhodamine chromophore resides beyond the polar head group region of the bilayer, we believe that structural perturbations to the acyl chain region of the bilayer will be minimal. Due to the extensive spectral overlap of the chromophores as well as the monotonic decreases in lifetime(s) with increasing optical acceptor concentration, we assert that these data are reflective of excitation transport in a

structurally heterogeneous system, where the short lifetime reflects efficient excitation transport when a Rhodamine-PE molecule is in close proximity to a cholesterol-rich region containing an NBD-cholesterol chromophore and the long lifetime data are related simply to the average distance between non-associated donor and acceptor species. Because the NBD-cholesterol fluorescence lifetime varies in a regular manner with the Rhodamine-PE concentration, we believe that the fast lifetime component contains information on the size of the cholesterol domains in which the NBD-cholesterol resides. For this system, the dominant mechanism for energy transfer to occur will be by dipolar coupling, as described by Förster, [40]

$$k_{DA} = \frac{\kappa^2 k_r^D}{n^4 R^6} \cdot 8.8x10^{17} \int \frac{\varepsilon_A(\bar{\nu}) f_D(\bar{\nu})}{\bar{\nu}^4} d\bar{\nu} = \frac{\kappa^2 k_r^D}{n^4} \left(\frac{R_0}{R} \right)^6 \qquad (3.1)$$

where k_{DA} is the rate constant for the transfer of energy from the donor to the acceptor. The κ term is a function of the geometric alignment of the donor and acceptor transition dipole moments, and for our experimental conditions, we approximate $\langle\kappa^2\rangle = 2/3$. While κ^2 can vary between 0 and 4, for our experimental geometries, κ^2 will lie in the region of 1. Lacking specific knowledge of the relative orientations of the donor and acceptor transition moments, we use the orientationally averaged value of $\kappa^2 = 2/3$. Any physically reasonable variations in κ^2 do not affect the interpretation of our data. The term k_r^D is the donor radiative decay rate constant in the absence of optical acceptor, n is the refractive index (n = 1.4, an approximate average of the organic (n~1.45), and the aqueous (n~1.33) regions of the bilayer) and R is the intermolecular D-A distance. The integral term is a measure of the spectral overlap between the emission spectrum of the

optical donor and the absorption spectrum of the acceptor. The spectral overlap term, combined with the several constants on the right hand side of Eq. 3.1 is typically referred to as the critical radius, R_0, a quantity which serves as an effective gauge of the range of this dipolar coupling process. We calculate R_0 for our donor-acceptor pair to be 51.4 Å, a value in good agreement with that of most organic chromophore pairs, ($R_0 \sim 50$ Å typically).[40-43] Based on this value of R_0, $k_r^D = 3.6 \times 10^8$ Hz, and k_{DA} between 1.8 and 2.2×10^9 Hz (the fast fluorescence lifetime range), we calculate R to be between 28.4 Å and 29.4 Å. If we had used a value of $\kappa^2 = 1$, the resulting R would be in the range of 30.4 to 31.4 Å, a difference that does not affect the physical picture of this system significantly. There are many geometric approximations that could be used to estimate the cholesterol domain size from this value of R, but if we presume these domains to be circular, R would approximate the radius of the circle. The area of the circle would thus be ca. 2500 $Å^2$. If the cholesterol molecules are stacked more or less end-on with respect to the plane of the circle, this area corresponds to ca. 100 molecules. For a circular domain of ca. 100 molecules, something on the order of 30 of these molecules will reside at the phase boundary, a structural situation that could influence the lifetime and dynamics of the NBD chromophore. Because of the size of the domains and translational motion within them, it is likely that the reorientation times we observe for this chromophore represent an average of interior and edge site dynamics. Given the time scales of the phenomena we report here, there will certainly be significant positional averaging of the NBD local environment due to diffusion within the cholesterol domains.

In the limit of acceptor molecules being distributed uniformly in the lipid phase, the Förster model predicts an increase in acceptor concentration would be related to the amount of Rhodamine-PE in closest proximity to the cholesterol-rich regions of the bilayers, yielding a monotonic relationship between acceptor concentration and fractional contribution of the fast decay to the overall NBD-cholesterol lifetime decay. The acceptor concentration-dependence of the lifetime pre-exponential factors, however, do not display this trend and are thus not consistent with a uniform distribution of acceptors in the lipid phase (Figure 3.4b). There could be several possible explanations for the decrease in the contribution from the fast lifetime component with increasing acceptor concentration, with the most likely being that chromophore-chromophore interactions of the Rhodamine-PE acceptor molecules is occurring in the phospholipid regions of the bilayer. This is a testable hypothesis.

To measure fluorescence anisotropy decays, we excite the samples with vertically polarized light and collect fluorescence transients polarized parallel ($I_{\parallel}(t)$) and perpendicular ($I_{\perp}(t)$) to the excitation polarization (Figure 3.5a). We construct the induced optical anisotropy function, R(t) from polarized emission intensity decays according to Eq. 3.2.

$$R(t) = \frac{I_{\parallel}(t) - I_{\perp}(t)}{I_{\parallel}(t) + 2I_{\perp}(t)} \tag{3.2}$$

The chemical information contained in these data resides in the decay functionality of R(t) (Figure 3.5b). For the experiments we report here, the chromophores are tethered to

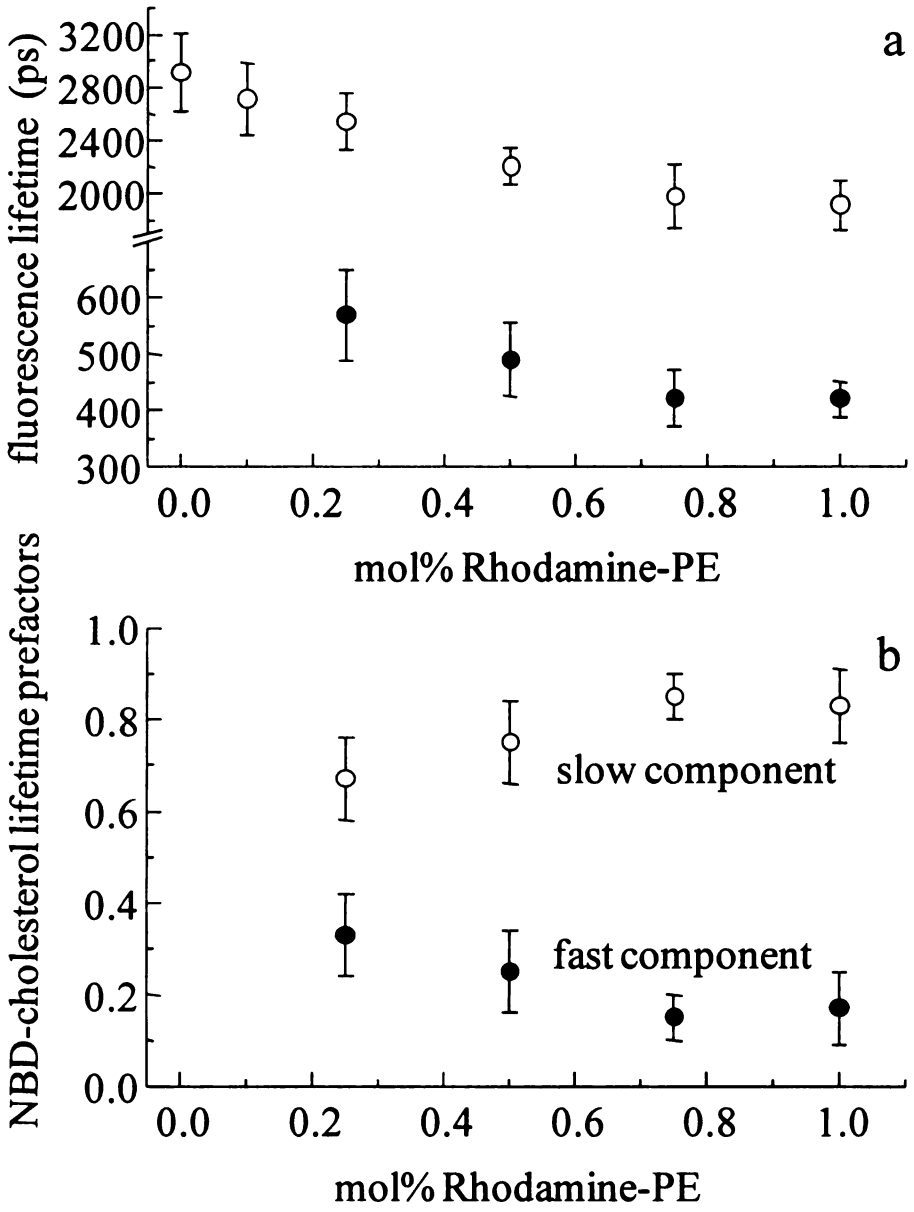

Figure 3.4. (a) Fluorescence lifetime(s) of NBD-cholesterol as a function of amount of Rhodamine-PE added to unilamellar vesicles. The appearance of two decay components is consistent with excitation transport in a heterogeneous system. (b) The fractional contribution of the fast fluorescent lifetime component of NBD-cholesterol as a function of Rhodamine-PE concentration.

membrane bilayer constituents, restricting degrees of freedom into which the initially anisotropic distribution can relax.

If Rhodamine-PE molecules are distributed uniformly in the phospholipid phase of the bilayer, over the concentration ranges we access, we should see no Rhodamine-PE concentration-dependence to its anisotropy decay. With interactions between acceptor chromophores, we would see the time constant for rhodamine chromophore motion increase with increasing Rhodamine-PE concentration, as is seen experimentally (Figure 3.6). Because the rhodamine chromophore is tethered to the polar head group of the phospholipid, and the dipolar and/or hydrogen bonding interactions between individual head groups dominate this region of the bilayer structure, a slowing of chromophore motion is associated with confinement. The NBD-cholesterol fluorescence lifetime data (Figure 3.4) and the Rhodamine-PE anisotropy data (Figure 3.6) are both consistent with the intermolecular interactions of the Rhodamine-PE chromophores in the phospholipid phase of the bilayer, where such interactions simultaneously slow the acceptor chromophore motion and increase the average donor-acceptor chromophore distance, thereby reducing the fractional contribution of the fast lifetime component.

As noted above, the rhodamine chromophore reorientation times increase with confinement because of their proximity to the polar head group region, where the lipid head groups interact strongly owing to dipolar and hydrogen-bonding interactions. The motional relaxation behavior of NBD-cholesterol appears to be different. As the concentration of Rhodamine-PE is increased to 1.0 mol% in the phospholipid phase, the

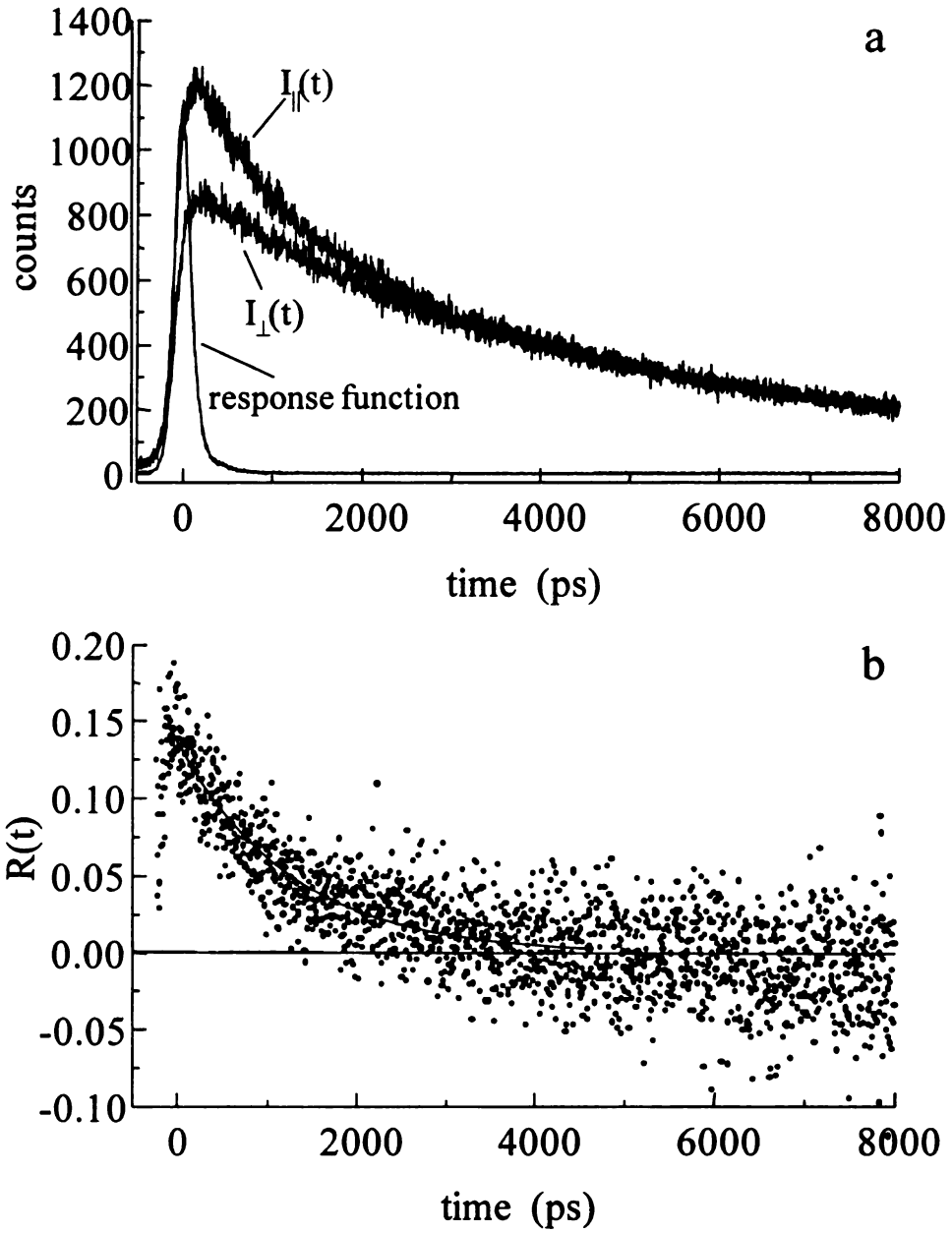

Figure 3.5. (a) Polarized emission transients for NBD-cholesterol in a unilamellar vesicle containing 33 mol% cholesterol, 11 mol% sphingomyelin and 56 mol% DMPC. The acquisition polarization of the transients is indicated in the figure relative to the vertical excitation pulse polarization. (b) Decay of the induced orientational anisotropy function, R(t), produced from the data shown in panel (a). The time constant of this anisotropy decay is 1362 ± 61 ps.

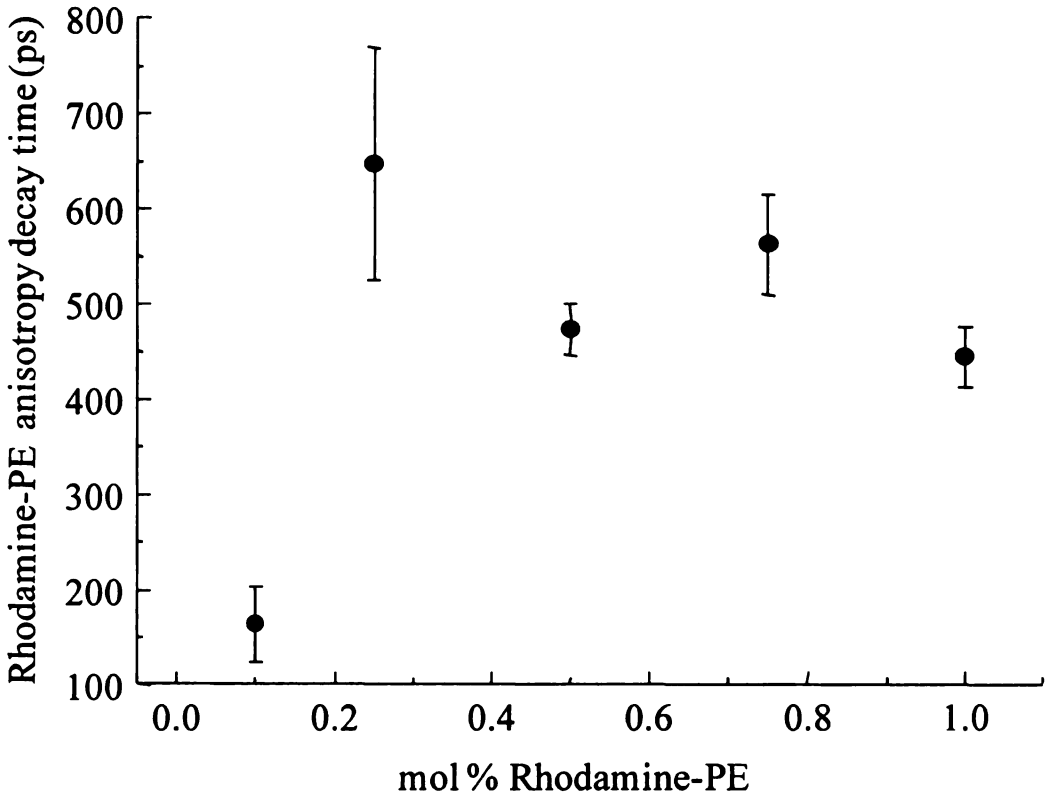

Figure 3.6. Dependence of Rhodamine-PE anisotropy decay time on Rhodamine-PE concentration.

reorientation dynamics of NBD-cholesterol become faster, exhibiting a feature analogous to a phase transition within the bilayer structure (Figure 3.7).

When confined within a membrane, a molecule is not free to sample all possible orientations with equal probability, and the hindered rotor model is appropriate for the treatment of such data.[44,45] For a planar membrane, R(t) does not decay to zero at long times; the residual steady state anisotropy results from the orientational constraints the membrane imposes on the chromophore. The hindered rotor model describes the motion of the restricted chromophore in the context of confinement within a conic volume of semiangle $2\theta_0$, where the angle θ is defined as the average tilt angle of the chromophore within the cone ($0° \leq \theta \leq 90°$).[44]

$$R(t) = R(\infty) + (R(0) - R(\infty))\exp(t/\tau) \tag{3.3}$$

The quantity τ contains information on the confining cone semi-angle θ_0 and the motion of the chromophore within the cone, D_w.

$$\tau = \frac{7\theta_0^2}{24D_w} \tag{3.4}$$

The quantity τ in Eq. 3.4 contains contributions from both θ_0 and D_w. Other work in our group has shown that both the structural freedom (θ_0) and effective rotor shape (Cartesian components of D_w) can vary with the composition of the bilayer.[34]

Previous work on the temperature-dependent reorientation of perylene sequestered in a DMPC bilayer showed a change in reorientation time by a factor of ca. 1.5 at the phase transition temperature for this lipid. The addition of 0.3 mol% of a DMPC analog with an unsaturation at the 9-position of the acyl chains yielded a 15

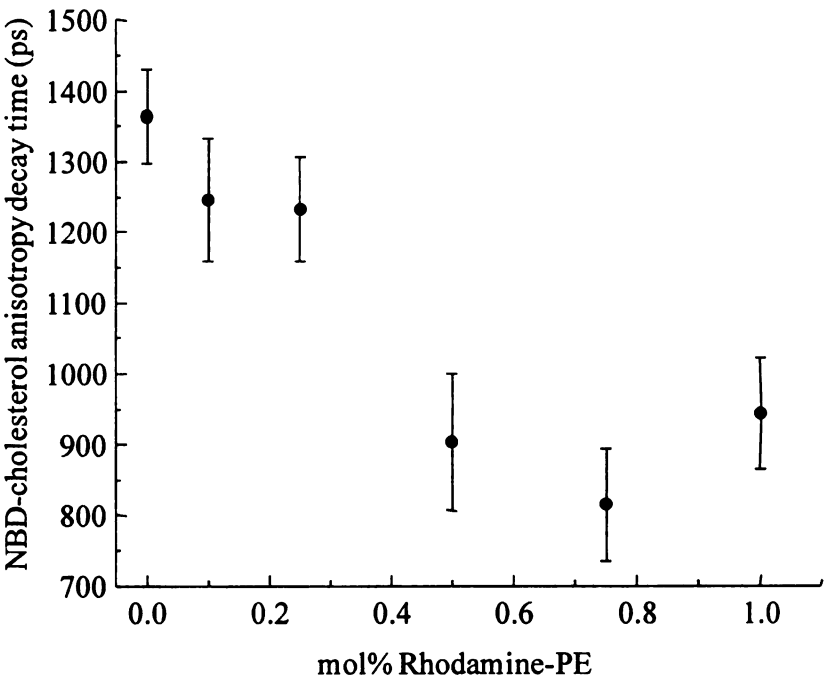

Figure 3.7. Dependence of NBD-cholesterol anisotropy decay time on Rhodamine-PE concentration.

degree reduction in phase transition temperature.[19] The presence of Rhodamine-PE affects the local environment of the NBD-cholesterol, as can be seen in the fluorescence anisotropy data (Figure 3.4). The functional form of the Rhodamine-PE concentration-dependence of NBD-cholesterol reorientation (at the fixed temperature of 27°C) resemble the phase transition data seen for perylene reorientation in DMPC vesicles. The phase transition for DMPC is known to be 24°C for the pure phospholipid,[46] and the addition of impurities lowers this phase transition temperature dramatically. If our data on NBD-cholesterol are indeed sensing a phase transition, it must be for a domain other than the phospholipids. We believe that we are sensing changes in the organization of the cholesterol-rich domains in these experiments. We understand this finding in the context of interacting Rhodamine-PE molecules producing "defect" sites in the lipid phase of the bilayer. The associated disorder of the lipid phase results in a corresponding change (loss) of order in the cholesterol phase.

It is tempting to estimate the viscosity of the bilayer region sensed by the NBD-cholesterol. Because we have not acquired fluorescence anisotropy data using both one- and two-photon excitation, it is not possible to determine the local viscosities unambiguously. If we assume that the NBD-cholesterol reorientation is characterized as a relatively spherical rotor, we can place bounds on the viscosity of the cholesterol-rich regions by comparing the experimental data to theoretical predictions. We have shown in earlier work that for the chromophore NBD tethered to a phospholipid acyl chain, the motional dynamics of this chromophore change significantly, from being a highly anisotropic rotor, with the dominant motion about its tethering bond in a pure

phospholipid bilayer, to being much closer to a spherical rotor in bilayers containing cholesterol.[34] Those data were obtained by direct comparison of one- and two-photon excited fluorescence anisotropy measurements, and we have not acquired the analogous information for the system under examination here. Nonetheless, this information suggests that the NBD chromophore reorients approximately as a spherical rotor in our systems. With this *ansatz*, we can estimate the rotational diffusion of NBD-cholesterol using the modified Debye-Stokes-Einstein equation.[47-49]

$$\tau_{OR} = (6D)^{-1} = \frac{\eta V f}{k_B T S} \tag{3.5}$$

This model has been discussed in detail before,[19,20,28,34] with the quantities η being solution viscosity, V representing solute hydrodynamic volume, f being the solvent-solute frictional interaction coefficient, and S representing the solute shape factor.

We estimate that the viscosity sensed by NBD-cholesterol varies from ca. 10 cP for low Rhodamine-PE concentrations to ca. 7 cP at higher Rhodamine-PE concentrations based on a comparison of the experimental data to values calculated from Eq. 3.5 (Table 3.1). This range of viscosities is reminiscent of our findings for DMPC bilayers in the region of their gel-to-fluid phase transition,[19] suggesting that both the lipid and cholesterol domains of model bilayer structures are similar in viscosity.

Table 3.1. Calculated viscosity dependence of the rotational diffusion coefficient and anisotropy decay time constant for NBD-cholesterol. The diffusion coefficients and reorientation times were calculated based on a hydrodynamic volume of 528 Å^3 [1] for the NBD-cholesterol molecule, f = 1, S = 1 and T = 298 K.

Viscosity (cP)	Rotational diffusion coefficient, D (Hz)	Reorientation time, τ_{OR} (ps)
5	2.60×10^8	640
7.5	1.73×10^8	960
10	1.30×10^8	1280
12.5	1.04×10^8	1600
15	8.68×10^7	1920

Conclusions

The data we have reported underscore the influence that comparatively small amounts of certain bilayer constituents can have on the overall properties of the system. These data are consistent with strong coupling between lipid- and cholesterol-rich phases determining the overall dynamics and fluidity of bilayer structures. Our fluorescence lifetime and anisotropy data indicate that the NBD chromophore tethered to cholesterol resides within the bilayer structure and that there is a significant dependence of the motional freedom of this chromophore on the composition of the phospholipid-rich regions of the bilayer. The rhodamine chromophore exists at the interface between the bilayer polar head groups and water, and our fluorescence anisotropy data for this chromophore indicates interactions between rhodamine chromophores even at relatively low concentrations. Such intermolecular interactions give rise to a step-wise change in the reorientation dynamics of the NBD-cholesterol chromophore that is reminiscent of a phase transition.

Literature Cited

(1) Edward, J. T. *Journal of Chemical Education* **1970**, *47*, 261.

(2) Keller, S. L. *Journal of Physics: Condensed Matter* **2002**, *14*, 4763.

(3) Keller, S. L. *Langmuir* **2003**, *19*, 1451.

(4) Keller, S. L.; McConnell, H. M. *Physical Review Letters* **1999**, *82*, 1602.

(5) Keller, S. L.; Radhakrishnan, A.; McConnell, H. M. *Journal of Physical Chemistry B* **2000**, *104*, 7522.

(6) Hinderliter, A.; Biltonen, R. L.; Almeida, P. F. F. *Biochemistry* **2004**, *43*, 7102.

(7) Sankaram, M. B.; Thompson, T. E. *Proceedings of the National Academy of Sciences of the USA* **1991**, *88*, 8686.

(8) Brown, D. A.; London, E. *Journal of Biological Chemistry* **2000**, *275*, 17221.

(9) de Almeida, R. F. M.; Loura, L. M. S.; Fedorov, A.; Prieto, M. *Journal of Molecular Biology* **2005**, *346*, 1109.

(10) de Almeida, R. F. M.; Fedorov, A.; Prieto, M. *Biophysical Journal* **2003**, *85*, 2406.

(11) De Almeida, R. F. M.; Loura, L. M. S.; Fedorov, A.; Prieto, M. *Biophysical Journal* **2002**, *82*, 823.

(12) Samsonov, A. V.; Mihalyov, I.; Cohen, F. S. *Biophysical Journal* **2001**, *81*, 1486.

(13) Wolf, C.; Koumanov, K.; Tenchov, B.; Quinn, P. J. *Biophysical Chemistry* **2001**, *89*, 163.

(14) Loura, L. M.; Fedorov, A.; Prieto, M. *Biochimica et Biophysica Acta* **2001**, *1511*, 236.

(15) McMullen, T. P. W.; Lewis, R. N. A. H.; McElhaney, R. N. *Current Opinion in Colloid & Interface Science* **2004**, *8*, 459.

(16) Chattopadhyay, A.; London, E. *Biochemistry* **1987**, *26*, 39.

(17) Chattopadhyay, A.; London, E. *Biochimica et Biophysica Acta* **1988**, *938*, 24.

(18) Scheidt, H. A.; Muller, P.; Herrmann, A.; Huster, D. *The Journal of Biological Chemistry* **2003**, *278*, 45563.

(19) Koan, M. M.; Blanchard, G. J. *Journal of Physical Chemistry B* **2006**, *in press*.

(20) Rasimas, J. P.; Berglund, K. A.; Blanchard, G. J. *Journal of Physical Chemistry* **1996**, *100*, 7220.

(21) Driessen, A. J.; van den Hooven, H. W.; Kuiper, W.; van de Kamp, M.; Sahl, H. G.; Konings, R. N.; Konings, W. N. *Biochemistry* **1995**, *34*, 1606.

(22) Mayer, L. D.; Hope, M. J.; Cullis, P. R. *Biochimica et Biophysica Acta* **1986**, *858*, 161.

(23) Unger, E. C.; MacDougall, P.; Cullis, P.; Tilcock, C. *Magnetic Resonance Imaging* **1989**, *7*, 417.

(24) Hunter, D. G.; Frisken, B. J. *Biophysical Journal* **1998**, *74*, 2996.

(25) MacDonald, R. C.; MacDonald, R. I.; Menco, B. P.; Takeshita, K.; Subbarao, N. K.; Hu, L. R. *Biochimica et Biophysica Acta* **1991**, *1061*, 297.

(26) Subbarao, N. K.; MacDonald, R. I.; Takeshita, K.; MacDonald, R. C. *Biochimica et Biophysica Acta* **1991**, *1063*, 147.

(27) Ladokhin, A. S. *Fluorescence Spectroscopy in Peptide and Protein Analysis*; John Wiley & Sons: Chichester, UK, 2000.

(28) DelaCruz, J. L.; Blanchard, G. J. *Journal of Physical Chemistry B* **2003**, *107*, 7102.

(29) DeWitt, L.; Blanchard, G. J.; LeGoff, E.; Benz, M. E.; Liao, J. H.; Kanatzidis, M. G. *Journal of the American Chemical Society* **1993**, *115*, 12158.

(30) Wang, T. Y.; Silvius, J. R. *Biophysical Journal* **2000**, *79*, 1478.

(31) Mukherjee, S.; Chattopadhyay, A. *Biochemistry* **1996**, *35*, 1311.

(32) Chattopadhyay, A.; Mukherjee, S. *Journal of Physical Chemistry B* **1999**, *103*, 8180.

(33) Rukmini, R.; Rawat, S. S.; Biswas, S. C.; Chattopadhyay, A. *Biophysical Journal* **2001**, *81*, 2122.

(34) Greenough, K. P.; Blanchard, G. J. *Journal of Physical Chemistry B* **2006**, *in review.*

(35) Kawato, S.; Kinosita, K., Jr.; Ikegami, A. *Biochemistry* **1977**, *16*, 2319.

(36) Kinosita, K., Jr.; Kawato, S.; Ikegami, A. *Biophysical Journal* **1977**, *20*, 289.

(37) Loura, L. M.; Fedorov, A.; Prieto, M. *Biophysical Journal* **2001**, *80*, 776.

(38) Loura, L. M. S.; Fedorov, A.; Prieto, M. *Journal of Physical Chemistry B* **2000**, *104*, 6920.

(39) Loura, L. M. S.; Fedorov, A.; Prieto, M. *Biochimica et Biophysica Acta, Biomembranes* **2000**, *1467*, 101.

(40) Forster, T. *Ann. Physik.* **1948**, *2*, 55.

(41) Birch, D. J. S.; Suhling, K.; Holmes, A. S.; Salthammer, T.; Imhof, R. E. *Pure and Applied Chemistry* **1993**, *65*, 1687.

(42) Ediger, M. D.; Fayer, M. D. *Journal of Chemical Physics* **1983**, *78*, 2518.

(43) Jones, G. M.; Wofsy, C.; Aurell, C.; Sklar, L. A. *Biophysical Journal* **1999**, *76*, 517.

(44) Lipari, G.; Szabo, A. *Biophysical Journal* **1980**, *30*, 489.

(45) Szabo, A. *Journal of Chemical Physics* **1984**, *81*, 150.

(46) Marsh, D. *Handbook of Lipid Bilayers*; CRC Press: Boca Raton, 1990.

(47) Perrin, F. *Journal de Physique et le Radium* **1936**, *7*, 1.

(48) Debye, P. Polar Molecules. In *Chemical Catalog Co.* New York, 1929.

(49) Zwanzig, R.; Harrison, A. K. *Journal of Chemical Physics* **1985**, *83*, 5861.

Chapter 4

THE ROLE OF PHOSPHOLIPID HEADGROUPS IN MEDIATING BILAYER ORGANIZATION. PERTURBATIONS INDUCED BY THE PRESENCE OF A TETHERED CHROMOPHORE

Introduction

Phospholipids are an essential component of plasma membranes,[1] and there is a significant, multidisciplinary research effort underway to understand the structural and compositional complexity of lipid bilayer structures. The use of model bilayer systems has attracted a great deal of attention because of their potential utility in the construction of chemical and biological sensor devices based on biomolecular recognition. Phospholipids self-assemble spontaneously in an aqueous environment to form a bilayer structure with the hydrophobic tails directed inward, toward one another and the headgroups exposed to the aqueous phase. This characteristic organization is responsible for the ability of biomembranes to act as barriers between two aqueous environments. It is clear that for such complex systems, both the acyl chain region and the polar headgroup region of the bilayer contribute to the overall organization.

As noted above, phase transitions have been seen in a variety of lipid bilayer structures. For a pure phospholipid the gel-to-fluid phase transition is well defined, with the transition temperature, T_m, depending sensitively on the length of the acyl chains and the presence and location of any unsaturations. The physical change that occurs at the gel-to-fluid phase transition is related to the organization of the aliphatic chains, with an increase in the number of *trans-gauche* conformers with increasing temperature.[2] The gel phase is a comparatively well-ordered state in which the translational mobility of the

bilayer constituents is thought to be limited. Above the phase transition temperature, in the fluid phase, the phospholipid aliphatic tails are more disordered,[3] leading to a decrease in the thickness of the bilayer,[4] and an increase in the rotational and lateral freedom of the phospholipid molecules. Lipid bilayers may exist in the gel phase or the fluid phase depending on the temperature, pressure, extent of hydration, and the structural identity of the phospholipids.

Many studies of bilayer systems have used fluorescent probes to interrogate the bilayer structure and dynamics. For example, we have established that the gel-to-fluid phase transition temperature is sensed by perylene sequestered in the nonpolar region of the lipid bilayer,[5] and the results of this work are in excellent agreement with the phase transition information recorded for the same lipid system using NMR measurements.[6] A more general question that we are interested in is whether or not the presence of the chromophore in a bilayer system can have a perturbative effect, yielding results that are not representative of the native bilayer system. We address this issue in this work, using a fluorescent probe localized at the polar headgroup region of the lipid bilayer. We have chosen to use a polar chromophore bound to the headgroup region of a phospholipid as the probe. Our choice is deliberate. For polar chromophores bonded to the phospholipid acyl chains, there is a well-established tendency for the chromophore to "loop back" so that it will be in relatively close proximity to the polar headgroup region,[7-12] a condition which is certainly perturbative to the bilayer structure. For a nonpolar chromophore, such as perylene, we have shown that the phase transition data we recover is the same as that for lipid bilayers that do not contain the chromophore. With the system chosen, we

are interrogating the portion of the bilayer above the polar headgroups, and the presence of the probe does not alter the organization of the acyl chains. To understand the role that this tethered chromophore plays in mediating bilayer organization, we have studied its concentration-dependent fluorescence behavior in unilamellar vesicle structures.

We use the lipid-tethered chromophore 1,2-dioleoyl-*sn*-glycero-3-phosphoethanolamine-N-lissamine rhodamine B sulfonyl ammonium salt (Rhodamine-PE). The rhodamine dyes are characteristically strong absorbers in the visible spectral region, and their relatively high fluorescence quantum yields and several nanosecond fluorescence lifetimes are well suited for use at the sub-monolayer level. The polar nature of the rhodamine chromophore, together with the characteristics listed above and previous work with rhodamines in our research group[13,14] render it suitable for the present study.

We focus on the rotational motion of Rhodamine-PE in the polar headgroup region as a function of its concentration and system temperature. We find that there is a significant dependence of the rotational relaxation dynamics and disorder in the bilayer structure with increasing chromophore concentration. These findings are augmented by steady state fluorescence data showing that at the highest chromophore concentrations there are some chromophore-chromophore interactions. Taken collectively, the data point to the need for caution in the use of fluorescent probes in bilayer structures, and that low concentrations of chromophore are required if the experimental data are to be useful in understanding the properties of the native bilayer.

Experimental

Vesicle Preparation. Phospholipids 1,2-dimyristoyl-*sn*-phosphatidylcholine (DMPC) and 1,2-dioleoyl-sn-glycero-3-phosphoethanolamine-N-lissamine rhodamine B sulfonyl ammonium salt (Rhodamine-PE) were purchased from Avanti Polar Lipids Inc. (Alabaster, AL) and used as received (Figure 4.1). For each sample, the lipids and the rhodamine probe were mixed in selected ratios so that the final concentrations of the samples were 1.5×10^{-3} M lipid, with the Rhodamine-PE concentration being 0.0025 mol%, 0.025 mol% or 0.25 mol%. The chloroform solvent was evaporated from the lipids and an appropriate volume of Tris® buffer (Sigma-Aldrich) was added to each mixture so that the lipid concentration was 1 mg/mL, consistent with the 1.5 mM concentration listed above. The buffer (10 mM, pH 7.8) was prepared using water from a Milli-Q Plus water purification system (Millipore, Bedford, MA). The mixtures were processed five times through a freeze-thaw-vortex cycle to ensure complete mixing of the constituents. Each cycle consisted of freezing the solution by immersion in liquid nitrogen for five minutes, followed by thawing via immersion in 60°C water (five minutes) and concluded with vortexing (approximately two minutes). After freeze-thaw-vortex processing, the solutions were immediately extruded once through two polycarbonate membrane filters with 400 nm pore diameter using a mini-extruder (Avanti Polar Lipids Inc.). The initially extruded vesicle suspension was subsequently extruded eleven times through two polycarbonate membranes (Avanti Polar Lipids Inc.), each with a nominal pore diameter of 100 nm. The resulting solution contained vesicles with a size

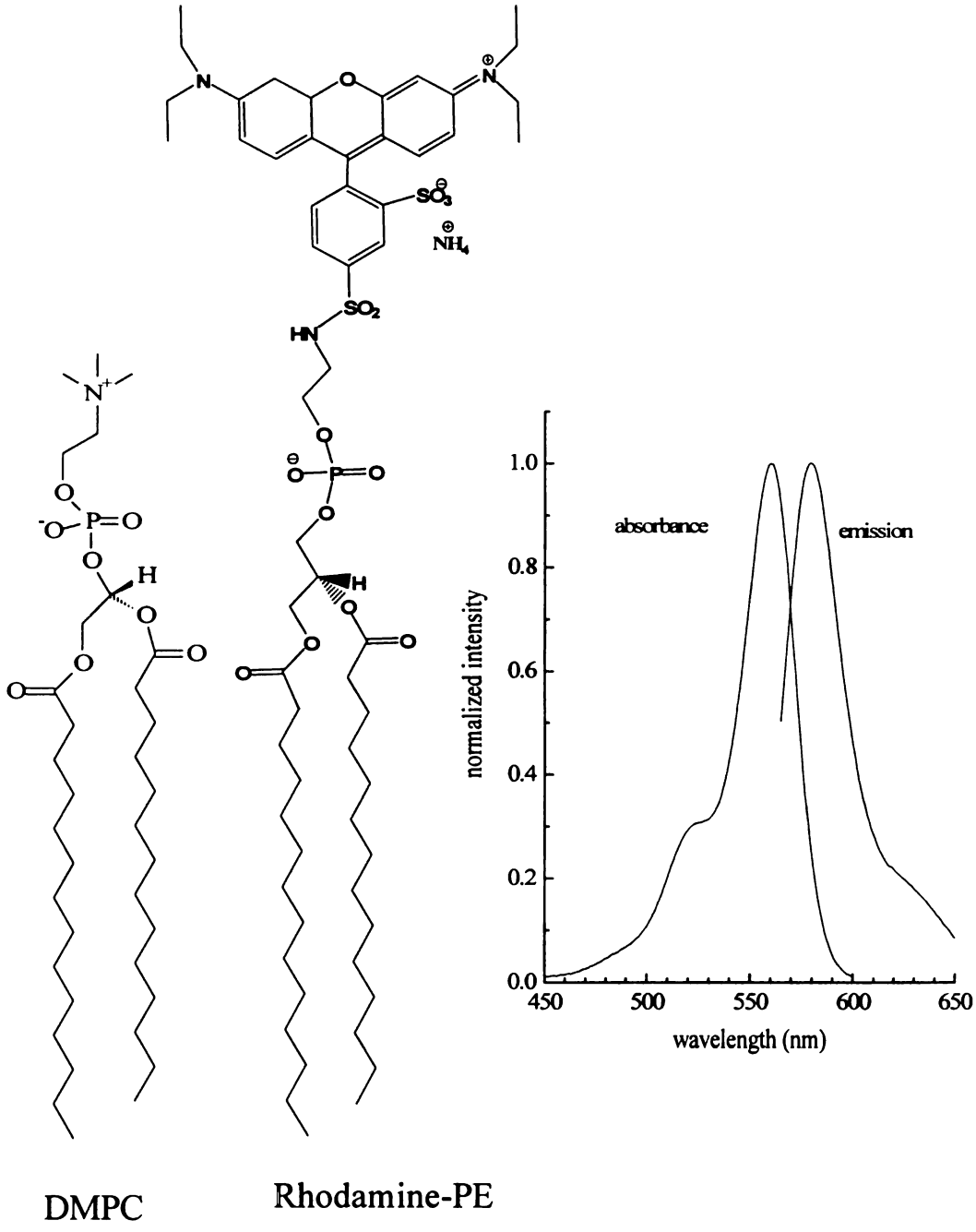

Figure 4.1. Left: Structures of the phospholipid DMPC and the chromophore-containing phospholipid Rhodamine-PE. Right: Solution phase absorption and emission spectra of Rhodamine-PE in ethanol. Spectra have been normalized for clarity of presentation.

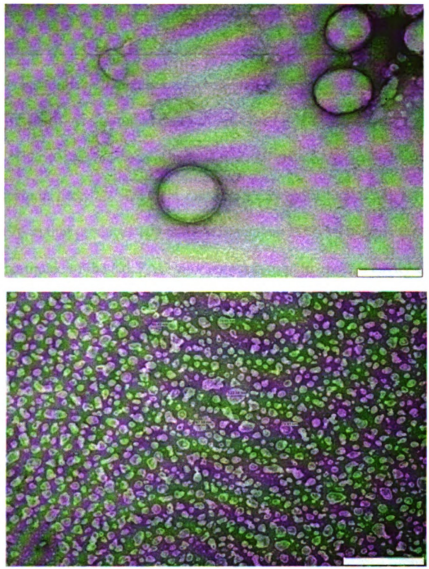

Figure 4.2. TEM images of vesicles produced by extrusion and used in this work. Top pane: Image of an isolated unilamellar vesicles of ca. 150 nm in diameter. Bottom pane: Image of multiple vesicles. The average diameter of vesicles was determined to be 84 ± 22 nm based on measurements made from this and other TEM images.

distribution centered around 85 nm diameter[15-20] with a standard deviation of 20 nm (Figure 4.2).

Time-resolved fluorescence measurements. Time-domain polarized fluorescence intensity decays were acquired using a time-correlated single-photon counting (TCSPC) system. This system has been described in detail elsewhere, and we briefly recap its salient features here.[21,22] The light source is a CW mode-locked Nd:YAG laser (Coherent Antares 76-s) that produces 100 ps 1064 nm pulses at 76 MHz repetition rate. The second harmonic of the Nd:YAG laser output is used to excite a cavity-dumped dye laser (Coherent 702-2) operated with Pyromethene 567 dye (Exciton) at ca. 550 nm. The output of this laser is ca. 75 mW average power, with 5 ps pulses at 4 MHz repetition rate. Sample fluorescence is detected with a microchannel plate – photomultiplier tube (MCP-PMT, Hamamatsu R3809U). The electronics used to temporally resolve the fluorescence transients included constant fraction discriminators for the signal and reference channels (CFD, Tennelec 454), and a time-to-amplitude converter/biased amplifier (TAC, Tennelec 864). The collection wavelength and polarization were computer controlled using LabVIEW® 7.1 code. The fluorescence lifetime data were collected at 54.7° with respect to the vertical excitation polarization, while the reorientation data were collected at polarizations parallel (0°) and perpendicular (90°) to the vertically-polarized incident light. The temperature of the sample was regulated to ± 0.1°C using a water-circulating bath (Neslab RTE-110) connected to a cooling jacket that holds the sample cuvette. All samples were allowed to equilibrate thermally for ten minutes prior to data acquisition.

Steady state spectroscopy. Steady state excitation and emission spectra were acquired for our vesicle samples for the purpose of characterizing the rhodamine band positions. We used a Spex Fluorolog 3 emission spectrometer for all measurements, set to a spectral bandpass of 3 nm for both excitation and emission monochromators.

Results and Discussion

The primary goal of this work is to understand the extent to which the presence of a tethered chromophore in a bilayer structure perturbs the organization of the bilayer. Clearly, this is an issue that can be addressed to a limited extent using spectroscopic methods, owing to the molecular length scale over which a fluorophore senses its local environment. In other words, regardless of chromophore concentration, the local environment sensed by the chromophore will be perturbed by the presence of the probe. This is, of course, a generic concern for any optical probe measurement and there is a significant body of knowledge that has been gained on bilayer and other structures using optical spectroscopic methods despite this intrinsic limitation. The concern we address in this work is not related to the local perturbation induced by the probe, but the longer length-scale disorder introduced to the bilayer by the presence of the chromophore. To address this issue we focus on the concentration-dependence of the tethered chromophore Rhodamine-PE in DMPC bilayers. We have measured the steady state and time-resolved fluorescence behavior of this chromophore incorporated into unilamellar vesicles of ca. 100 nm diameter, at three different chromophore concentrations; 0.0025 mol%, 0.025 mol% and 0.25 mol%. Our data reveal a change in the organization of the bilayer structure and a change in the local dynamics experienced by the Rhodamine-PE chromophore as a function of concentration.

As we present our data on the concentration-dependence of the Rhodamine-PE spectral and dynamical behavior, we also report these data as a function of temperature. The reason for reporting the temperature-dependence of these data is that DMPC is

known to exhibit a gel-to-fluid phase transition at 24°C, and we are interested in determining whether or not this structural transition in the acyl chain region of the bilayers can be sensed by a chromophore that is tethered to the headgroup region. While we clearly do not expect an effect as dramatic as was reported for perylene in the bilayer acyl chains, the organization of a bilayer represents a balance of interactions between headgroup and acyl chain regions, and it is of fundamental interest to understand if such interactions can be sensed by a headgroup-bound chromophore.

Steady state spectroscopy. We have measured the steady state emission behavior of Rhodamine-PE in unilamellar vesicles as a function of chromophore concentration and system temperature, and we show these results in Figure 4.3. There are two trends to note in these data. The first is that for the lower two chromophore concentrations, 0.0025 mol% and 0.025 mol%, the emission spectra appear to be identical and are characterized by a maximum at 587 nm. For the 0.25 mol% concentration vesicles, the emission spectrum is shifted to the red by 5 nm and the band profile is different than for the lower concentrations. For all Rhodamine-PE concentrations, there is no discernible change in the steady state emission spectra with temperature, indicating that the optical response of this chromophore is not sensitive to structural changes in the acyl chain region of the bilayer to which they are tethered.

The spectral shift seen for the higher concentration Rhodamine-PE indicates that this chromophore is interacting with neighboring chromophores. This is not a surprising result based on geometric considerations alone. For vesicles containing 0.0025 mol% Rhodamine-PE, the average separation between chromophores is ca. 160 nm, assuming a

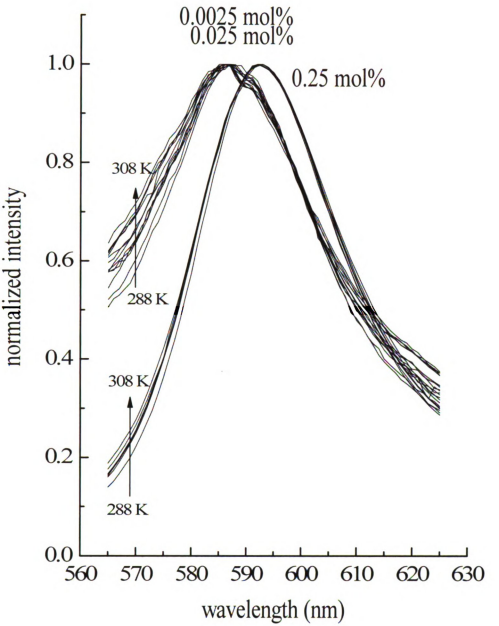

Figure 4.3. Steady state emission spectra of Rhodamine-PE in DMPC vesicles. The chromophore concentrations are 0.0025 mol%, 0.025 mol% and 0.25 mol%, as indicated. Temperature-dependence of the emission band profiles is also indicated.

homogeneous distribution of chromophores and a phospholipid size of 64 $Å^2$/molecule[23]. For vesicles containing 0.025 mol% Rhodamine-PE, the average separation between chromophores is 50 nm, and for 0.25 mol% Rhodamine-PE, the average spacing is 16 nm. For the lower concentrations, it is reasonable to expect little or no discernible chromophore-chromophore interaction, but for the 0.25 mol% system, the average distance is sufficiently short that there will be significant chromophore-chromophore interactions. By way of comparison, a distance of 16 nm is about twice what one would expect for the Förster critical transfer radius, R_0. We will return to a discussion of this point because of the effect that donor-donor excitation transport can have on reorientation measurements.[24-26]

In addition to the steady state spectroscopic data, we have performed time-resolved lifetime and anisotropy decay measurements on Rhodamine-PE in DMPC vesicles. The purpose of these measurements is to gain insight into the molecular scale environment(s) of the chromophores. The interpretation of the experimental reorientation data is somewhat more complex than the standard, solution phase treatment because the rhodamine chromophore is attached to the polar lipid headgroups, a structural condition that gives rise to an infinite time anisotropy. The magnitude of the infinite time anisotropy depends on the extent to which the chromophore is constrained to move within a fixed conic volume.[27,28] For such a system, there are two relevant temporal regions in the data, and the information of interest is derived from the induced orientational anisotropy decay function, R(t), in Eq. 4.1.

$$R(t) = \frac{I_{\parallel}(t) - I_{\perp}(t)}{I_{\parallel}(t) + 2I_{\perp}(t)} \tag{4.1}$$

The experimental fluorescence transients, $I_{\parallel}(t)$ and $I_{\perp}(t)$ (Figure 4.4a), are the emission intensities polarized parallel and perpendicular with respect to the vertically polarized incident excitation pulse.

The theoretical basis used to interpret fluorescence anisotropy data depends on the local environment in which the chromophore is present. The hindered rotor model is used when the motional freedom of a molecule is restricted, as is the case here.[28-31] This restriction may be the result of incorporation of the chromophore within a confined area such as a bilayer structure, or may occur when the chromophore is tethered to an interface. The fact that the chromophore distribution is unable to re-randomize completely following excitation results in a non-zero infinite-time anisotropy, $R(\infty)$. For such systems, R(t) exhibits the functional form shown in Eq. 4.2,

$$R(t) = R(\infty) + (R(0) - R(\infty))\exp(-t/\tau_{HR}) \tag{4.2}$$

where $R(\infty)$ is the infinite time anisotropy and R(0) is the zero time anisotropy (Figure 4.4b). The term R(0) is determined by the angle between the excited and emitting transition dipole moments of the chromophore, and $R(\infty)$ is a gauge of the orientational confinement that the chromophore experiences. The term τ_{HR} is related to the orientational relaxation of the chromophore within its confining volume, and is approximated by Eq. 4.3,[27,28]

$$\tau_{HR} = \frac{7\theta_0^2}{24D_w} \tag{4.3}$$

where θ_0 is the semi-angle of the confining cone. The fundamental quantity of interest is D_w, the so-called wobbling diffusion constant. This quantity reflects the ability of the

tethered chromophore to move within its restricted environment. To evaluate D_w, we need both θ_0 and τ_{HR}. The time constant τ_{HR} is available from the experimental R(t) data, and we show these data as a function of chromophore concentration and system temperature in Figure 4.5a. The cone angle θ_0 is related to the limiting values R(0) and R(∞), and what information can be extracted from these data. The semi-angle of the conic confining volume of the chromophore is related to the zero- and infinite-time anisotropies by Eq. 4.4,[27]

$$\left[\frac{R(\infty)}{R(0)}\right]^{1/2} = 0.5\left(\cos\theta_0\left(1+\cos\theta_0\right)\right) \tag{4.4}$$

We have calculated values for θ_0 (Eq. 4.4) as a function of chromophore concentration and temperature (Figure 4.5b). We consider the temperature and concentration-dependencies of these data individually.

The τ_{HR} data shown in Figure 4.5a do not appear to exhibit a temperature dependence that is related to the known gel-to-fluid phase transition in DMPC at 24°C. This is not a surprising result because the chromophore is not located within the acyl chain region of the bilayer, where the structural phase transition is known to occur. It is also possible that, at least for the higher Rhodamine-PE concentration, that the presence of the chromophore is itself influencing the phase transition temperature. One interesting feature of these data is the dependence of the recovered relaxation time τ_{HR} on the chromophore concentration. There are several possible explanations for these data, but the fact that the concentration-dependence is non-monotonic suggests that the explanation is more complicated than a single effect, such as the effect of donor-donor excitation

transport, for example. It is also noteworthy that the time constants for orientational relaxation also trend toward longer times with increasing temperature. This finding outwardly appears counter-intuitive because the local viscosity of the bilayer environment is expected to decrease with increasing temperature, an effect which could give rise to shorter τ_{HR} values with increasing temperature, if the acyl chains played a role in mediating the chromophore local environment. The other possible explanation for such data is that the volume in which the chromophore can move is increasing in size with increasing temperature, and for this situation the chromophore would require longer to re-randomize its orientation within the larger conic volume. This is a testable hypothesis, through the measurement of the restricting cone angle.

We show in Figure 4.5b the dependence of the cone semi-angle on chromophore concentration and system temperature. There are several interesting trends in these data. It is clear that the 0.0025 mol% Rhodamine-PE vesicles exhibit a smaller cone angle than that of either the 0.025 mol% or 0.25 mol% Rhodamine-PE vesicles. These data, by themselves, point to the role that the chromophore plays in mediating the organization of the bilayer structures. For the higher probe concentrations, there is clearly less order in the bilayer structure, but it is not clear from these data that the concentration of the probe, above a certain point, changes the bilayer organization. As expected, the cone angles increase with temperature in all cases, consistent with increasing thermal disorder in these bilayers.

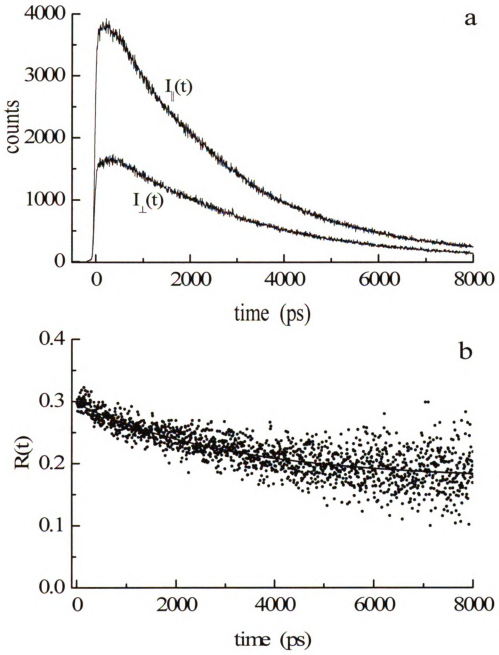

Figure 4.4. (a) Experimental polarized fluorescence transients for Rhodamine-PE in 100 nm diameter DMPC vesicles. (b) Induced orientational anisotropy function, R(t), generated from the data shown in panel (a).

Neither the concentration nor the temperature dependence of τ_{HR} (Figure 4.5a) or θ_0 (Figure 4.5b) by themselves provide a clear picture of how the bilayer is changing as a result of these two experimental variables. As noted above, the fundamental quantity of interest is D_w (Eq. 4.3), and with the τ_{HR} and θ_0 information extracted from the experimental data, we can determine D_w as a function of chromophore concentration and temperature (Figure 4.6). These data contain several interesting trends, and we consider the concentration-dependence first.

It is clear from Figure 4.6 that D_w increases measurably with increasing Rhodamine-PE concentration. As noted above, the quantity D_w reflects the ability of the chromophore to move within its spatially restricted volume, and we ascribe this change to the disorganization introduced to the bilayer structure by the presence of the chromophore itself. Because the chromophore is connected to the lipid headgroup, the notion of conical confinement is less clear, perhaps, than if the chromophore were connected to the acyl chain. Because of the location of the chromophore, the species providing the most confinement will be the phosphocholine headgroups adjacent to the chromophore. As disorder increases in the acyl chain region of the bilayer, the corresponding organization of the headgroup region will also change, giving rise to the effect we detect through the chromophore concentration-dependence of D_w. It is clear from these data that the presence of the chromophore does indeed perturb the organization of the bilayer.

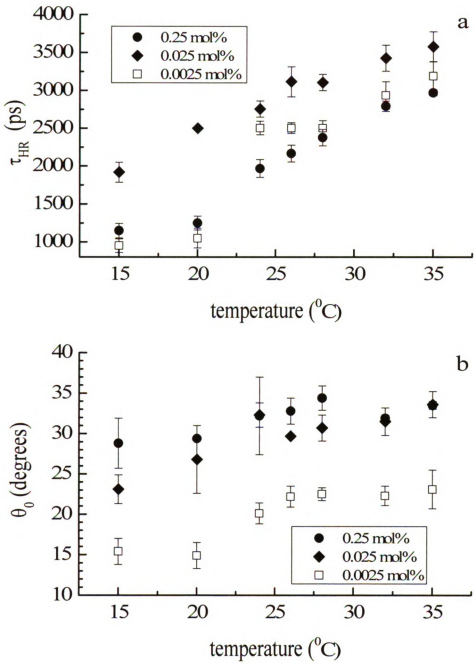

Figure 4.5. (a) Time constants (Eq. 4.2) extracted from anisotropy data for Rhodamine-PE in DMPC vesicles as a function of chromophore concentration and system temperature. (b) Confining cone semi-angle measurements from the experimental data (Eq. 4.4).

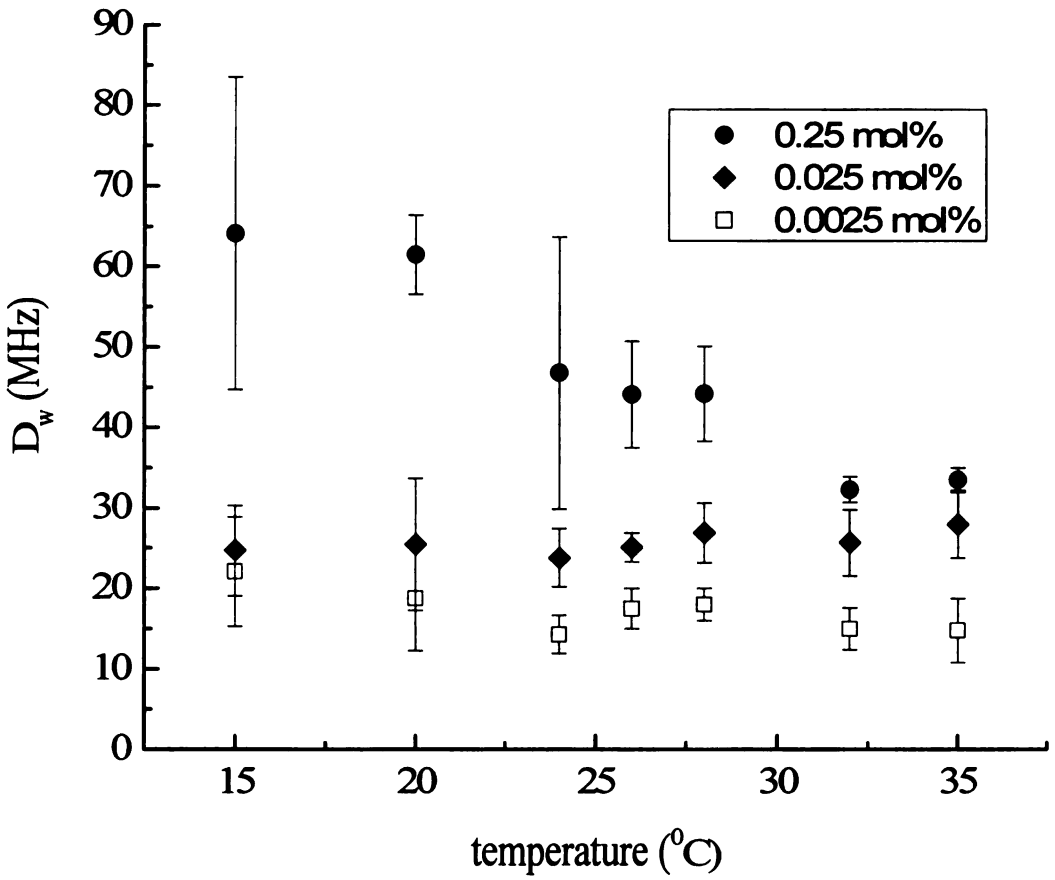

Figure 4.6. Dependence of D_w on chromophore concentration and system temperature. The quantity D_w is calculated from Eq. 4.3 using the experimentally derived quantities τ_{OR} and θ_0.

The second noteworthy finding is that D_w remains essentially constant with temperature for the lower chromophore concentrations, but it *decreases* with increasing temperature for 0.25 mol% Rhodamine-PE. This finding can be understood in terms of the cooperative effects of acyl chain dynamics and headgroup dynamics in a bilayer system. We have reported previously that perylene reorientation within the nonpolar region of DMPC bilayers manifests an increase in D with increasing temperature.[5] It is clear from the perylene data that increasing the temperature of the bilayer structure makes the acyl regions of the bilayers less viscous, thus increasing the mobility of chemical species in the nonpolar region. Because the headgroups are covalently bound to the aliphatic tails, we assert that the mobility of the headgroups must, of necessity, experience a change in (translational) mobility as well. The fact that we observe experimentally a constant or decreasing chromophore D_w with increasing temperature is consistent with a limited number of physical conditions for our bilayers.

For the low chromophore concentrations, where no temperature dependence is seen in D_w, we understand this behavior in the context of our orientational anisotropy measurements not being sensitive to translational diffusion phenomena. For the lower chromophore concentrations, there is a sufficiently low chromophore density that under all conditions the chromophores respond as individual entities. The reason that D_w exhibits little or no change with temperature for these systems is that the chromophore is in an environment dominated by the lipid headgroup region and the water overlayer. This region of the bilayer system is not expected to change significantly over the temperature range we examined, and this expectation is supported by the functional form

of our data. For the highest chromophore concentration, where the chromophores are, on average, 16 nm apart, it is possible that interactions between chromophores would give rise to slower motion, consistent with our findings. In addition to the temperature-dependent change in dynamics, such chromophore-chromophore interactions would produce changes in spectroscopic band shape, and we observe this effect clearly (Figure 4.3). While it may be tempting, based on the translational diffusion coefficients derived for our perylene data,[5] to estimate the extent or frequency of chromophore-chromophore interactions, we refrain from making this calculation because we do not have any independent means of estimating the energetics of this process.

It is also important to recognize that, for these measurements, donor-donor excitation transport can contribute to the functional form of the anisotropy decay for high chromophore concentrations.[24-26] The mechanism of such excitation transport is dipolar coupling, with the length scale over which this process operates being similar to that for the more widely considered Förster donor-acceptor energy transfer. The chromophores are nominally separated by ca. two Förster critical radii at the highest concentration, and the signature of this process is the loss of polarization with time as the hopping excitation(s) sample the orientational distribution present in the system. The separation of motional and excitation transport processes is often difficult, relying on measuring the concentration-dependence of the anisotropy decay over the appropriate concentration range. We have not mapped out the concentration-dependence of R(t) for this system with sufficient resolution to cleanly separate these two processes. The fact that our data for the highest chromophore concentration does manifest a temperature-dependence

where the lower concentrations do not suggests that there is at least some contribution from donor-donor transport in this system, and this is a matter which is currently under investigation.

Conclusions

We have found that the steady state and time-resolved fluorescence behavior of the chromophore Rhodamine-PE in DMPC bilayers can be used to interrogate organization within the bilayer system. A long-standing issue with any fluorescent probe method is the extent of the perturbation introduced to the system by the probe itself. We find direct evidence for such perturbations with the chromophore concentration and system temperature dependence of the steady state and time-resolved fluorescence of Rhodamine-PE in DMPC. Specifically, we find that the emission spectral profiles of this chromophore depend on the chromophore concentration, with a red-shifted emission spectrum seen for the highest chromophore concentration. Such a spectral shift is consistent with chromophore-chromophore interactions. The findings of the steady state data are supported by the time-resolved experimental results. We recover concentration- and temperature-dependent anisotropy decay dynamics for this chromophore, with no apparent simple relationship between the measured decay time constant and the properties of the bilayer system. As has been seen previously for solution phase systems, the anisotropy decay time constant can vary for reasons not related to changes in the rotational diffusion constant.[32] In this case, where we use the hindered rotor model to interpret our dynamical data,[27,28] we find that it is also important to account for changes in the extent to which the chromophore is restricted, and this is manifested in the confining cone semi-angle, θ_0. This system property also does not, by itself provide full insight into the bilayer system. When both of these experimentally-derived quantities are considered, and the fundamental quantity D_w is extracted, an intuitive physical picture

emerges. As the chromophore concentration is increased, D_w increases as a result of disorganization within both the head group and acyl chain region of the bilayer structure. For 0.25 mol% Rhodamine-PE we observe a decrease in D_w with increasing temperature, a phenomenon consistent with chromophore-chromophore interactions which serve to slow the motion of the individual chromophores. This interpretation of the data is consistent with the steady state emission spectra, which show significant inter-chromophore interactions. Extracting the relative contribution to D_w from excitation transport for this system is a difficult task, and current work is under way to elucidate the role of this process more clearly. The larger significance of this work, however, is the understanding that low chromophore concentrations must be used in fluorescence probe measurements if the properties of the bilayer itself are to be interrogated.

Literature Cited

(1) Bagatolli, L. A.; Gratton, E. *Biophysical Journal* **2000**, *78*, 290.

(2) Pabst, G.; Amenitsch, H.; Kharakoz, D. P.; Laggner, P.; Rappolt, M. *Physical Review E: Statistical, Nonlinear, and Soft Matter Physics* **2004**, *70*, 021908/1.

(3) Stevens, B. C.; Ha, T. *Journal of Chemical Physics* **2004**, *120*, 3030.

(4) Nagle, J. F. *Annual Review of Physical Chemistry* **1980**, *31*, 157.

(5) Koan, M. M.; Blanchard, G. J. *Journal of Physical Chemistry B* **2006**, *110*, 16584.

(6) Oraedd, G.; Lindblom, G. *Biophysical Journal* **2004**, *87*, 980.

(7) Chapman, C. F.; Liu, Y.; Sonek, G. J.; Tromberg, B. J. *Photochemistry and Photobiology* **1995**, *62*, 416.

(8) Chattopadhyay, A.; London, E. *Biochimica et Biophysica Acta, Biomembranes* **1988**, *938*, 24.

(9) Fery-Forgues, S.; Fayet, J.-P.; Lopez, A. *Journal of Photochemistry and Photobiology, A: Chemistry* **1993**, *70*, 229.

(10) Feng, Z. V.; Spurlin, T. A.; Gewirth, A. A. *Biophysical Journal* **2005**, *88*, 2154.

(11) Mazeres, S.; Schram, V.; Tocanne, J.-F.; Lopez, A. *Biophysical Journal* **1996**, *71*, 327.

(12) Mukherjee, S.; Chattopadhyay, A.; Samanta, A.; Soujanya, T. *Journal of Physical Chemistry* **1994**, *98*, 2809.

(13) Dela Cruz, J. L.; Blanchard, G. J. *Journal of Physical Chemistry A* **2001**, *105*, 9328.

(14) Dela Cruz, J. L.; Blanchard, G. J. *Journal of Physical Chemistry A* **2002**, *106*, 10718.

(15) Mayer, L. D.; Hope, M. J.; Cullis, P. R. *Biochimica et Biophysica Acta* **1986**, *858*, 161.

(16) Hunter, D. G.; Frisken, B. J. *Biophysical Journal* **1998**, *74*, 2996.

(17) MacDonald, R. C.; MacDonald, R. I.; Menco, B. P.; Takeshita, K.; Subbarao, N. K.; Hu, L. R. *Biochimica et Biophysica Acta* **1991**, *1061*, 297.

(18) Driessen, A. J.; van den Hooven, H. W.; Kuiper, W.; van de Kamp, M.; Sahl, H. G.; Konings, R. N.; Konings, W. N. *Biochemistry* **1995**, *34*, 1606.

(19) Unger, E. C.; MacDougall, P.; Cullis, P.; Tilcock, C. *Magnetic Resonance Imaging* **1989**, *7*, 417.

(20) Subbarao, N. K.; MacDonald, R. I.; Takeshita, K.; MacDonald, R. C. *Biochimica et Biophysica Acta* **1991**, *1063*, 147.

(21) DelaCruz, J. L.; Blanchard, G. J. *Journal of Physical Chemistry B* **2003**, *107*, 7102.

(22) DeWitt, L.; Blanchard, G. J.; LeGoff, E.; Benz, M. E.; Liao, J. H.; Kanatzidis, M. G. *Journal of the American Chemical Society* **1993**, *115*, 12158.

(23) Lague, P.; Zuckermann, M. J.; Roux, B. *Biophysical Journal* **2001**, *81*, 276.

(24) Gochanour, C. R.; Fayer, M. D. *Journal of Physical Chemistry* **1981**, *85*, 1989.

(25) Ediger, M. D.; Fayer, M. D. *Journal of Chemical Physics* **1983**, *78*, 2518.

(26) Baumann, J.; Fayer, M. D. *Journal of Chemical Physics* **1986**, *85*, 4087.

(27) Lipari, G.; Szabo, A. *Biophysical Journal* **1980**, *30*, 489.

(28) Szabo, A. *Journal of Chemical Physics* **1984**, *81*, 150.

(29) Karpovich, D. S.; Blanchard, G. J. *Langmuir* **1996**, *12*, 5522.

(30) Kinosita, K., Jr.; Ikegami, A.; Kawato, S. *Biophysical Journal* **1982**, *37*, 461.

(31) Kinosita, K., Jr.; Kawato, S.; Ikegami, A. *Biophysical Journal* **1977**, *20*, 289.

(32) Blanchard, G. J.; Wirth, M. J. *Journal of Chemical Physics* **1985**, *82*, 39.

Chapter 5

GAUGING THE EFFECT OF IMPURITIES ON LIPID BILAYER PHASE TRANSITION TEMPERATURE

Introduction

Phospholipid bilayers have attracted a great deal of interest because of their central role in cellular function and the potential for the use of model bilayer systems in chemical and biological sensing applications. As our understanding of phospholipid bilayers has developed, the structural and compositional complexity of this family of molecular assemblies has become more apparent. It is now known that natural bilayer structures contain 100 or more constituents,[1] and for simple model systems comprised of as few as two or three different species, phase separations have been observed.[2-6] While phase segregation remains to be seen for biologically-derived bilayers, it is likely that these compositionally heterogeneous structures are characterized by small, fluid domains that are beneath our ability to resolve. Our interest in phospholipid bilayers lies in their potential utility as supported bilayer membranes, a structural motif useful in the creation of selective chemical sensing systems based on biological molecules such as enzymes and trans-membrane proteins. We are investigating the fluidity and phase segregation behavior of model bilayer structures in an effort to optimize these films for incorporation of selected biomolecules in their active form. We focus in this work on the composition-dependence of bilayer fluidity.

Phospholipids self-assemble spontaneously to form a bilayer structure with the

hydrophobic tails directed toward the center, and the head groups exposed to the aqueous phase. Phase transitions have been seen in a variety of bilayers, and it is thought that at the so-called gel-to-fluid melting transition temperature, T_m, the hydrocarbon tails undergo a change from being predominantly *trans* to a structural configuration characterized by a significant number of *trans-gauche* conformers.[7] The characteristic phase transition temperature (T_m) for a phospholipid depends sensitively on the aliphatic chain length and the presence and location of any unsaturations in the aliphatic chain(s), and such phase transitions have been detected by a number of techniques, ranging from calorimetry[8] to fluorescence spectroscopy[9] and spin labeling.[10] For temperatures below T_m, the lipid aliphatic tails are said to exist in the gel phase, a comparatively well-ordered state where translational mobility of the bilayer constituents is thought to be limited. Above the phase transition temperature, the phospholipid aliphatic tails exist in a more disordered fluid phase,[11] characterized by more motional freedom and consequently, more lateral freedom. Lipid bilayers may exist in the gel phase or the fluid phase depending on the temperature, pressure, extent of hydration, and the structural identity of the phospholipids.[12] This phase transition has received a great deal of research attention, both experimental and theoretical, because the phase transition temperature is related to the energetics of lipid-lipid interactions within the bilayer, and phospholipid phase transitions are considered to be important in regulating the activities of membrane-associated proteins.[13,14]

There is a significant body of literature focused on measuring T_m for selected phospholipid bilayer systems.[11-25] We have undertaken the present study for two reasons.

The first is to evaluate the utility of fluorescent probe molecules sequestered within the nonpolar regions of lipid bilayers to detect phase transitions. The second purpose of this work is to evaluate the effect of impurities within the bilayers on the characteristic T_m for the resulting system. Both of these issues are of great potential importance because of the information content of the fluorescence experiments in addition to the phase transition temperature. While there has been a great deal of work focused on understanding structural phase transitions in bilayer systems, there remains the issue of the characteristic length scale over which the change in organization at the phase transition is seen. By working with systems containing controlled amounts of impurities, and comparing microscopic viscosity data to phase transition temperatures, we can assess whether or not the change in organization associated with a phase transition is reflected accurately by molecular-scale changes in the nonpolar region of the bilayer on the molecular scale.

For these experiments we use the chromophore perylene. Perylene is a planar polycyclic aromatic hydrocarbon with a well characterized linear optical response. Its nonpolar nature makes it well suited to incorporation within the acyl chain region of lipid bilayers. In this work, we focus on the rotational motion of perylene within the bilayer nonpolar region as a function of temperature. Not only is rotational diffusion more sensitive to local environment than fluorescence lifetime, but the details of the rotational motion provide a gauge of the bilayer viscosity. While perylene has been used previously in the study of bilayer systems, our direct picosecond time-resolved measurements afford more detail than has been available from either steady state or phase-resolved fluorescence measurments.[26,27]

The phase transition behavior of phospholipids bilayers from the gel phase to the fluid phase has been studied in great detail previously.[15-25,28] The phase transition temperatures of many phospholipids are well-documented, especially for those phospholipids containing no unsaturations. For some systems, even more specific information is known, such as changes in partial specific molar volume, for example.[28] However, there are comparatively fewer reports on the effect of "impurities" on T_m for a phospholipid bilayer. The work we report here, using 1,2-dimyristoyl-*sn*-phosphatidylcholine (DMPC) and 1,2-dimyristoleoyl-*sn*-glycero-3-phosphocholine (14:1 PC) as the phospholipid and "impurity", respectively, demonstrate that even well ordered phospholipid bilayers are characterized by a viscosity of 14.5 ± 2.5 cP in the gel phase and 8.5 ± 1.5 cP in the fluid phase. When 14:1 PC is introduced to a DMPC bilayer, we observe a dramatic decrease in the gel-to-fluid transition temperature from 24°C for the pure DMPC bilayer, with a gradual approach to a new phase transition temperature of ca. 4°C for concentrations of 14:1 PC on the order of 1 mol%. These findings point to the relatively small amount of impurity required to disrupt the phase transition temperature of a bilayer, even though the local viscosity of the bilayers did not sense a corresponding change in order.

Experimental

Vesicle Preparation. Phospholipids 1,2-dimyristoyl-*sn*-phosphatidylcholine (DMPC) and 1,2-dimyristoleoyl-*sn*-glycero-3-phosphocholine (14:1 PC) were purchased from Avanti Polar Lipids Inc. (Alabaster, AL) and used as received. Both lipids are >99% pure, with the details of the analyses being provided on Avanti's web site (www.avantilipids.com). Perylene was purchased from Sigma-Aldrich (Milwaukee, WI) and used without further purification. For each sample, the lipids and the perylene probe were mixed in selected ratios so that the final concentrations of the samples were 2.9 x 10^{-4} M lipid and 1 x 10^{-5} M perylene. The chloroform solvent was evaporated and an appropriate volume of Tris® buffer (Sigma-Aldrich) was added to each mixture so that the lipid concentration was 1 mg/mL. The buffer (10 mM, pH 7.8) was prepared using purified water from a Milli-Q Plus water purification system (Millipore, Bedford, MA). The mixtures were processed five times through a freeze-thaw-vortex cycle to ensure complete mixing of the constituents. Each cycle was comprised of freezing the solution by immersion in liquid nitrogen for five minutes, followed by thawing via immersion in 60°C water (five minutes) and concluded with vortexing (approximately two minutes). After freeze-thaw-vortex processing, the solutions were extruded once through two polycarbonate membrane filters with 400 nm pore diameter using a mini-extruder (Avanti Polar Lipids Inc.). The initially extruded vesicle suspension was then extruded eleven times through two polycarbonate membranes (Avanti Polar Lipids Inc.) with a nominal pore diameter of 100 nm. Extrusions were performed at room temperature. The resulting

solution contained vesicles with a size distribution centered around 100 nm diameter (Figure 5.1).[29-34]

Time-resolved fluorescence measurements. Time-domain polarized fluorescence intensity decays were acquired over a range of temperatures using a time-correlated single-photon counting (TCSPC) system. This system has been described in detail elsewhere, and we briefly recap its salient features here.[35,36] The light source is a CW mode-locked Nd:YAG laser (Coherent Antares 76-s) that produces 100 ps 1064 nm pulses at 76 MHz repetition rate. The third harmonic of the Nd:YAG laser output is used to excite a cavity-dumped dye laser (Coherent 702-2) operated with Stilbene 420 dye (Exciton) at ca. 430 nm. The output of this laser is ca. 25 mW average power, with 5 ps pulses at a 4 MHz repetition rate. Sample fluorescence is detected with a microchannel plate – photomultiplier tube (MCP-PMT, Hamamatsu R3809U) and the electronics used to temporally resolve the fluorescence transients were a constant fraction discriminator (CFD, Tennelec 454) and a time-to-amplitude converter/biased amplifier (TAC, Tennelec 864). The collection wavelength and polarization were computer controlled using LabVIEW® 7.0 code. The fluorescence lifetime data were collected at 54.7° with respect to the vertical excitation polarization, while the reorientation data were collected at polarizations parallel (0°) and perpendicular (90°) to the vertically-polarized incident light. The temperature of the sample was regulated to ± 0.1°C using a water-circulating bath (Neslab RTE-110) connected to a cooling jacket that holds the sample cuvette. All samples were allowed to thermally equilibrate for ten minutes prior to data acquisition.

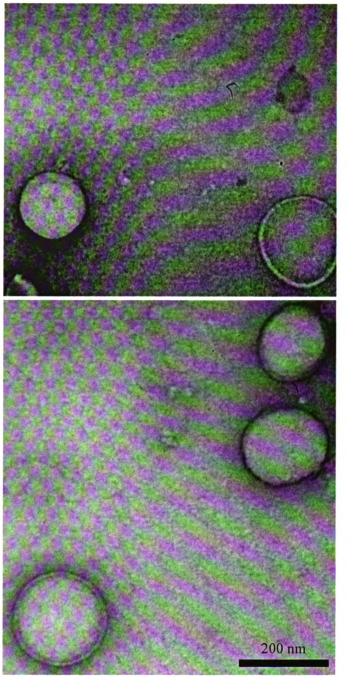

Figure 5.1. Transmission electron microscope images of a unilamellar vesicle used in this work. The scale bar for both images is shown in the lower right corner.

Steady state spectroscopy. Steady state excitation and emission spectra (not shown) were acquired for our vesicle samples for the purpose of characterizing the perylene band positions. We used a Spex Fluorolog 3 emission spectrometer for all measurements, set to a spectral bandpass of 2 nm for both excitation and emission monochromators.

Results and Discussion

As noted above, there are two major goals of this work. The first is to demonstrate the feasibility of using a chromophore imbedded in the non-polar region of a lipid bilayer structure to sense the gel-to-fluid phase transition temperature. The second purpose of this work is to achieve a more quantitative understanding of the effect that an impurity has on the phase transition temperature of vesicles comprised primarily of the phospholipid DMPC. The chosen "impurity" for this series of experiments is 1,2-dimyristoleoyl-*sn*-glycero-3-phosphocholine, a 14-carbon phospholipid that closely resembles DMPC, but contains one *cis*-unsaturation at the 9- position in each acyl chain (14:1 PC, Figure 5.2). This choice of "impurity" was intended to introduce irregularities in the bilayer structures in a relatively well controlled manner. We consider the utility of perylene as an optical probe of bilayer phase transitions first.

The gel-to-fluid transition temperature of pure DMPC has been established to be 24°C,[37] and we find that perylene exhibits a discontinuous change in its rotational diffusion dynamics in DMPC unilamellar vesicles at this temperature (Figure 5.3). Phenomenologically, perylene functions as a phase transition probe likely because the chromophore is sequestered within the portion of the bilayer structure that is thought to undergo the greatest structural change at the point of phase transition from the gel to the fluid phases. It is fair to consider that the perylene itself may be responsible for some perturbation of the bilayer structure. While this possibility must be considered for any fluorescent probe experiment, we believe that the perturbation imposed on the bilayer by

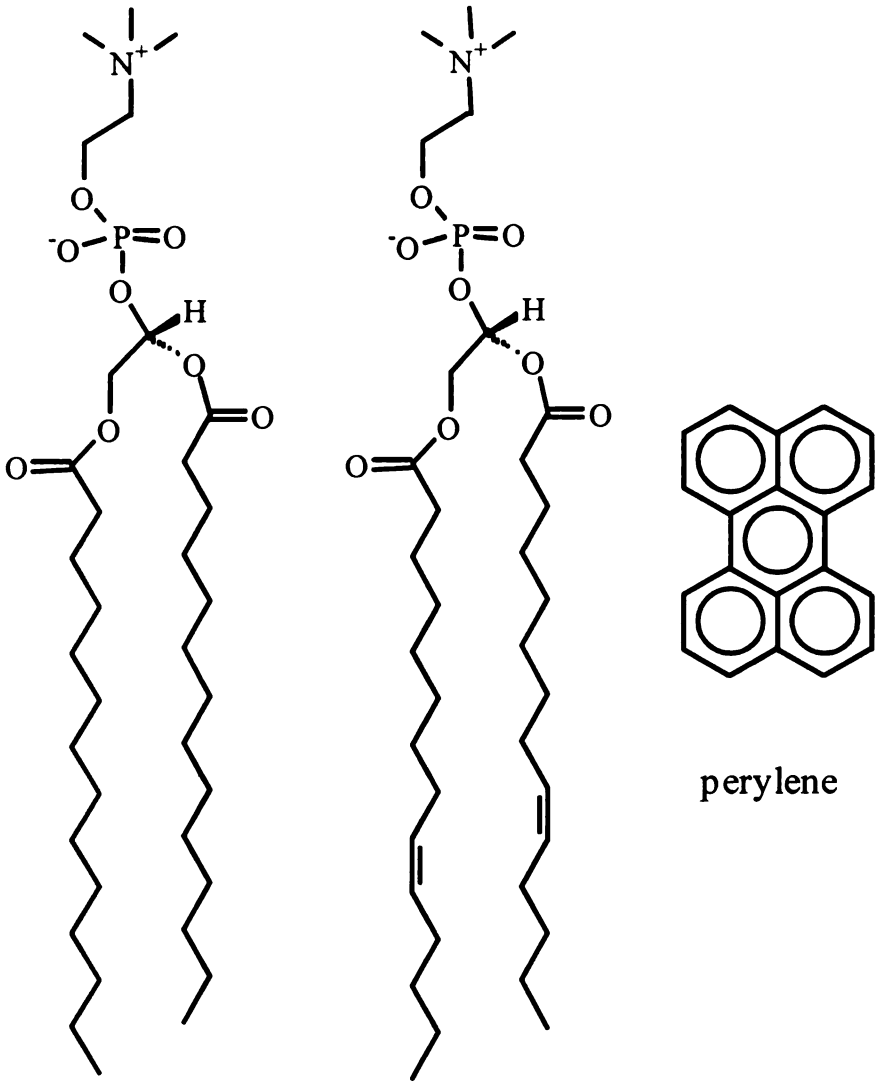

Figure 5.2. Structures of DMPC, 14:1 PC and perylene.

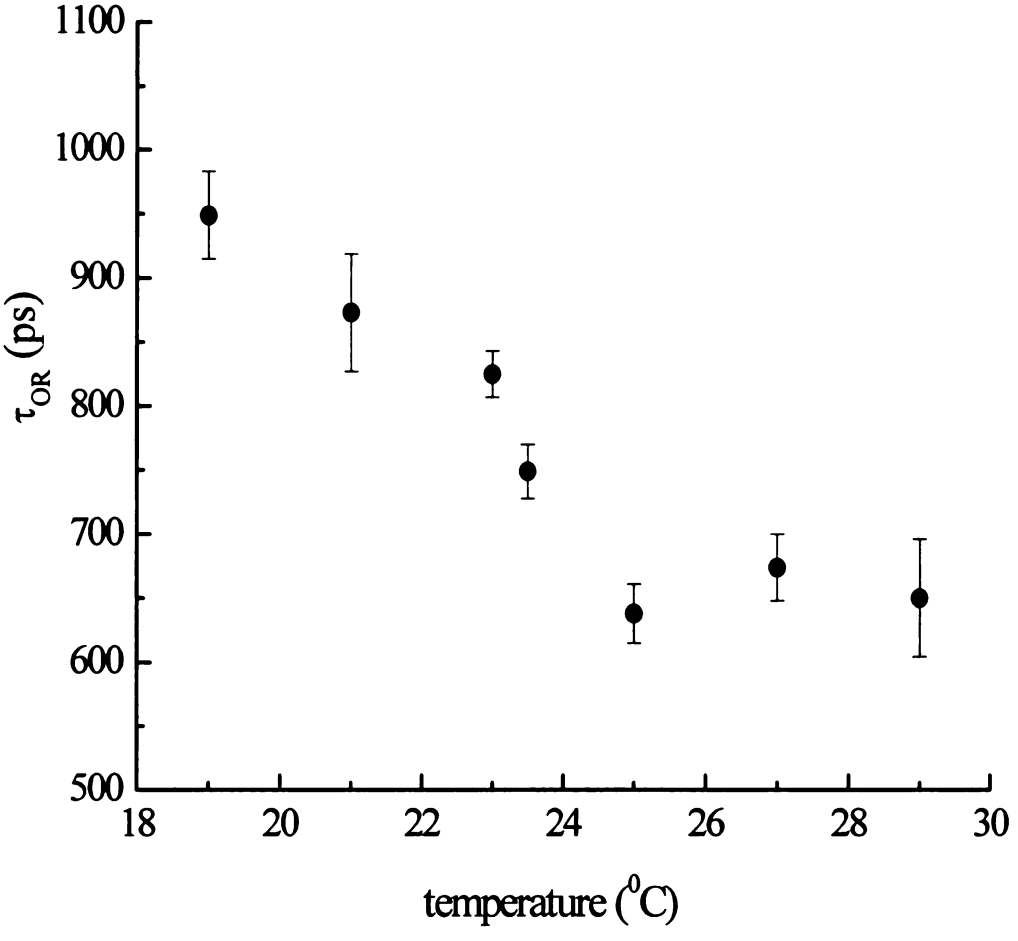

Figure 5.3. Reorientation time of perylene in unilamellar vesicles comprised of DMPC as a function of temperature. There is a discontinuous change in τ_{OR} at the gel-to-fluid phase transition temperature. Error bars are $\pm 1\sigma$ for at least four individual determinations at each temperature.

perylene is modest. Our reasons for this assertion are that, with perylene, we observe the same phase transition temperature for DMPC that has been measured by other methods.[37] With the addition of relatively small amounts of 14:1 PC, we observe changes in the phase transition temperature for the bilayer system. Thus, even if the perylene does perturb the bilayer structure, it is constant for all of our measurements and the changes in phase transition temperature associated with the introduction of DMPC are manifested by large changes in the phase transition temperature. Apparently, the planar structure of the perylene molecule can be accommodated within the nonpolar bilayer region with less disruption than the presence of *cis* defects in the chains themselves.

In addition to the ability of perylene to sense the phase transition temperature of DMPC, the measurements we perform provide other valuable information on the nonpolar interior region of these bilayers. We determine transient fluorescence anisotropy dynamics through the induced optical anisotropy function, R(t) (Eq. 5.1)

$$R(t) = \frac{I_{\parallel}(t) - I_{\perp}(t)}{I_{\parallel}(t) + 2I_{\perp}(t)} \tag{5.1}$$

where $I_{\parallel}$(t) and $I_{\perp}$(t) are the emission intensities polarized both parallel and perpendicular to the incident vertically polarized excitation pulse. The chemical information contained in these experiments resides in the decay functionality of R(t), and this information differs for chromophores that exist in free solution versus those confined within a membrane structure. In general, a chromophore can produce an anisotropy decay with up to five exponential components, but owing to symmetry considerations and experimental signal-to-noise limitations, it is highly unusual to observe more than two

decay components in R(t). These decay components can be related to the Cartesian components of the rotational diffusion constant, D, and to the orientation(s) of the excited and emitting transition dipole moments relative to the molecular structure.

The reorientation dynamics of perylene are well understood in a variety of environments. The excited and emitting transition dipole moments of perylene are known to reside along its long in-plane axis, which is typically assigned as the x-axis. In this scheme, the short in-plane axis is designated y and the z-axis is perpendicular to the chromophore π-system plane. For this molecule, a single exponential anisotropy decay is taken to indicate perylene reorienting as a prolate rotor ($D_x > D_y = D_z$) and a two-component anisotropy decay is indicative of reorientation as an oblate rotor ($D_z > D_x = D_y$). We find experimentally that perylene reorients as a prolate rotor, rendering the recovered time constant $\tau_{OR} = 6D_z^{-1}$.[38] It is significant for several reasons that we recover a single exponential anisotropy decay for all measurements. First, our earlier work on perylene in n-alkane bulk solvents revealed a change in the effective rotor shape of the chromophore as the length of the alkane exceeded the length of the perylene long axis.[38] The fact that we do not observe this same change suggests that the perylene may reside in a region that is not spanned continuously by discrete aliphatic chains. Such a finding is consistent with perylene residing near the center of the nonpolar region of the bilayer. The second reason that this finding is significant is that the reorientation time constants both above and below the phase transition are directly comparable to one another, allowing the straightforward extraction of local viscosity information (*vide infra*). While the use of perylene as a probe of bilayer microviscosity has been questioned before,[27] we

believe that perylene is reporting accurately on microscale changes in analogous molecular environments across the gel-to-fluid phase transitions in these bilayers, and that on both sides of the phase transition, the probe sweeps out the same ellipsoidal volume of rotation. At the very least, the relative changes in local environment across the bilayer phase transition are reflected accurately in the perylene reorientation data. We consider next the relationship between the recovered reorientation time constant and the local environment of the chromophore.

The modified Debye-Stokes-Einstein equation relates the measured reorientation time to the quantities of interest.[39-41]

$$\tau_{OR} = \frac{\eta V f}{k_B T S} \tag{5.2}$$

This model has been discussed extensively before, and we will not attempt a detailed review here. The quantities of interest here are η, the viscosity of the medium surrounding the reorienting chromophore, V is the solute hydrodynamic volume, f is a solvent-solute frictional interaction coefficient, and S is a shape factor to account for the non-spherical shape of the reorienting chromophore. This model has been shown to be in reasonable agreement with experimental data for a wide variety of systems. While this model assumes a continuum medium surrounding the reorienting moiety, which is clearly not an accurate description because the molecular motion we sense is averaged over many configurations of the local environment, the approximation of a continuum is phenomenologically reasonable. Using the calculated hydrodynamic volume of perylene (225 $Å^3$) and the experimental reorientation data, we can extract information on the viscosity of the lipid bilayers. These data lie in the range of ca. 14.5 cP for the gel phase

and ca. 8.5 cP for the fluid phase (Table 5.1). These values are broad averages over a range of experimental conditions, but they are nonetheless important because they provide significant insight into the fluidity of these bilayer structures, and the influence that structural disorder has on this property.

To place these values in context, there has been a good deal of interest in the viscosity of bilayers because this property is a gauge of membrane fluidity and thus the mobility of membrane constituents. Our understanding of bilayer structures has evolved substantially over time, and with it has come a range of estimates for the viscosity of bilayers. Initially it was thought that bilayers were characterized by a viscosity of ca. 100 cP,[1] with subsequent estimates being revised downward. A recent estimate of plasma membrane viscosity was that it was similar to "crocodile fat on a warm summer's day."[1] Absent accurate viscosity data on warm crocodile fat, we chose to quantitate the viscosity of the bilayer structures directly. The range of viscosities we recover from our measurements are in a range one would expect for either a long chain alkanol such as nonanol or decanol, (8.7 – 10.5 cP)[42] or for an extensively hydrogen-bonded liquid such as ethylene glycol (ca. 16 cP).[43] Our findings, based on the fluorescence anisotropy data we report here, are consonant with other literature reports. X-ray diffraction experiments [44,45] and simulation studies[11] have shown that phospholipids in the gel phase pack less tightly than a crystal, but still exhibit short-range order. In the gel phase, the lipids are situated in a nominally hexagonal lattice pattern and the fatty acid chains are extended fully.[11] Our use of a nonpolar chromophore places the probe in a location ideally suited

Table 5.1. Viscosities of DMPC unilamellar vesicles as a function of 14:1 PC concentration.

	Gel Phase			Fluid Phase		
Mol % 14:1 PC	**τ_{OR} (ps)**	**T (K)**	**η (cP)**	**τ_{OR} (ps)**	**T (K)**	**η (cP)**
0.0	825 ± 18	296	15.0 ± 0.3	638 ± 23	298	9.0 ± 0.1
0.3	646 ± 38	282	11.9 ± 0.7	408 ± 67	283	7.1 ± 1.2
0.7	850 ± 43	277	14.5 ± 0.7	453 ± 37	278	7.7 ± 0.6
1.0	767 ± 73	277	13.0 ± 1.2	588 ± 60	278	10.0 ± 1.0
1.5	1061 ± 26	271	17.6 ± 0.4	539 ± 5	273	9.0 ± 0.1

to the detection and characterization of changes in bilayer structure associated with the phase transition.

With the ability to detect phase transitions in bilayer structures using perylene as an optical "sensor," we turn our attention to the effect of impurities on the phase transition temperature and local organization of DMPC bilayers. To evaluate this issue, we have made samples containing comparatively small amounts of 14:1 PC as an impurity (0.3 mol%, 0.7 mol%, 1.0 mol% and 1.5 mol%), and have measured the transition temperatures of the vesicle solutions using perylene reorientation. We show the temperature-dependent reorientation data in graphical form in Figures 5.4 and 5.5, for DMPC vesicles containing varying amounts of 14:1 PC. We find that there is a regular progression in T_m, decreasing with increasing amounts of 14:1 PC (Figure 5.6). For 0.3 mol% 14:1 PC, we observe a 15°C decrease in T_m, indicating that even relatively small amounts of a structural impurity can give rise to marked changes in the organization of bilayers. We note that experiments on bilayers comprised of 5 mol% 14:1 PC did not yield a phase transition temperature in the range we can access (as low as -15°C). Given that as few as three molecules per thousand can disrupt the organization of a bilayer substantially, it is fair to question whether or not the viscosity of the bilayers changes with the addition of 14:1 PC. As shown in Table 5.1, we recover viscosities that are possibly slightly different than for vesicles of pure DMPC, but the fact that we are measuring the reorientation times at substantially different temperatures makes a direct comparison of viscosity values for the different vesicles difficult. That said, for all of the viscosity data we report, the fluid phase viscosities lie in the range of 8.5 ± 1.5 cP and the

gel phase viscosities are in the range of 14.5 ± 2.5 cP. These are measurably different values for the two phases, but there appears to be no discernible trend in either phase with respect to the amount of 14:1 PC present. Thus, even though the longer range organization that is characterized by T_m is compromised by the presence of 14:1 PC, the local environment(s) sensed by perylene in either the gel or fluid phases is not influenced measurably by the presence of the structural impurity.

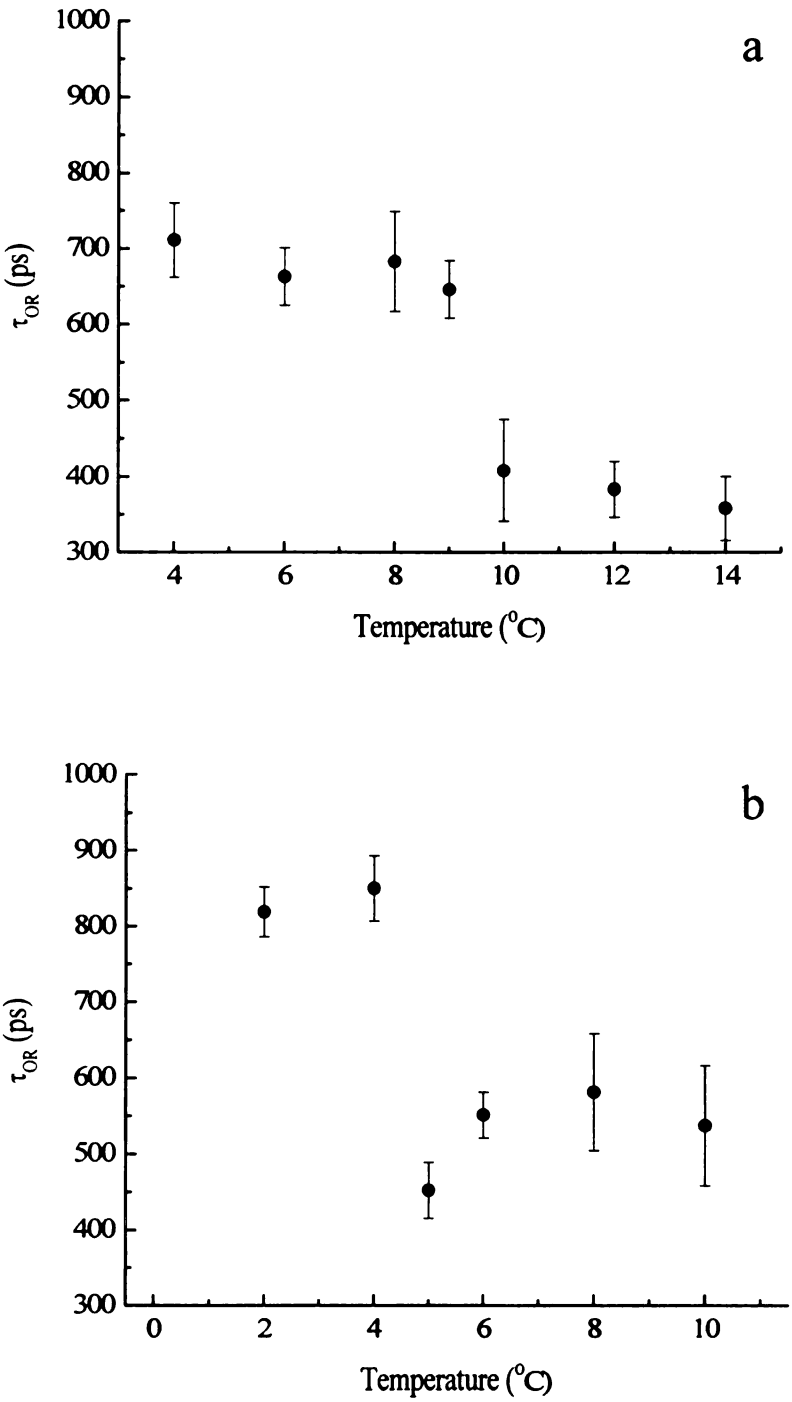

Figure 5.4. Reorientation time of perylene in DMPC unilamellar vesicles containing (a) 0.3 mol% 14:1 PC and (b) 0.7 mol% 14:1 PC as a function of temperature. Error bars are ± 1σ for at least four individual determinations at each temperature.

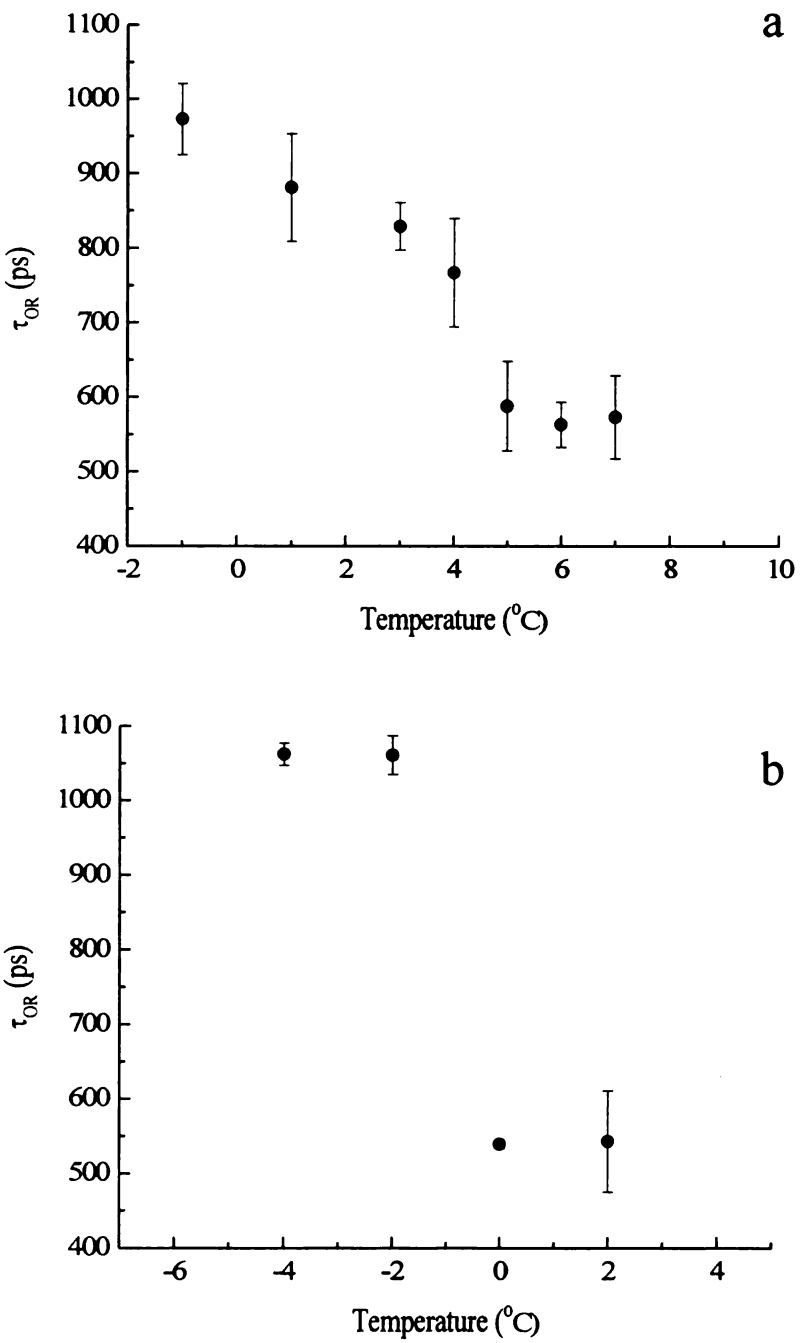

Figure 5.5. Reorientation time of perylene in DMPC unilamellar vesicles containing (a) 1.0 mol% 14:1 PC and (b) 1.5 mol% 14:1 PC as a function of temperature. Error bars are ± 1σ for at least four individual determinations at each temperature.

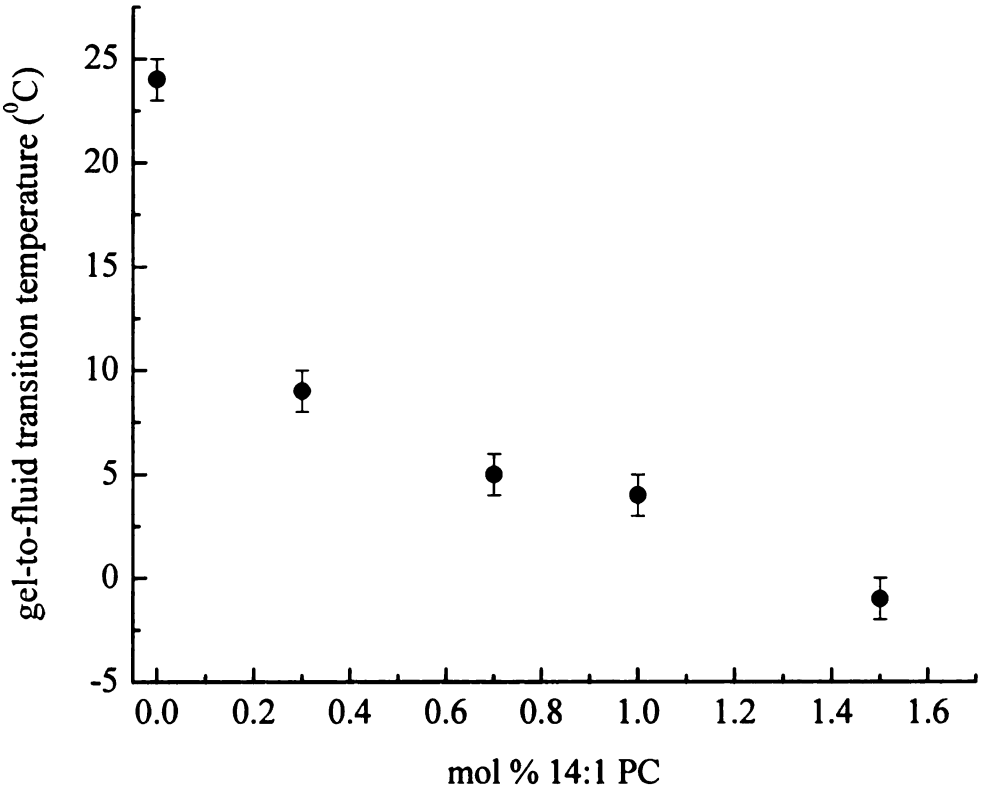

Figure 5.6. Variation of measured T_m in DMPC unilamellar vesicles as a function of 14:1 PC concentration.

The perylene reorientation data provide information on the effective local viscosity of the DMPC bilayer. This information can be used to estimate the translational diffusion coefficient, D_T, of perylene in these systems according to the Stokes-Einstein equation,[46]

$$D_T = \frac{k_B T}{6\pi R\eta} \tag{5.3}$$

Where R is the radius of the diffusing species and η is the viscosity. To estimate R, we use the hydrodynamic volume of perylene (225 $Å^3$) and presume a spherical shape, yielding R = 3.77 Å. We present the calculated values of D_T for our systems in Table 5.2. The data show that for all of these systems, there is an increase of a factor of ca. 1.5 in D_T across the phase transition, and that, even with the addition of 14:1 PC, D_T changes only modestly. It is, of course, important to consider how our values of D_T (~40 $\mu m^2/s$ below T_m, ~65 $\mu m^2/s$ above T_m) compare to other reports of D_T. Our values for D_T are in excellent qualitative agreement with those reported for tethered fluorophores in phospholipid monolayers, where D_T values between 15 and 110 $\mu m^2/s$ were reported, depending on the compression applied to the phospholipid LB monolayer.[47]

We provide the calculated D_T values in Table 5.2 with a couple of caveats. The first is that our bilayer structures could be a heterogeneous system, because we do not know the extent to which the 14:1 PC tends to aggregate within the bilayers. In this limit, the translational diffusion coefficient we report would not be an accurate representation of the frustrated translational diffusion that would occur in a heterogeneous system. The other caution is that both Eqs. 5.2 and 5.3 were derived for a solute contained within a

Table 5.2. Calculated translational diffusion coefficients for perylene in DMPC unilamellar vesicles as a function of 14:1 PC concentration. Viscosities were determined from τ_{OR} data with use of Eq. 5.2, and D_T values were calculated according to Eq. 5.3.

	Gel Phase			Fluid Phase		
Mol % 14:1 PC	**T (K)**	**η (cP)**	**D_T ($\mu m^2/s$)**	**T (K)**	**η (cP)**	**D_T ($\mu m^2/s$)**
0.0	296	15.0 ± 0.3	38 ± 1	298	9.0 ± 0.1	64 ± 1
0.3	282	11.9 ± 0.7	46 ± 3	283	7.1 ± 1.2	77 ± 11
0.7	277	14.5 ± 0.7	37 ± 2	278	7.7 ± 0.6	70 ± 5
1.0	277	13.0 ± 1.2	41 ± 4	278	10.0 ± 1.0	54 ± 5
1.5	271	17.6 ± 0.4	30 ± 1	273	9.0 ± 0.1	59 ± 1

continuum solvent, and for rotational diffusion measurements, there can be significant deviation from model predictions for cases where the solute and solvent molecules become similar in size. This deviation reflects a complex solvent-solute frictional interaction that must involve molecular-scale steric and dipolar processes. The microscale viscosities we infer from the reorientation data could, in principle, be off by a scaling constant, rendering our D_T values uniformly high or low, but the scaling constant should be essentially the same for all measurements. The change in D_T across the phase transition is thus reflected accurately in our reported results. With this frame of reference, we believe that the relatively modest changes in D_T across the phase transition for our systems is more consistent with a change in the extent of organization within the bilayer than with any substantial changes in free volume within the bilayer.

Conclusions

We have evaluated the utility of fluorescence anisotropy as a means of characterizing gel-to-fluid phase transitions in phospholipid bilayer structures. We find that perylene reorientation is a sensitive measure of the bilayer phase transition and that the incorporation of impurities has a substantial and measurable effect on this phase transition temperature. We have incorporated perylene, a nonpolar polycyclic aromatic hydrocarbon, into lipid bilayer structures consisting of pure DMPC and in bilayers containing DMPC with 0.3 mol%, 0.7 mol%, 1.0 mol% and 1.5 mol% of 14:1 PC over a range of temperatures surrounding the phase transition for these systems. Despite this mesoscopic structural effect, the local environment of the perylene probe is not affected substantially by the addition of 14:1 PC. Our viscosity data above and below the phase transition temperature provide quantitative information on the fluidity of this family of bilayer structures.

Literature Cited

(1) Edidin, M. *Nature Reviews. Molecular Cell Biology* **2003**, *4*, 414.

(2) Discher, B. M.; Maloney, K. M.; Grainger, D. W.; Sousa, C. A.; Hall, S. B. *Biochemistry* **1999**, *38*, 474.

(3) Keller, S. L.; McConnell, H. M. *Physical Review Letters* **1999**, *82*, 1602.

(4) Samsonov, A. V.; Mihalyov, I.; Cohen, F. S. *Biophysical Journal* **2001**, *81*, 1486.

(5) Subramaniam, S.; McConnell, H. M. *Journal of Physical Chemistry* **1987**, *91*, 1715.

(6) Yechiel, E.; Edidin, M. *Journal of Cell Biology* **1987**, *105*, 755.

(7) Pabst, G.; Amenitsch, H.; Kharakoz, D. P.; Laggner, P.; Rappolt, M. *Physical Review E: Statistical, Nonlinear, and Soft Matter Physics* **2004**, *70*, 021908/1.

(8) Suurkuusk, J.; Lentz, B. R.; Barenholz, Y.; Biltonen, R. L.; Thompson, T. E. *Biochemistry* **1976**, *15*, 1393.

(9) Lentz, B. R.; Barenholz, Y.; Thompson, T. E. *Biochemistry* **1976**, *15*, 4521.

(10) Shimshick, E. J.; McConnell, H. M. *Biochemistry* **1973**, *12*, 2351.

(11) Stevens, B. C.; Ha, T. *Journal of Chemical Physics* **2004**, *120*, 3030.

(12) Kranenburg, M.; Smit, B. *Journal of Physical Chemistry B* **2005**, *109*, 6553.

(13) Epand, R. M. *Biochemical Society Transactions* **1997**, *25*, 1073.

(14) Tocanne, J. F.; Cezanne, L.; Lopez, A.; Piknova, B.; Schram, V.; Tournier, J. F.; Welby, M. *Chemistry and Physics of Lipids* **1994**, *73*, 139.

(15) Korreman, S. S.; Posselt, D. *European Physical Journal E: Soft Matter* **2000**, *1*, 87.

(16) Lewis, R. N.; McElhaney, R. N. *Biochemistry* **1990**, *29*, 7946.

(17) Marsh, D.; Watts, A.; Knowles, P. F. *Biochimica et Biophysica Acta, Biomembranes* **1977**, *465*, 500.

(18) Morrow, M. R.; Davis, J. H. *Biochemistry* **1988**, *27*, 2024.

(19) Prenner, E. J.; Lewis, R. N.; Kondejewski, L. H.; Hodges, R. S.; McElhaney, R. N. *Biochimica et Biophysica Acta* **1999**, *1417*, 211.

(20) Mason, J. T. *Methods in Enzymology* **1998**, *295*, 468.

(21) Mabrey, S.; Sturtevant, J. M. *Proceedings of the National Academy of Sciences* **1976**, *73*, 3862.

(22) Mantsch, H. H.; McElhaney, R. N. *Chemistry and Physics of Lipids* **1991**, *57*, 213.

(23) McElhaney, R. N. *Chemistry and Physics of Lipids* **1982**, *30*, 229.

(24) Parasassi, T.; Gratton, E.; Yu, W. M.; Wilson, P.; Levi, M. *Biophysical Journal* **1997**, *72*, 2413.

(25) Watts, A.; Spooner, P. J. *Chemistry and Physics of Lipids* **1991**, *57*, 195.

(26) Khan, T. K.; Chong, P. L. G. *Biophysical Journal* **2000**, *78*, 1390.

(27) Lakowicz, J. R.; Knutson, J. R. *Biochemistry* **1980**, *19*, 905.

(28) Watts, A.; Marsh, D.; Knowles, P. F. *Biochemistry* **1978**, *17*, 1792.

(29) Mayer, L. D.; Hope, M. J.; Cullis, P. R. *Biochimica et Biophysica Acta* **1986**, *858*, 161.

(30) Hunter, D. G.; Frisken, B. J. *Biophysical Journal* **1998**, *74*, 2996.

(31) MacDonald, R. C.; MacDonald, R. I.; Menco, B. P.; Takeshita, K.; Subbarao, N. K.; Hu, L. R. *Biochimica et Biophysica Acta* **1991**, *1061*, 297.

(32) Driessen, A. J.; van den Hooven, H. W.; Kuiper, W.; van de Kamp, M.; Sahl, H. G.; Konings, R. N.; Konings, W. N. *Biochemistry* **1995**, *34*, 1606.

(33) Unger, E. C.; MacDougall, P.; Cullis, P.; Tilcock, C. *Magnetic Resonance Imaging* **1989**, *7*, 417.

(34) Subbarao, N. K.; MacDonald, R. I.; Takeshita, K.; MacDonald, R. C. *Biochimica et Biophysica Acta* **1991**, *1063*, 147.

(35) DelaCruz, J. L.; Blanchard, G. J. *Journal of Physical Chemistry B* **2003**, *107*, 7102.

(36) DeWitt, L.; Blanchard, G. J.; LeGoff, E.; Benz, M. E.; Liao, J. H.; Kanatzidis, M. G. *Journal of the American Chemical Society* **1993**, *115*, 12158.

(37) Marsh, D. *Handbook of Lipid Bilayers*; CRC Press: Boca Raton, 1990.

(38) Jiang, Y.; Blanchard, G. J. *Journal of Physical Chemistry* **1994**, *98*, 6436.

(39) Perrin, F. *Journal de Physique et le Radium* **1936**, *7*, 1.

(40) Debye, P. *Polar Molecules*; Chemical Catalog Co.: New York, 1929.

(41) Zwanzig, R.; Harrison, A. K. *Journal of Chemical Physics* **1985**, *83*, 5861.

(42) Blanchard, G. J. *Journal of Physical Chemistry* **1988**, *92*, 6303.

(43) Lipari, G.; Szabo, A. *Biophysical Journal* **1980**, *30*, 489.

(44) Janiak, M. J.; Small, D. M.; Shipley, G. G. *Biochemistry* **1976**, *15*, 4575.

(45) Tristram-Nagle, S.; Zhang, R.; Suter, R. M.; Worthington, C. R.; Sun, W. J.; Nagle, J. F. *Biophysical Journal* **1993**, *64*, 1097.

(46) Eimer, W.; Pecora, R. *Journal of Chemical Physics* **1991**, *94*, 2324.

(47) Peters, R.; Beck, K. *Proceedings of the National Academy of Sciences* **1983**, *80*, 7183.

Chapter 6

INTERROGATING THE ROLE OF LIPOSOME SIZE IN MEDIATING THE DYNAMICS OF A CHROMOPHORE IN THE ACYL CHAIN REGION OF A PHOSPHOLIPID BILAYER

Introduction

Lipid bilayer structures are essential to life processes, and as such have attracted a great deal of attention. It is well known that phospholipids will self-assemble spontaneously to form a bilayer structure in an aqueous environment, and under some conditions the most stable form is that which closes on itself, leaving no exposed "edges." Such spherical bilayer structures are commonly referred to as liposomes or vesicles, and they can be formed in a range of sizes, from ca. 100 nm or less to ca. 10 μm in diameter. This structural format has found widespread use because such structures can be suspended in an aqueous environment and can be manipulated with relative ease.

These outwardly simple structures are characterized by a range of subtle molecular interactions that collectively account for why the bilayer structure closes on itself. For example, it is known that there are phase transitions in lipid bilayer structures that are related to the organization of the phospholipid acyl chains. At a characteristic temperature, T_m, the hydrocarbon chains undergo a structural change from being predominantly *trans* in configuration to a structure characterized by a one or more *trans-gauche* conformers per chain.[1] For temperatures below the T_m, the lipid aliphatic tails are said to exist in a gel phase, a well-ordered state in which the translational mobility and diffusion of the bilayer constituents is thought to be comparatively limited. Above the

phase transition temperature, the phospholipid aliphatic tails exist in a disordered, fluid-like phase,[2] characterized by more motional and lateral freedom of bilayer constituents.[3-5] Some of the techniques that have been used in the past to measure this phase transition include differential scanning calorimetry,[6] fluorescence spectroscopy[7] and spin labeling.[8]

Because the phase transition temperature is related to the energetics of lipid-lipid interactions within the bilayer, and phospholipid phase transitions are considered to be important in regulating the activities of membrane-associated proteins,[9,10] there is a significant body of literature focused on measuring T_m for selected phospholipid bilayer systems.[2,9-22] The phase transitions seen for the acyl regions of phospholipid bilayers do not, however, provide a complete picture of bilayer organization. Vesicle geometry is also thought to contribute to the properties of the bilayer structure, with the dominant issue for this case being the extent to which surface curvature influences the organization of the acyl chains. This is a topic that has been considered extensively in the literature,[23-26] and there is some experimental evidence that bilayer surface curvature can influence the dynamics of the bilayer constituents. Indeed, it is the purpose of this paper to examine the influence of bilayer surface curvature on the dynamics of a chromophore imbedded in the acyl chain region. We find that the perylene reorientation depends sensitively on the size of the liposome in which it is incorporated.

To understand the role of lipid bilayer curvature in mediating the dynamics of an imbedded chromophore, we have constructed unilamellar vesicles of the phospholipid DMPC containing 10^{-6} M perylene as the probing chromophore. The diameter of prepared liposomes is controlled using the extrusion method,[27-33] where polycarbonate

membranes with defined pore sizes are used as the medium for extrusion. As the pore sizes in the polycarbonate membranes increase, the radius of curvature of the vesicles decreases, and we have established the relationship between membrane pore size and the resulting liposome diameter based on dynamic light scattering (DLS) measurements. We are interested in two issues. The first is to understand whether or not there is a relationship between vesicle size and phase transition temperature, and the second is to understand whether or not the size of the vesicle influences the chromophore dynamics. We find that for the smaller vesicles ($\leq$ 800 nm diameter) the phospholipid gel to fluid phase transition can be detected through the reorientation dynamics of perylene, and this finding is in agreement with our earlier report.[34] We also find that the dynamics of the perylene chromophore change markedly and abruptly with increasing liposome size. This finding suggests that as curvature in the bilayer becomes less pronounced, the perylene chromophore relocates within the bilayer structure. We discuss possible chromophore locations within the bilayer that are consistent with this finding. Our data imply that, for smaller vesicles, the chromophore locates preferentially in one of the bilayer leaflets, although which leaflet is not able to be discerned from our measurements.

Experimental

Vesicle Preparation. The phospholipid 1,2-dimyristoyl-*sn*-phosphatidylcholine (DMPC) was purchased from Avanti Polar Lipids Inc. (Alabaster, AL) and used as received. Perylene was purchased from Sigma-Aldrich (Milwaukee, WI) and used without further purification. The lipid and the perylene probe were mixed so that the final concentration was 2.9×10^{-4} M DMPC and 1×10^{-6} M perylene in the initial chloroform solution. The chloroform solvent was evaporated and an appropriate volume of Tris® buffer (Sigma-Aldrich, Milwaukee, WI) was added to the sample so that the resulting lipid concentration was 1 mg/mL. The buffer (10 mM, pH 7.8) was prepared using purified water from a Milli-Q Plus water purification system (Millipore, Bedford, MA). The mixture was processed five times through a freeze-thaw-vortex cycle to ensure complete mixing of the lipid and fluorescent probe. Each cycle consisted of freezing the solution by immersion in liquid nitrogen for five minutes, followed by thawing in a 60°C water bath (five minutes) and vortexing (approximately two minutes). After freeze-thaw-vortex processing, the solution was extruded eleven times through a polycarbonate membrane (Avanti Polar Lipids Inc., Alabaster, AL) with pores of a given diameter (ranging from 100 nm to 5 μm). Extrusions[27-33] were performed at room temperature.

Time-resolved fluorescence measurements. Time-domain polarized fluorescence intensity decays were acquired over a range of temperatures using a time-correlated single-photon counting (TCSPC) system. This system has been described in detail elsewhere, and we briefly recap some of its features here.[35,36] The light source is a CW mode-locked Nd:YAG laser (Coherent Antares 76-s) that produces 100 ps 1064 nm

pulses at 76 MHz repetition rate. The third harmonic of the Nd:YAG laser output is used to excite a cavity-dumped dye laser (Coherent 702-2) operated with Stilbene 420 dye (Exciton) at ca. 430 nm. The output of this laser is ca. 25 mW average power, with 5 ps pulses at a 3.8 MHz repetition rate. Sample fluorescence is detected with a microchannel plate – photomultiplier tube (MCP-PMT, Hamamatsu R3809U) and the electronics used to temporally resolve the fluorescence transients are constant fraction discriminators (CFD, Tennelec 454) and a time-to-amplitude converter/biased amplifier (TAC, Tennelec 864). The collection wavelength and polarization are computer-controlled using LabVIEW® 7.1 code. The fluorescence lifetime data were collected at 54.7° with respect to the vertical excitation polarization, and the reorientation data were collected at polarizations parallel (0°) and perpendicular (90°) to the vertically-polarized incident light. The temperature of the sample was regulated to ± 0.1°C using a water-circulating bath (Neslab RTE-110) connected to a cooling jacket that surrounds the sample cuvette. All samples were allowed to thermally equilibrate for ten minutes prior to data acquisition.

Steady state spectroscopy. Steady state excitation and emission spectra (Figure 6.1) were acquired for our vesicle samples for the purpose of characterizing the perylene band positions. We used a Spex Fluorolog 3 emission spectrometer for all measurements, set to a spectral bandpass of 2 nm for both excitation and emission monochromators.

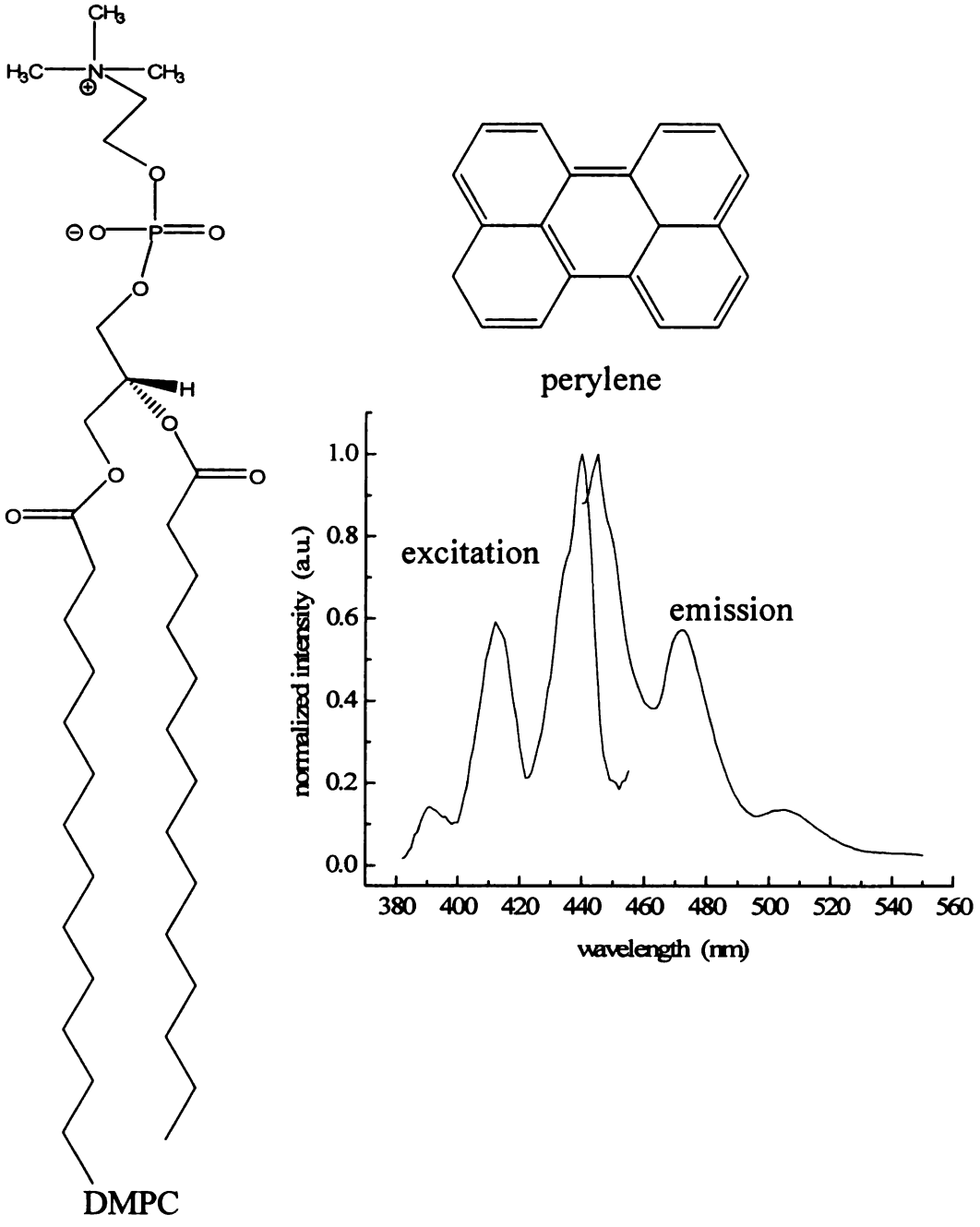

Figure 6.1. Structures of the phospholipid, DMPC and the chromophore, perylene. Bottom right: Steady state absorption and emission spectra of perylene in DMPC vesicles. Spectra have been normalized for clarity of presentation.

Dynamic light scattering. Dynamic light scattering (DLS) was performed with a Protein Solutions DynaPro-MS/X system (Wyatt Technology Corporation, Santa Barbara, CA) on DMPC/perylene liposome solutions to determine mean vesicle sizes and size distribution. Liposome solutions were diluted by a factor of fifty with buffer and placed in a polyethylene cuvette for measurement. We find that there is a direct correspondence between DLS-measured vesicle size and the nominal pore diameter of the extrusion membrane (Table 6.1 and Figure 6.2).

Table 6.1. Comparison of extrusion membrane pore diameter to the experimental diameter of the extruded vesicles. Experimental diameters were determined by DLS measurements. Uncertainties are ± 1σ for three individual determinations.

Extrusion nominal pore diameter (nm)	Measured mean vesicle diameter (nm)
100	106 ± 3
200	193 ± 14
400	417 ± 8
600	610 ± 16
800	817 ± 23
1000	1050 ± 69
2000	2108 ± 21
3000	3028 ± 83
5000	(not measurable)

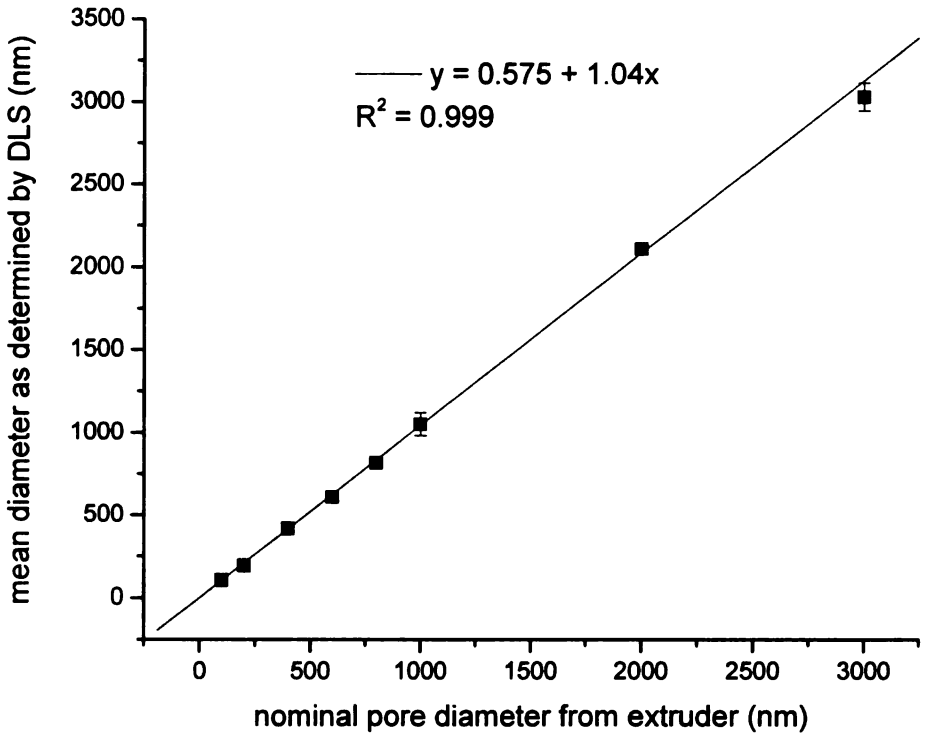

Figure 6.2. Plot showing the linear relationship between the nominal pore diameter in the extruder membrane and the measured diameter of DMPC/perylene vesicles from DLS.

Results and Discussion

The purpose of this work is to understand the dynamics of perylene in DMPC vesicles and how those dynamics depend on the temperature of the system and the diameter of the vesicles. As noted above, phospholipids are known to undergo phase transitions that are related to the organization of their acyl chains, and in a previous study we reported that the reorientation dynamics of perylene imbedded within DMPC bilayers are sensitive to this phase transition.[34] The interrogation of a phase transition in a lipid bilayer system requires some consideration of where in the system the probe resides as well as the characteristic length scale of the structural changes in the bilayer relative to the length scale sensed by chromophore reorientation. In an attempt to address these issues, we have studied perylene imbedded in a series of DMPC unilamellar vesicles of controlled diameter. Our findings relating to the temperature- and vesicle-size dependence of the recovered perylene dynamics reveal several interesting structural features. We consider the significance of each of these bodies of data after initial consideration of the perylene dynamics we recover.

In our previous report we found that perylene imbedded in 100 nm diameter unilamellar DMPC vesicles was sensitive to the phase transition of the bilayer from the gel to fluid phase.[34] Further, with the addition of 14:1 PC, even in small amounts, there was a marked change in the observed phase transition temperature. To characterize the reorientation dynamics of perylene, we combined the experimental fluorescence transients to form the induced orientational anisotropy function, R(t),

$$R(t) = \frac{I_{\parallel}(t) - I_{\perp}(t)}{I_{\parallel}(t) + 2I_{\perp}(t)} \tag{6.1}$$

and from the functional form of R(t) we inferred the motional dynamics of the perylene chromophore. The theory for the interpretation of R(t) is well established, and the number of exponential decays contained in this function is related to the shape of the molecule and its motion relative to the orientations of the excited and emitting transition moments.[37] Perylene has been studied extensively before,[38-41] and can exhibit either a single exponential decay or a two-component exponential decay of R(t), depending on whether it reorients as a Type I or a Type II rotor. We use Type I and Type II designations rather than the more widely used prolate and oblate terms because of the potential ambiguity with the latter. For a Type I rotor, the unique rotational axis is coincident with the transition moment, and for a Type II rotor, the unique rotational axis is perpendicular to the transition moment. For the purposes of this discussion, we assign the perylene long in-plane axis as *x* (coincident with the $S_1 \leftarrow S_0$ transition dipole moment), the short in-plane axis as *y* and *z* is the axis perpendicular to the molecular π system plane. For a Type I rotor ($D_x \neq D_y = D_z$) under these axis assignments, we expect the functional form of R(t) to be,

$$R(t) = 0.4\exp(6D_z t) \tag{6.2}$$

and for a Type II rotor ($D_z \neq D_x = D_y$),

$$R(t) = 0.1\exp(-(2D_x + 4D_z)t) + 0.3\exp(-6D_x t) \tag{6.3}$$

In our earlier work we recovered anisotropy decay functions consistent with a single exponential decay, and in this work we recover anisotropy functions that can be

resolved as two-component decays. The results are consistent with one another (*vide infra*), and indicate that perylene reorients as a Type II rotor in the DMPC vesicles we have formed. The data reported previously[34] were characterized by a limited S/N ratio, thereby allowing the resolution of two anisotropy decay components (Figure 6.3). When the experimental time constants we report here are reduced to a single weighted average time constant, the results are the same as the time constants reported in the earlier work (Figure 6.4). Because we can resolve two anisotropy decay components for perylene, it is possible to determine D_z and D_x, and substantial information is contained in these rotational diffusion constants. We have examined how these quantities vary with vesicle size and system temperature. We consider first the temperature dependence of these rotational diffusion constants.

We show in Figures 6.5 the temperature-dependent reorientation dynamics of perylene in unilamellar vesicles from 100 nm to 800 nm diameter (Figure 6.5a) and 1000 nm to 5000 nm diameter (Figure 6.5b). We present these data in the form of weighted average time constants to make direct correspondence with data we have reported previously. The temperature-dependent reorientation data show a subtle change in dynamical behavior in the vicinity of the transition temperature for vesicles up to 800 nm diameter (Figure 6.5a), but for vesicles 1000 nm and larger (Figure 6.5b), there is no discernible change in probe dynamics near the phase transition temperature. This finding suggests that either there is a change in the nature of the phospholipid phase transition or there is a change in the location of the probe within the bilayer structure. We will return to a discussion of this point following consideration of the vesicle-size dependence of the

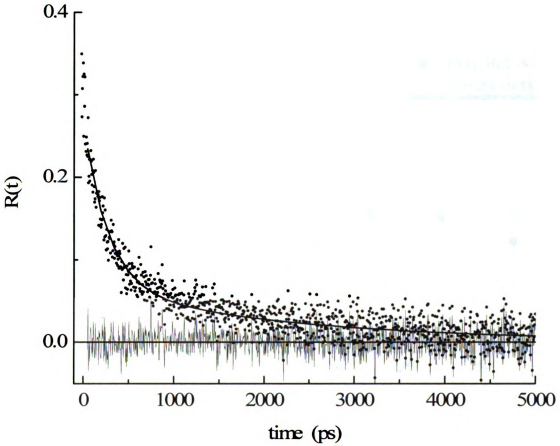

Figure 6.3. Anisotropy data for perylene in 100 nm diameter DMPC vesicles at 25°C, showing a decay that is best fit by two exponential components. The fitted line is indicated as the solid line and the residuals of the fit are shown centered around the zero line. The fitted function is $R(t) = A_1\exp(-t/\tau_1) + A_2\exp(-t/\tau_2)$, where $A_1 = 0.07 \pm 0.01$, $\tau_1 = 271 \pm 6$ PS, $A_2 = 0.20 \pm 0.01$ and $\tau_2 = 2238 \pm 56$ ps.

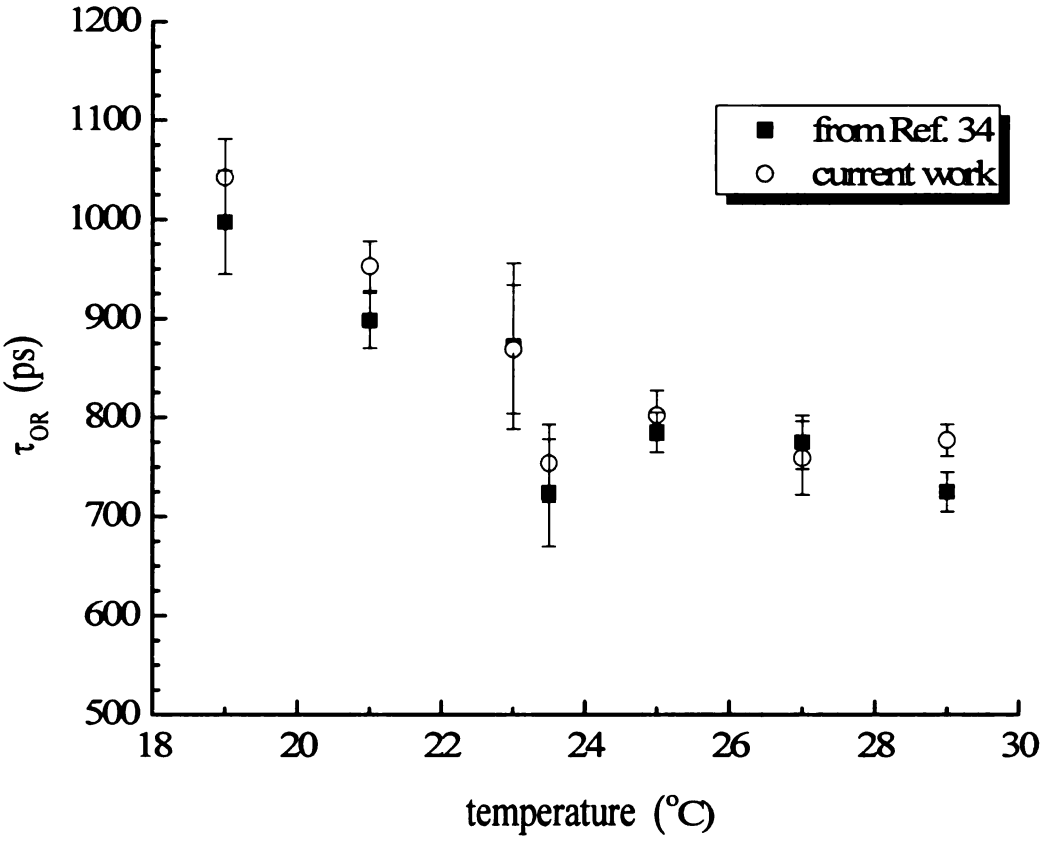

Figure 6.4. Reorientation times obtained for 100 nm diameter vesicles containing DMPC and perylene. The data from the earlier work were single time constants, while the data from the current work represent weighted averages of two time constants.

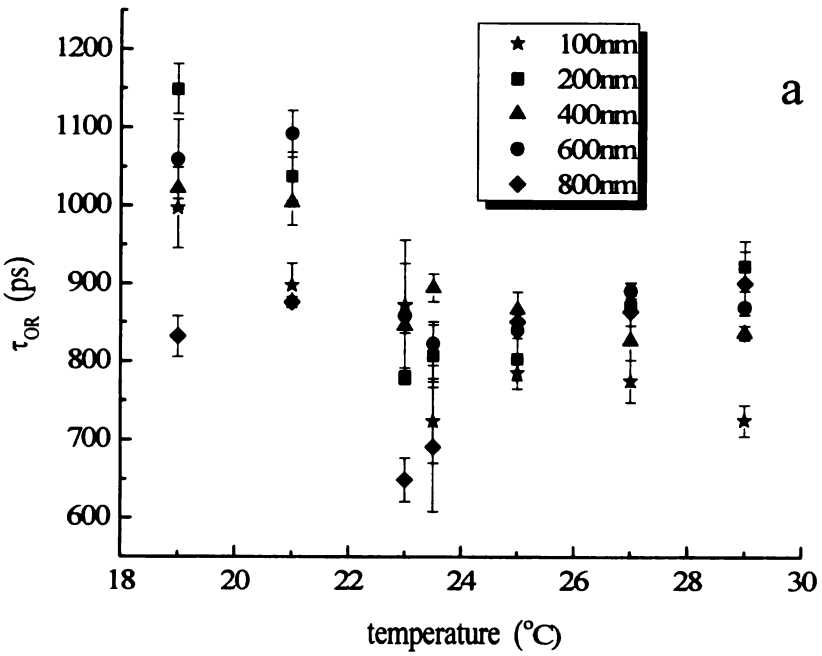
a
100nm
200nm
400nm
600nm
800nm
τ_{OR} (ps)
temperature (°C)

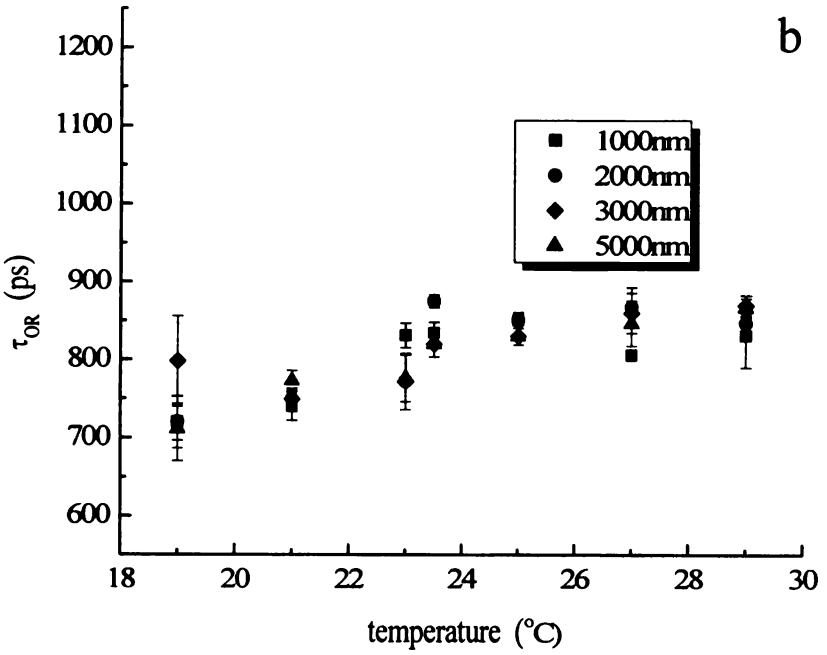
b
1000nm
2000nm
3000nm
5000nm
τ_{OR} (ps)
temperature (°C)

Figure 6.5. Reorientation times obtained for perylene in DMPC vesicles as a function of temperature and vesicle diameter. (a) 100-800 nm vesicle diameters. (b) 1000-5000 nm vesicle diameters.

data. We note that there is the possibility that the vesicles could change in size during the phase transition, which we cannot readily account for. However, based on past research,[42,43] there was a minimal change in the average diameter of phospholipid vesicles over a temperature range that included the gel-to-fluid phase transition.

We were interested in using the measured reorientation times of perylene within the lipid vesicles to calculate the rotational diffusion coefficient, D, as a function of temperature. As a Type II rotor, the shorter recovered time constant, $\tau_{1,OR}$, is related to one of the Cartesian components of the rotational diffusion constant by Eq. 6.4.[37]

$$\tau_{1,OR} = \frac{1}{6D_z} \tag{6.4}$$

The longer recovered time constant $\tau_{2,OR}$, is related to two Cartesian components of the rotational diffusion constant by Eq. 6.5.[37]

$$\tau_{2,OR} = \frac{1}{2D_x + 4D_z} \tag{6.5}$$

When both anisotropy decay time constants are used, and the quantities D_x and D_z are extracted (Eq. 6.5), it is clear that D_z is larger than D_x in all cases, and that the most pronounced change in dynamics occurs for D_z (Figure 6.6).

The temperature-dependent data for a given vesicle size reveals a subtle change in anisotropy decay dynamics in the region of the DMPC phase transition, but the most marked functional dependence of the data is seen when the vesicle size-dependence is plotted for a given temperature. We show these data for 19°C in Figures 6.7-6.8, noting

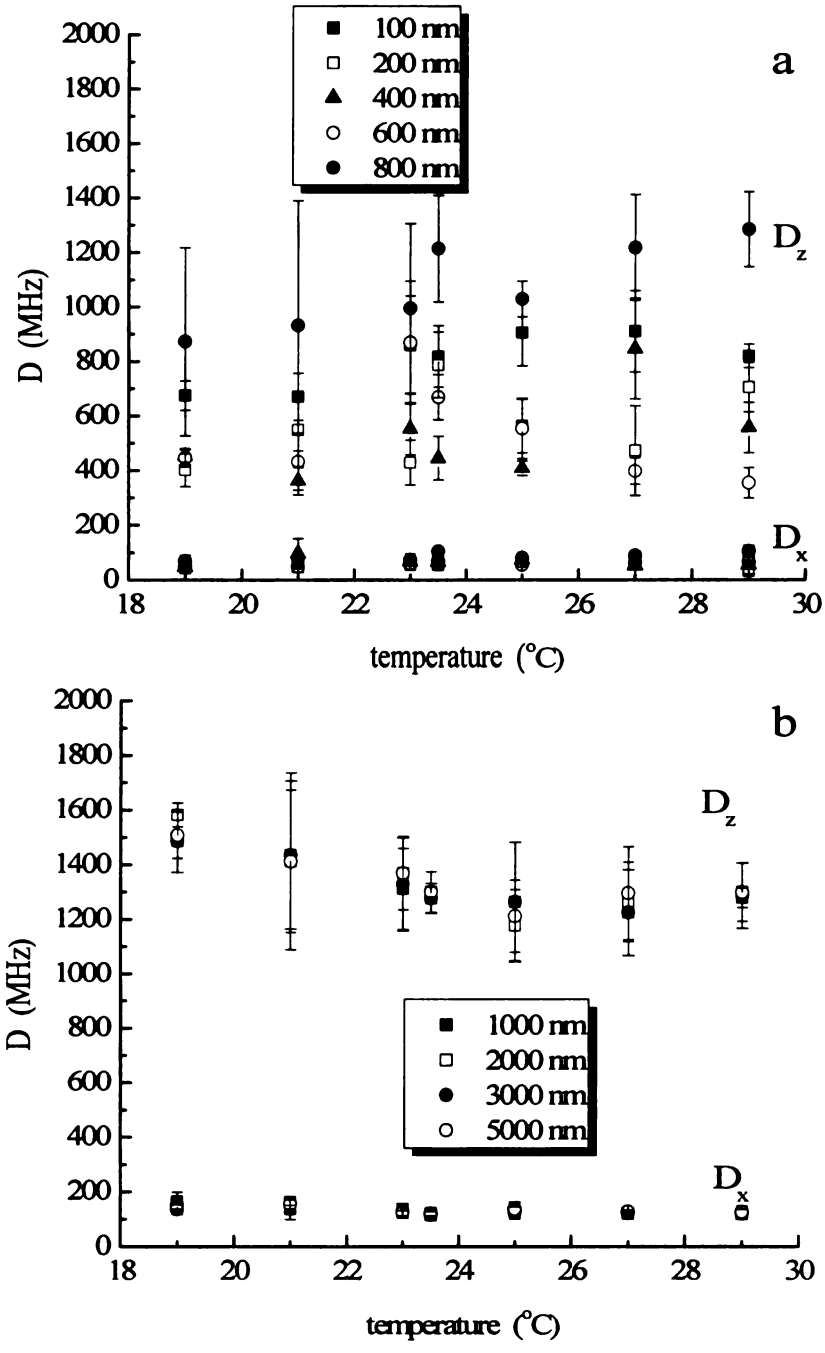

Figure 6.6. Cartesian components of the diffusion coefficient, D_x and D_z, obtained for perylene in DMPC vesicles as a function of temperature and vesicle diameter. (a) 100-800 nm vesicle diameters. (b) 1000-5000 nm vesicle diameters.

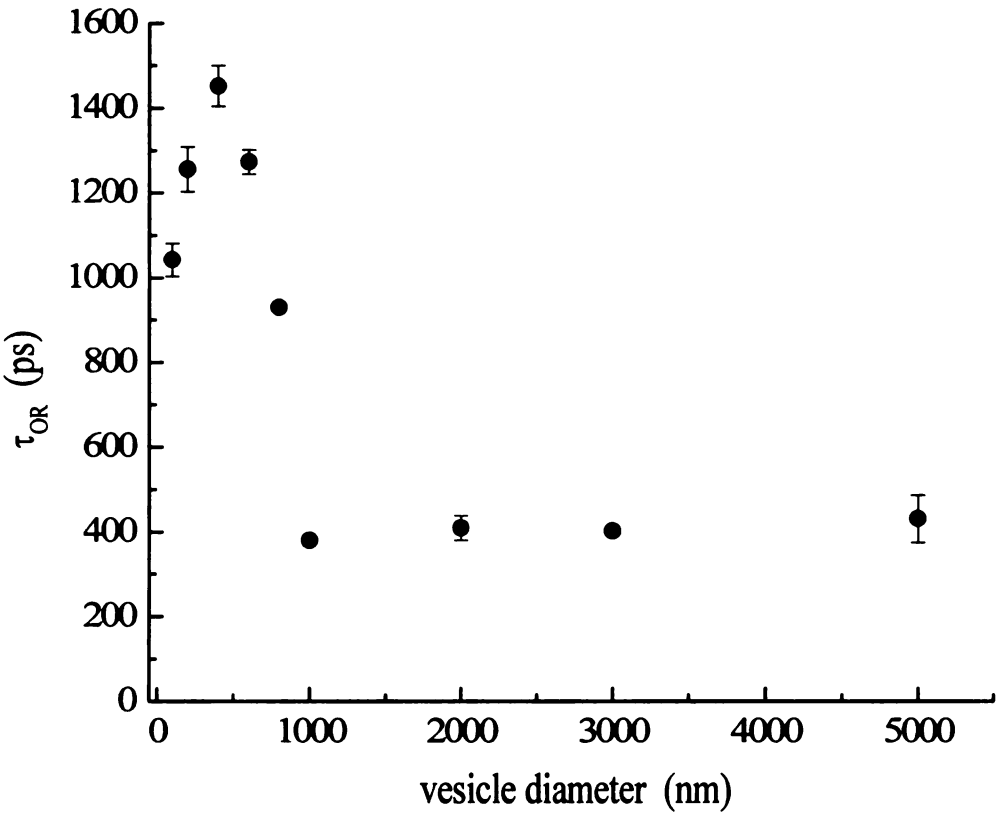

Figure 6.7. Reorientation times obtained for perylene in DMPC vesicles as a function of vesicle diameter at 19°C.

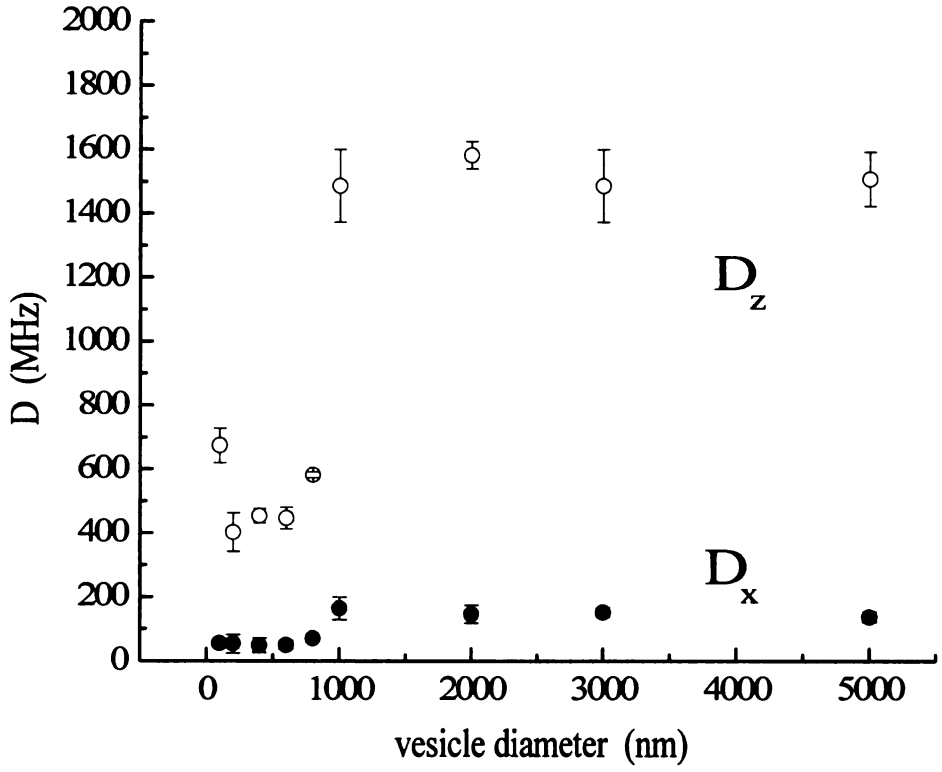

Figure 6.8. Cartesian components of the diffusion coefficient, D_x and D_z, obtained for perylene in DMPC vesicles as a function of vesicle diameter at 19°C.

that the data at other temperatures exhibit the same size dependence. The anisotropy decay data change in a step-wise manner; for vesicles smaller than 800 nm diameter we observe $D_z \sim 600$ MHz and $D_x \sim 60$ MHz ($D_z/D_x \sim 10$). For vesicles 1000 nm diameter and larger, we recover $D_z \sim 1500$ MHz and $D_x \sim 150$ MHz ($D_z/D_x \sim 10$). While theaspect ratio of the perylene motion remains substantially the same, the reorientation rate of the chromophore increases by a factor of ca. 2.5 for a small change in vesicle diameter. As noted above, we observe the same behavior at temperatures above and below the DMPC phase transition temperature. Such a change in dynamics indicates that there is a marked change in the local environment of the chromophore as the vesicle diameter changes from 800 nm to 1000 nm.

Using the calculated Cartesian components (D_x, D_y and D_z) of the rotational diffusion constant, D, we can calculate D based on Eq. 6.6.

$$D = \frac{D_x + D_y + D_z}{3} \tag{6.6}$$

The rotational diffusion constant can then be related to the local environment in which the chromophore resides based on the modified Debye-Stokes-Einstein equation,[44-46]

$$\frac{1}{6D} = \frac{\eta V f}{k_B T S} \tag{6.7}$$

where η is the viscosity of the medium surrounding the reorienting chromophore, V is the hydrodynamic volume of the chromophore, f is a frictional term to account for solvent-solute interactions, k_B is the Boltzmann constant and T is the temperature in Kelvin. The term S is a shape factor determined from Perrin's equations[44] to account for the nonspherical shape of the chromophore, and we calculate from Perrin's equations that S =

Table 6.2. Calculated viscosity at 19°C for the vesicles with varying diameters.

Vesicle diameter (nm)	Calculated viscosity (cP)
100	8.0 ± 0.8
200	12.4 ± 2.7
400	11.4 ± 1.6
600	11.5 ± 1.2
800	8.7 ± 0.3
1000	3.5 ± 0.3
2000	4.2 ± 1.4
3000	3.5 ± 0.3
5000	3.5 ± 0.2

0.70.[47] For each of the systems, using the calculated rotational diffusion constant from Eq. 6.6 and the hydrodynamic volume for perylene (225 $Å^3$),[48] the viscosity, η, was calculated. While the average viscosity for each sample remained approximately constant over the temperature range that we studied (19-29°C), we observed a decrease in the average viscosity in vesicles with diameters greater than 800 nm. Table 6.2 shows the calculated viscosity as a function of vesicle diameter at 19°C.

The experimental data (at ca. 1000 nm diameter vesicle size) indicate that there is a change in the chromophore local environment. This change could be the result of either an alteration of the bilayer structure of DMPC, or it could result from a change in the location of the chromophore in the bilayer structure. It is known that for vesicles, curvature in the system gives rise to asymmetric bilayers.[23-26] This bilayer asymmetry, in the case of the bilayers we use in this work, must come in the form of the number of lipids contained in the inner and outer leaflets, and likely also the packing of the acyl chains. Experimental data on some small vesicles (< 200 nm in diameter) indicates that, in terms of x-ray measurements, any difference between phosphocholine inner and outer leaflets cannot be resolved.[49] Our dynamical data on perylene rotational motion within the bilayers indicate, however, that chromophore access to different environments is modulated by the size of the vesicles, implicating curvature as a factor in this finding. There is also a large literature, mostly in the form of molecular dynamics simulations, that indicates that curvature in bilayers does occur and gives rise to asymmetric bilayers.[23-26]

Our data do not point to a specific change in chromophore location with increasing vesicle size, but there are several aspects of these findings that provide inferential insight into the organization of the system. The first point is that the chromophore dynamics become faster with increasing vesicle size. While the most noticeable change occurs for D_z, the ratio of D_z/D_x remains close to constant for all of the vesicle sizes we have measured. The fact that the diffusion coefficients increase by a factor of ca. 2.5 over the small change in vesicle size points to the perylene moving to a region of lower viscosity. Given the nonpolar nature of the chromophore, we suggest that the perylene is moving from being predominantly within the acyl chains for small vesicles to residing primarily in the region between the leaflets for the more planar structures. The second, and related point of interest is that the change in dynamics is seen at the same vesicle size where the motion of perylene appears to stop sensing the acyl chain gel-to-fluid phase transition. Such a change in what the chromophore senses implies that the chromophore is not in intimate contact with the portion of the bilayer that is affected most by the phase transition for larger vesicles. Again, a change of location from within the acyl chains to between the leaflets is consistent with this observation.

If the assignment of the perylene moving from the acyl chain region to the inter-leaflet region with increasing vesicle size is correct, an implication of this assignment is that, because there is necessarily an asymmetry between the inner and outer leaflets for small vesicles, the perylene chromophore will preferentially reside in one of the leaflets for small vesicles, owing to more favorable packing. It is possible that the organizational difference between the inner and outer leaflets is negligible,[49] but unfortunately, it is not

possible at this point, using simple DMPC vesicles, to evaluate the role of bilayer asymmetry in mediating perylene dynamics in small vesicles.

Conclusions

We have used fluorescence anisotropy measurements as a means of interrogating the local environment in lipid vesicle systems of varying diameter. We found that we could detect the DMPC gel-to-fluid phase transition temperature in vesicles with diameters of 800 nm or less and could resolve differences in D_z, over the temperature range encompassing the phase transition. With vesicles 1000 nm to 5000 nm in diameter, the transition temperature could not be resolved and there was no discernable trend in the rotational dynamics of perylene sequestered within the lipid bilayer. Examining how the reorientation data varied with vesicle size, however, revealed a marked change in chromophore dynamics with increasing vesicle size. The data suggest that the perylene changes location within the bilayer structure as curvature is reduced. This finding underscores the critical role that bilayer curvature can play in mediating dynamics and local environment. Further work with more complex bilayer structures will provide insight into cooperative roles that bilayer constituents may play in altering the influence of curvature at the molecular level.

Literature Cited

(1) Pabst, G.; Amenitsch, H.; Kharakoz, D. P.; Laggner, P.; Rappolt, M. *Physical Review E: Statistical, Nonlinear, and Soft Matter Physics* **2004**, *70*, 021908/1.

(2) Stevens, B. C.; Ha, T. *Journal of Chemical Physics* **2004**, *120*, 3030.

(3) Van Zoelen, E. J. J.; De Kruijff, B.; Van Deenen, L. L. M. *Biochimica et Biophysica Acta, Biomembranes* **1978**, *508*, 97.

(4) De Kruijff, B.; Van Zoelen, E. J. J.; Van Deenen, L. L. M. *Biochimica et Biophysica Acta, Biomembranes* **1978**, *509*, 537.

(5) Gerritsen, W. J.; Henricks, P. A. J.; De Kruijff, B.; Van Deenen, L. L. M. *Biochimica et Biophysica Acta, Biomembranes* **1980**, *600*, 607.

(6) Suurkuusk, J.; Lentz, B. R.; Barenholz, Y.; Biltonen, R. L.; Thompson, T. E. *Biochemistry* **1976**, *15*, 1393.

(7) Lentz, B. R.; Barenholz, Y.; Thompson, T. E. *Biochemistry* **1976**, *15*, 4521.

(8) Shimshick, E. J.; McConnell, H. M. *Biochemistry* **1973**, *12*, 2351.

(9) Epand, R. M. *Biochemical Society Transactions* **1997**, *25*, 1073.

(10) Tocanne, J. F.; Cezanne, L.; Lopez, A.; Piknova, B.; Schram, V.; Tournier, J. F.; Welby, M. *Chemistry and Physics of Lipids* **1994**, *73*, 139.

(11) Kranenburg, M.; Smit, B. *Journal of Physical Chemistry B* **2005**, *109*, 6553.

(12) Korreman, S. S.; Posselt, D. *European Physical Journal E: Soft Matter* **2000**, *1*, 87.

(13) Lewis, R. N.; McElhaney, R. N. *Biochemistry* **1990**, *29*, 7946.

(14) Marsh, D.; Watts, A.; Knowles, P. F. *Biochimica et Biophysica Acta, Biomembranes* **1977**, *465*, 500.

(15) Morrow, M. R.; Davis, J. H. *Biochemistry* **1988**, *27*, 2024.

(16) Prenner, E. J.; Lewis, R. N.; Kondejewski, L. H.; Hodges, R. S.; McElhaney, R. N. *Biochimica et Biophysica Acta* **1999**, *1417*, 211.

(17) Mason, J. T. *Methods in Enzymology* **1998**, *295*, 468.

(18) Mabrey, S.; Sturtevant, J. M. *Proceedings of the National Academy of Sciences of the United States of America* **1976**, *73*, 3862.

(19) Mantsch, H. H.; McElhaney, R. N. *Chemistry and Physics of Lipids* **1991**, *57*, 213.

(20) McElhaney, R. N. *Chemistry and Physics of Lipids* **1982**, *30*, 229.

(21) Parasassi, T.; Gratton, E.; Yu, W. M.; Wilson, P.; Levi, M. *Biophysical Journal* **1997**, *72*, 2413.

(22) Watts, A.; Spooner, P. J. *Chemistry and Physics of Lipids* **1991**, *57*, 195.

(23) Parthasarathy, R.; Yu, C.-h.; Groves, J. T. *Langmuir* **2006**, *22*, 5095.

(24) Cooke, I. R.; Deserno, M. *Biophysical Journal* **2006**, *91*, 487.

(25) Lubensky, T. C.; MacKintosh, F. C. *Physical Review Letters* **1993**, *71*, 1565.

(26) Baumgaertner, A. *Journal of Chemical Physics* **1994**, *101*, 9060.

(27) Driessen, A. J.; van den Hooven, H. W.; Kuiper, W.; van de Kamp, M.; Sahl, H. G.; Konings, R. N.; Konings, W. N. *Biochemistry* **1995**, *34*, 1606.

(28) Hope, M. J.; Bally, M. B.; Webb, G.; Cullis, P. R. *Biochimica et Biophysica Acta, Biomembranes* **1985**, *812*, 55.

(29) Hunter, D. G.; Frisken, B. J. *Biophysical Journal* **1998**, *74*, 2996.

(30) MacDonald, R. C.; MacDonald, R. I.; Menco, B. P.; Takeshita, K.; Subbarao, N. K.; Hu, L. R. *Biochimica et Biophysica Acta* **1991**, *1061*, 297.

(31) Mayer, L. D.; Hope, M. J.; Cullis, P. R. *Biochimica et Biophysica Acta* **1986**, *858*, 161.

(32) Subbarao, N. K.; MacDonald, R. I.; Takeshita, K.; MacDonald, R. C. *Biochimica et Biophysica Acta* **1991**, *1063*, 147.

(33) Unger, E. C.; MacDougall, P.; Cullis, P.; Tilcock, C. *Magnetic Resonance Imaging* **1989**, *7*, 417.

(34) Koan, M. M.; Blanchard, G. J. *Journal of Physical Chemistry B* **2006**, *110*, 16584.

(35) DeWitt, L.; Blanchard, G. J.; LeGoff, E.; Benz, M. E.; Liao, J. H.; Kanatzidis, M. G. *Journal of the American Chemical Society* **1993**, *115*, 12158.

(36) Dela Cruz, J. L.; Blanchard, G. J. *Journal of Physical Chemistry A* **2001**, *105*, 9328.

(37) Chuang, T. J.; Eisenthal, K. B. *Journal of Chemical Physics* **1972**, *57*, 5094.

(38) Labhart, H.; Pantke, E. R. *Chemical Physics Letters* **1973**, *23*, 482.

(39) Zinsli, P. E. *Chemical Physics* **1977**, *20*, 299.

(40) Klein, U. K. A.; Haar, H. P. *Chemical Physics Letters* **1979**, *63*, 40.

(41) Christensen, R. L.; Drake, R. C.; Phillips, D. *Journal of Physical Chemistry* **1986**, *90*, 5960.

(42) Cornell, B. A.; Fletcher, G. C.; Middlehurst, J.; Separovic, F. *Biochimica et Biophysica Acta, Biomembranes* **1981**, *642*, 375.

(43) Ceuterick, F.; Heremans, K.; De Smedt, H.; Nieuwenhuysen, P.; Clauwaert, J. *Chemical Physics Letters* **1979**, *62*, 341.

(44) Perrin, F. *Journal de Physique et le Radium* **1936**, *7*, 1.

(45) Zwanzig, R.; Harrison, A. K. *Journal of Chemical Physics* **1985**, *83*, 5861.

(46) Debye, P. Polar Molecules. In *Chemical Catalog Co.* New York, 1929.

(47) Jiang, Y.; Blanchard, G. J. *Journal of Physical Chemistry* **1994**, *98*, 6436.

(48) Edward, J. T. *Journal of Chemical Education* **1970**, *47*, 261.

(49) Kucerka, N.; Pencer, J.; Sachs, J. N.; Nagle, J. F.; Katsaras, J. *Langmuir* **2007**, *23*, 1292.

Chapter 7

CONCLUSIONS AND FUTURE WORK

In this dissertation, we used Time Correlated Single Photon Counting (TCSPC) and fluorescence recovery after pattern photobleaching (FRAPP) to study the fluorescence lifetime and rotational and translational dynamics of various chromophores located in different regions of lipid bilayers, with most emphasis on unilamellar vesicles. In doing so, we were able to study the dynamics of lipid bilayer structures and determine which factors affect the organizational and structural properties of the systems.

In Chapter 2, we found that two methods of lipid vesicle preparation, extrusion and sonication, yielded the same translational and rotational dynamic results for the tethered NBD chromophore that was used, despite any differences that were observed in the physical appearance, size and size distribution of the samples. While the addition of cholesterol into these systems made the lipid bilayers more fluid, the results were the same, regardless of the method of preparation.

In Chapter 3, we found that the lipid bilayer constituents were highly interactive in our systems, and any changes in one region gave rise to corresponding structural changes in other bilayer regions. The dynamics of the tethered rhodamine chromophore, located near the head group region of the lipid bilayer, showed the existence of interactions between these chromophores, which were mediated by the NBD chromophore dynamics in cholesterol rich domains.

The effect of increasing chromophore concentration in the lipid vesicles was studied in Chapter 4, where it was found that both the steady state and dynamical

properties of tethered rhodamine change with concentration, in a manner that is consistent with the introduction of disorganization to the lipid bilayers. This finding underscored the necessity in using low chromophore concentrations for our studies.

We found in Chapter 5 that we could use a nonpolar chromophore, perylene, together with its reorientation times to determine the phase transition temperature in selected lipid bilayer systems. We were able to use the data that we obtained to approximate the viscosity, as sensed by this probe, in the nonpolar regions of the lipid bilayers. We also found that the incorporation of an unsaturated lipid into the system, in varying concentrations, caused substantial changes in the measured transition temperature of the system.

In Chapter 6, we varied the diameters of the lipid vesicles (from 100 nm to 5 μm) and used the rotational reorientational dynamics of perylene to sense the phase transition. We found that we could resolve the phase transition in the vesicles with diameters less than 1 μm. In the larger vesicles, the rotational dynamics of perylene were not as fully resolved.

Future work with this project would involve tethering lipid vesicles onto planar substrates in order to study additional properties of bilayer systems including the movement of transmembrane proteins. The incorporation of proteins and additional bilayer constituents into the systems, including cholesterol and sphingomyelin, would serve to make the lipid bilayers systems more realistic and aid in the design of future model membranes.

We now realize the necessity in using lower concentrations of chromophores in spectroscopic studies, and we are further interested in comparing the information obtained from these studies to electrochemical experiments. The fusion of vesicles onto a conductive substrate would allow us the ability to measure the electrochemical signal across the membrane and use the membranes as biosensors. Additionally, it would be constructive to be able to visualize and size the various domains within lipid bilayers using fluorescence microscopy to further verify the exact location of the fluorescent probes.